Rowan University
Rowan Digital Works

Theses and Dissertations

7-18-2017

High throughput analysis of the penetration of iron oxide/ polyethylene glycol nanoparticles into multicellular breast cancer tumor spheroids

Jonathan Robert Gabriel
Rowan University

Follow this and additional works at: https://rdw.rowan.edu/etd

 Part of the Biomedical Engineering and Bioengineering Commons

Recommended Citation

Gabriel, Jonathan Robert, "High throughput analysis of the penetration of iron oxide/polyethylene glycol nanoparticles into multicellular breast cancer tumor spheroids" (2017). *Theses and Dissertations*. 2454.
https://rdw.rowan.edu/etd/2454

This Thesis is brought to you for free and open access by Rowan Digital Works. It has been accepted for inclusion in Theses and Dissertations by an authorized administrator of Rowan Digital Works. For more information, please contact graduateresearch@rowan.edu.

www.manaraa.com

HIGH THROUGHPUT ANALYSIS OF THE PENETRATION OF IRON OXIDE/POLYETHYLENE GLYCOL NANOPARTICLES INTO MULTICELLULAR BREAST CANCER TUMOR SPHEROIDS

by

Jonathan Robert Gabriel

A Thesis

Submitted to the
Department of Mechanical Engineering
College of Engineering
In partial fulfillment of the requirement
For the degree of
Master of Science in Mechanical Engineering
at
Rowan University
March 10, 2016

Thesis Chair: Vince Beachley, Ph.D.

www.manaraa.com

© 2016 Jonathan Robert Gabriel

www.manaraa.com

Dedication

For my parents, Michael and Traci Gabriel, and my grandmother Fredelle.

www.manaraa.com

Acknowledgements

I would like to thank my advisor Dr. Vincent Beachley for his direction, mentoring, and insightful advice during my graduate career. I wish also to thank my Advisory Committee members Dr. Tom Merrill, Dr. Jennifer Vernengo, and Dr. Wei Xue, for your efforts I am truly grateful.

Thank you Dr. Robi Polikar for the introduction to Rowan's graduate engineering program by way of panel discussion at The College of New Jersey in the fall of 2013. Your enthusiasm piqued my interests to consider the budding ground of Rowan University as a prime location to continue my education.

I am grateful to the philanthropist and humanist, Henry Rowan for inspiration and motivation stemming from his ironic quote, "My only regret is that I did not work hard enough," shared with me by Dr. Merrill. Thank you for making this unique learning experience possible.

Most importantly, I would like to recognize the support of my parents, Michael and Traci Gabriel, my brother Eric, my grandmother Fredelle, and all other close family and friends who provided encouragement during this process. Through your everlasting guidance and understanding, this work was made possible, and given meaning beyond the context of these pages.

www.manaraa.com

Abstract

Jonathan Robert Gabriel
HIGH THROUGHPUT ANALYSIS OF THE PENETRATION OF IRON OXIDE/POLYETHYLENE GLYCOL NANOPARTICLES INTO MULTICELLULAR BREAST CANCER TUMOR SPHEROIDS
2015-2016
Vince Beachley, Ph.D.
Master of Science in Mechanical Engineering

The purpose of this study was to design and optimize a system for the high-throughput analysis of multicellular tumor spheroids (MCTS), and validate the system through the study of a complex biological model. The system was successfully created and optimized, allowing the histological recovery of MCTS at rates up to 90% for microarrays of 24-spheroids. Arrays of 96-spheroids were recovered at rates up to 86%. The system was used to study the penetration of 5k Da-polyethylene coated superparamagnetic iron-oxide nanoparticles (5k-PEG SPIONs) into HTB-126 breast cancer spheroids cultured to a mean diameter of 486 μm (± 25.2 μm). Results were compared to an identical study using 2D cultures. Positive staining for the SPION dosage of 100 μg/mL in 2D culture regardless of incubation time was observed along with a lack of staining for all other concentrations in both 2D and 3D. SPION incubation led to necrosis in breast cancer spheroids after 3 days.

www.manaraa.com

Table of Contents

www.manaraa.com

Table of Contents (Continued)

www.manaraa.com

Table of Contents (Continued)

www.manaraa.com

Table of Contents (Continued)

www.manaraa.com

List of Figures

www.manaraa.com

List of Figures (Continued)

www.manaraa.com

List of Tables

www.manaraa.com

Chapter 1

Introduction

1.1. Motivation

Biomedical cell culture and analysis techniques developed in the first decade of the 19th century remain the chosen research methods in many laboratories of today. Since this time, our fundamental knowledge of cellular and tissue biology has greatly changed; however, our analytical methodologies have failed to keep up to pace. It is irrefutable that more efficient tools and cost-effective methods are necessary to propel biology, specifically cancer biology and drug development, through the 21st century. The widespread application of recent technological advances has the potential to improve outcomes for many patients now and in the future through improved drugs and personalized medicine.

It is unfortunate that the pharmaceutical industry is primarily a business and only secondarily a means for the improvement of humankind. As a result, more economically favorable products may be pursued in place of developing those with the greatest potential to impact and cure disease. This idea substantiates the need for developing testing platforms to produce better drugs more rapidly, while tailoring them to patient specific needs, at a fraction of the cost.

www.manaraa.com

The future of drug development lies in mechanistic approaches which are superior to their empirical counterparts in identifying novel therapeutic targets. Many assays for drug development have been developed, but no single assay can firmly predict the usefulness of a potential candidate. We present a system, with the ability to interface with existing immunohistochemical techniques that is high-throughput and uses 3D culture systems as the fundamental diagnostic tool. 3D culture systems have been proven time and again to be far more relevant than their out-dated, 2D counterparts. This is because 3D culture systems accurately represent the 3D tumor microenvironment consisting of cells and the surrounding extracellular matrix (ECM). Improvements in cellular biology, tissue engineering, materials science, and micro/nanofabrication will only benefit the future of 3D culture.

In recent times, innovative discovery techniques have elucidated new drug targets leading to the development of novel compounds to act upon them. However, only about 5% of these compounds successfully progress through the development funnel, ultimately becoming useful treatments. For every 5,000 to 10,000 compounds in the pharmaceutical development funnel, only one will successfully make it to market. In the United States in 2013, the Food and Drug Administration approved only 27 new medications; nine of these were orphan drugs. The European Medical Agency did not surpass this to a great extent,

www.manaraa.com

recommending 81 medications for approval (up from 57 in 2012). Many drugs fail during the most expensive phase, phase III clinical trials. The result is a cost of approximately $1.5 billion USD to bring a single drug to market. This cost is necessary to make up for failed compounds in a company's pipeline. One potential reason for the high attrition rate is the use of 2D culture by pharmaceutical companies as an initial screening tool. The use of 3D cultures in the pharmaceutical business is likely limited, with little public evidence of any use. Implications of 2D culture high-throughput screening (HTS) approaches include the passing of drugs which may ultimately fail, and the screening out of others which may have become truly beneficial. Additionally, no two patients ever have the exact same disease state. The term "cancer" refers to over one hundred different diseases with patient specific genetic effects. There exists a definite need for a system that can use a patient's own cells, incorporate the more relevant 3D microenvironment, and have the ability to be tested and analyzed in a high-throughput manner. The future of oncology therapeutics is 3D culture, and there is no reason that it should not be used ubiquitously in 2016.

1.2. Objective

The objectives of this research were as follows: (1) to develop a system or process for conducting high-throughput analysis of multicellular tumor spheroids with the ability to acquire regionally based biochemical information,

www.manaraa.com

and (2) to validate it through a complex biological model involving drug penetration, showing the power of the methodologies of the system.

The specific aims included: (1) a complete review of the current state of the field including rationale for 3D culture, spheroid generation methodologies, and analysis methods amenable to high-throughput testing; (2) optimization of procedures for the creation and analysis of a spheroid microarray including (a) microarray mold design and fabrication, (b) spheroid culture techniques, (c) spheroid harvesting and transfer techniques, (d) microarray fabrication reagents and techniques, (e) array processing reagents and methodology, and (f) histological sectioning and staining; (3) quantification of the effectiveness of the system through (a) determination of the number of spheroids recovered, (b) degree of tilt during sectioning of the microarray, (c) processing effects of histological samples, and (d) the value proposition of the system through time and money saved to a user versus conventional methods; (4) validation of the system's effectiveness through a 3D study involving two dosages and multiple time points to characterize the penetration of superparamagnetic iron-oxide nanoparticles into breast cancer spheroids, and compare these to a parallel 2D study; (5) develop an automated/mechanical system for spheroid transfer from culture plates to microarray mold to increase the speed of microarray fabrication and reduce the cost of the system.

www.manaraa.com

We hypothesized the system would be capable of recovering at least 90% of spheroids embedded into blocks of 24-wells through a range equivalent to one-third of the diameter of the initial spheroid, and at least 70% of spheroids from blocks of 96-wells through the same range. We anticipate an increased efficiency of study greater than 1000% compared to conventional methods based on time and money saved. We believe sectioning will occur in-plane with an error no greater than 100 micrometers of tilt over the length of the array (0.382 degrees of tilt). Finally, we anticipate dosage and incubation time dependent effects on nanoparticle penetration in the validation study, but are unsure which will have a more profound effect.

Future developments related to this project will (1) improve the design of the mold and process, pushing spheroid recovery above 95% for all array sizes, (2) fabricate a completely automated system capable of spheroid placement into the microarray, and (3) improve processing and histological techniques to section microarrays to 10 μm and below.

1.3. Organization of Thesis

This chapter (*Chapter 1*) contains an overview of the motivations and objectives of the research reported in the thesis. This chapter should act as an outline for the experiments performed, data and results expected, and rationale for said experiments.

www.manaraa.com

Chapter 2 is an in-depth and complete literature review on the current state of 3D culture and its implications for drug development and experimental biology. *Chapter 2* will be condensed and submitted to Pathology & Oncology Research as a review paper. What differentiates *Chapter 2* from other literature review papers on this topic is its focus on analytical methods for spheroids with the ability to acquire regionally based biochemical information without ultra-expensive imaging equipment available only in top research laboratories. The paper then proposes the methods discussed here as a prospective solution.

Chapter 3 consists of a thorough description of the methodologies invented, refined and analyzed to solve the problem of high-throughput immunohistochemistry of multicellular tumor spheroids (MCTS). This chapter represents a bulk of the experimental work of the thesis. The system is complete, fully characterized, and at a level of quality substantial for formal research. Recommendations for future iterations of design are recommended. *Chapter 3* will be slightly modified and submitted to the journal *Tissue Engineering Part C: Methods*.

Chapter 4 contains a validation study for the system, with a comparison experiment between a 2D and a 3D culture system. It is unfortunate that no publishable results were obtained from this preliminary study; however, it remains to show the power of the system, serving its purpose in this thesis. This

www.manaraa.com

study is currently under repeat and will be combined with *Chapter 3* for journal submission.

Chapter 5 presents a solution for the mechanically automated transfer of spheroids between culture plates and the microarray mold. Motivation for this chapter came as the result of suggestions from a recent grant review desiring more automation in the process. This chapter covers the rationale, design, and functional procedure. This chapter should be treated as confidential as it contains drawings and pictures of non-secured intellectual property.

Chapter 6 presents a conclusion of the work in this paper and recommendations for the future.

www.manaraa.com

Chapter 2

A Review of 3D Spheroid Cultures as a Tool for Biomedical and Cancer Research: Needs, Rationale and Implications for the Future

2.1. The Current State of Drug Development

Methods currently employed in biomedical research laboratories and the pharmaceutical industry to discover novel cancer therapeutics use often incorporate techniques developed in the first decade of the 19th century. Only as recently as the 1970s has the industry seen a moderate shift towards more clinically relevant methods, methods involving the third dimension of cell culture [1]. More efficient tools and cost-effective methods are needed to conduct the preclinical screening of anti-cancer drugs to propel these technologies through the 21st century. Unfortunately, many pharmaceutical companies operate around the basis of profit and do not necessarily produce the best possible treatments for patients, but those that are economically favorable. This idea substantiates the need to develop testing platforms that produce better drugs more rapidly, while tailoring them to individual needs of patients for a fraction of the cost.

There is a recent shift in the anticancer drug discovery process from empirical to mechanistic approaches [2, 3]. Empirical methods involve testing a

www.manaraa.com

drug on a culture of cells and measuring the resulting viability[1] of the cells without cognizance for the underlying mechanisms causing change. Mechanistic approaches revolve around identifying molecular targets as the basis for drug design. Recent research in genomics and proteogenomics has elucidated many new molecular targets for researchers and pharmaceutical companies to design therapeutic agents to act upon [4]. All drugs follow a similar process of design and development leading to their clinical use. The process begins with identifying a druggable target as the result of a mechanistic or similar biological study. Once the target is identified and characterized, *in silico* modeling is used to develop an array of lead compounds to act on this target. These compounds are synthesized, beginning the pre-clinical testing. Difficulties begin with sifting through large numbers of initial compounds using a set of standardized, high-throughput screens. Both *in vitro* analyses on appropriate cell lines, and *in vivo* studies on relevant animal models are performed. Each drug is fully characterized using pharmacokinetic and pharmacological tests to determine absorption, distribution, metabolism and excretion properties. Further cytotoxicity tests are performed to predict drug safety. The tests determine potential therapeutic usefulness. Compounds that successfully navigate pre-

[1] viability or another property that is a result of the entire culture's population. This is in comparison to a specific cellular event that can be tracked through biochemical analysis to individual cells or a specific organelle, protein, or gene across many cells.

www.manaraa.com

clinical testing are employed in human clinical trials, the most important of all tests [1]. Many assays have been developed, but the ability of any particular assay to predict *in vivo* efficacy in humans has not been firmly established [4].

While biotech innovations have greatly increased the pool of potential new therapeutic compounds, only 5-10% of compounds reaching clinical trials successfully progress through development. For every 5,000 to 10,000 compounds entering the pipeline, only one will make it to market. The large number of failures along the development process makes the cost of a successful compound greater than $1.5 billion USD in the 2010s [5]. Failure is generally due to either a lack of clinical efficacy or unacceptable human toxicity. Clinically predictive *in vitro* models have obvious advantages in terms of their ability to save time and money. Unfortunately, many of the current systems, including cell-based and xenograft models, are unreliable and non predictive of the pathophysiology they hope to represent; failure most often occurs during the latest and most expensive stages of testing, human clinical trials. Therefore, it is absolutely imperative that more highly predictive, cell-based *in vitro* models are created to screen out poorly performing compounds earlier in the development funnel. Eliminating useless candidates more quickly will reduce costs, wastes, and the ethical dilemmas associated with clinical trials, especially those of

www.manaraa.com

failure. Furthermore, it allows prioritizing the most promising candidates and accelerates their path to market [1].

At this stage, assay methodologies are split into two distinct paths. The first involves the automation and miniaturization of HTS to create ultra-HTS approaches, which are considered by some so distant to the *in vivo* environment that their outputs are relatively useless [4]. The other path involves creating assays of intermediate complexity to gain deeper insights to the mechanisms that operate at the cellular level. Each set of assays has its benefits and limitations. There are three general categories based on the mode of operation and predictive capacities [4]. Generic cellular assays study the proliferation, viability and cytotoxicity in response to external stimuli. These assays are more broad, but may provide confirmation for the continuation of a compound's research. Failure at this step is not necessarily adequate grounds for disqualification. Other assays study signal transduction pathways such as ion channels, second messengers, and kinase activation. The third class of assays study events at the genetic level with regards to transcription, translation and the regulation of such processes. Unfortunately, none of these assays can definitively predict whether a compound's candidacy should be pursued or terminated. The current drug development process uses a combination of assays to build a library of potential new compounds that will move on to the next step. Surely many promising

www.manaraa.com

compounds may be left behind. Additionally, we know that many compounds passing this stage will fail, costing the system millions of dollars. The lack of clinical value of these assays may be attributed to the fact that 2D systems do not accurately predict the 3D environment.

Developments in 3D culture techniques have paralleled research in tissue engineering, hoping to more accurately represent the 3D microenvironment. Some techniques able to create reproducible cultures exhibiting viability and differentiation from isolated primary tissue include spinner flask culture, various perfusion and fed-batch techniques, and the tumor fragment spheroid model [4]. These methodologies will be discussed further in *2.6 Three Dimensional Culture Techniques*.

Currently, there exists an effort to develop tumor specific testing platforms that employ the patient's own primary cancer cells. The result is a highly individualized test which attempts to recreate the specific disease pathophysiology of the individual patient. One example of these tests is the *ex vivo* ATP-based chemosensitivity assay. Unfortunately it relies on the 2D culturing of tumor cells isolated from primary tissue biopsies [6]. Problems with this method include a limited number of useful cells extracted from the biopsy, and the potential modulation of cell morphology upon expansion in 2D culture. Here, we see a definite need for a system that can use a patient's own cells,

www.manaraa.com

incorporate the more relevant 3D microenvironment, and have the ability to be tested and analyzed in a high-throughput manner.

2.2. The Need for *In vitro* Models with Increased Physiological Relevance

There is an increased demand for *in vitro* models that capture more complexity than what is observed through 2D monolayer culture [7]. It is firmly established that 2D monolayer culture does not accurately represent the *in vivo* micromilieu. The development of tissue and quasi-organ 3D *in vitro* models from human cells have the potential to "bridge-the-gap" between standard monolayer culture, and more complex models such as animal and human testing [7]. The best method for creating 3D cell structures has yet to be determined, but it is speculated that better drugs will be developed as a result of testing on more realistic systems [1]. Initial "stop/go" decisions in the drug development process are often made after tests on monolayer cultures. These are not the most physiologically relevant [1]. For the pharmaceutical industry, it is imperative to screen out poorly performing compounds at the earliest possible stages for cost effectiveness. Many researchers believe the best way to improve *in vitro* screening of candidates is to use 3D multicellular tumor spheroid (MCTS) testing as a critical part of the process [1]. Since many treatments lose their efficacy in the 3D environment, spheroids are thought to be a tool for negative selection, identifying compounds that perform poorly *in vivo*. More recently molecular

www.manaraa.com

targets and signaling pathways have been found to play a role exclusively in 3D making the spheroid model a positive selection tool in drug development initiatives [8-12].

2.2.1. Predictive capacity of animal, xenograft and humanized models is limited. Many reports have stated the limited predictive value of routine drug screening tactics [3, 13, 14]. This information adds additional support to the need for developing more complex 3D models to adequately mimic the *in vivo* pathophysiological environment in hopes of forever replacing monolayer culture and animal testing [4]. The optimization of preclinical and pre-animal testing systems will alleviate economical burdens while also diffusing ethical concerns associated with clinical testing. Additionally, improved tests will optimize and streamline the selection of clinically effective drugs from the growing pool of potential candidates [4]. The US National Cancer Institute Developmental Therapeutic Program uses a few different multi cell-line screens, and one hollow fiber model, to predict xenograft activity. Xenograft models involve transplanting human tumors into immunodeficient animals, and studying the effects of the drug on the tumor. These types of models are thought to be one step closer to human models than standard animal testing, although they do come with drawbacks such as unnatural biochemical interactions, and significantly different, compromised immune systems. As for the cell line

www.manaraa.com

models, it was shown that the 60-cell line screen was slightly more predictive than the hollow fiber model in determining which compounds should proceed to animal and xenograft testing. However, no significant correlation was shown between any single *in vitro* or *in vivo* preclinical model and actual clinical results [4].

Rodent models will still be necessary for pharmacokinetic[2] and toxicological[3] evaluation of potential new therapeutic agents for decades. However, spheroids have the potential power to greatly reduce the number of animal models needed, and to delay their use in the process. In this way, spheroids may not only alleviate ethical and economic concerns, but also make up for the fact that animal models are not very indicative of human *in vivo* testing results, and thus clinical efficacy [4]. MTSC models look to "bridge the gap" between 2D culture and animal/human testing by employing explanted human cells in a more natural, and physiologically relevant way. Adding MTSC as a tool in the drug development arsenal will give researchers a stronger testing foundation and better information to move forward.

Animal models give researchers information that may not be discerned from any current *in vitro* methods, but they often fail to capture the *in vivo* response that is seen in humans. For example, the number one reason for the

[2] dosage, formulation, administration, and half-life
[3] both systemic and organ specific

www.manaraa.com

failure of drugs in clinical trials is liver toxicity not predicted by animal models [15]. Furthermore, many pathogens and immune responses are species specific. One attempt to create a better model involves 'humanizing' mice. Humanized mice are almost completely immunodeficient mice which show high rates of human cell engraftment, can support human tissue differentiation and growth, and generate well-differentiated multilineage human hematopoietic cells after hematopoietic stem cell transplantation. These models are useful for studying human hematology and immunology *in vivo*. More recently, genes have been introduced into these mice to allow for the production of important human cytokines with direct influence on the immunological response [16]. These techniques provide valuable information but remain expensive, challenging and have limits recapitulating the dynamics of the human body. Questions have also been raised against the validity of these models as research has shown fundamental differences in telomerase regulation and cytokine compatibility between rodents and humans [15].

2.2.2. The engineering journey to more predictive models. To create increasingly predictive *in vitro* models, attempts must be made to replicate the functional hierarchy present in tissues beginning with microvasculature, as transport phenomena are crucial to understanding biological systems. Additionally, better models should recreate microscale flows through the

www.manaraa.com

interstitial space, blood and lymphatic networks, and the apical ducts [7]. The challenge of recreating microvasculature remains a significant barrier to fully functional *in vitro* systems [7]. Microvascular considerations are important for *in vitro* models as these mechanisms govern the bulk transport of signaling and regulatory molecules, along with those required for sustaining life. These flows lead to a profound impact on tissue proliferation, morphology, and differentiation *in vivo*. This will be expanded upon further in *Section 2.4, The Mechanical and Chemical Properties of the In Vitro Microenvironment and their Influences on Cellular Biochemistry*.

The use of a patient's primary cells for *in vivo* testing is preferable but limited by availability. Primary cells have a reduced ability to expand and are largely variable in morphology. Studies involving human primary cells may also be hindered by ethical considerations [4]. The lack of primary human material is the limiting step for high-throughput screening (HTS); systems employing established cell lines are considered secondary. The result is a demand for more advanced *in vitro* test systems based on secondary cells in the pharmaceutical industry. In tests with secondary material, generating the required number of cells is no longer an issue; however, tests involving secondary cell lines in place of those using primary cells may not accurately represent the pathophysiology of the patient's specific disease state [4].

www.manaraa.com

The field of stereolithography has accelerated allowing researchers to fabricate well toleranced materials into the low end of the microscale range. These systems are able to produce scaffolds large enough (0.1 - 10 cm) with finely tuned features such as walls, pores, and channels adequate for cell penetration, proliferation, communication and pre-vascularization (0.2 - 11 mm). In time, technology may improve to allow even finer features to facilitate the fine-scale cell organization truly necessary for *in vitro* tissue engineered models. Some manufacturing systems are emerging that allow the necessary resolution to move into the nanofabrication territory, but these technologies must be properly adapted to work with biological systems [7].

Many researchers recommend a collaborative environment between academic institutions and the pharmaceutical industry to prove the predictive value of 3D systems, while optimizing use and allowing for integration into the current drug development process. Advances in tissue engineering, such as the creation of bioreactors and 3D scaffolds, have created numerous new 3D culture technologies. More work must be done in fully characterizing each of these systems and evaluating their individual potential to replicate necessary functions of pathological tumors *in vivo* [4].

"A principle component of this failure results from our lack of understanding of, and inattention to, how to culture cells specifically so that they

www.manaraa.com

phenotypically represent their *in vivo* counterparts" [17]. It is accepted without dispute that cells behave in accordance to their environment and culture conditions. Altering factors such as culture mediums and supplementation, initial cell density, and culturing surfaces and techniques leads to high variability in quantitative and qualitative outputs such as proliferation, differentiation, migration and apoptosis[4]. It is believed that each of these factors affects both random and target-specific screening approaches, creating a "butterfly effect" of cell culture. Further understanding of the cellular microenvironment and its impact on cellular phenotype is necessary to design increasingly accurate models.

2.3. Two Dimensional Cell Culture and its Limitations

The fundamental principles of cell culture were first developed in 1907 by Harrison and colleagues, who showed sustained cell maintenance outside the original body of origin. Specifically, pre-differentiated neural tissue was taken from frog embryos and placed in a drop of lymph. The solution was hung off a sterile coverslip in a moist environment and cultured for some time. This setup was actually quite similar to initial methods of hanging drop culture, occurring much later in the century. Since its inception, almost every step of the cell culture process has been optimized. Developments include culture containers

[4] programmed cell death through signal transduction

www.manaraa.com

coated with optimal chemicals for cell attachment and synthetic culture mediums that outperform their blood plasma predecessors. Additionally, new culture mediums are cheaper, reproducible and antigen free. Antibiotics and antifungal agents have been developed to mitigate potential contamination sources arising during normal culture. Small iterations over past decades have improved culture techniques, while the internet has made vast knowledge bases available to any research laboratory wishing to join the quest [1].

Traditional methods of culture involve the growth of a cell monolayer in a flat culture vessel, typically a flask or Petri dish. Culture chambers are made of plastic and coated with substrates to aid cellular attachment. Cells are grown in a mixture of culture medium, serum and antibiotics. Other additives such as L-glutamine and insulin may be added depending on the needs of a specific cell lineage. Additionally, the cell medium may contain phenol red as a pH indicator. Phenol red transitions from yellow to red between pH values of 6 and 8. The ideal eukaryotic cell's physiological pH is tightly regulated between 7.35 and 7.45. Therefore, fresh culture medium appears red and turns orange-to-yellow when acidic metabolites accumulate. Medium must be changed before the solution becomes fully yellow in color. Cultures are incubated at physiological temperature of 37ºC for optimal enzyme activity and 5% CO_2 saturation to maintain bicarbonate concentration for cell pH buffering systems.

www.manaraa.com

Once cells reach confluence, they are detached from the culture flask using trypsin and/or ETDA, and reseeded in a new flask at approximately 10% of the confluent concentration. This is called sub-culture. It is performed to prevent cell senescence and nutrient exhaustion. The process of sub-culturing a line of cells increases its passage number by one. It is important to keep track of the number of passages as some cell lines lose proliferative and viability capabilities as well as important morphological characteristics at passage numbers as low as five [1]. Many cancer cell lines have been immortalized meaning their genes have been engineered for indefinite proliferation without the loss of viability. The cells of Henrietta Lacks, who died in 1951, have been around since the 1950s and are still used today.

The need to create *in vitro* assays which produce biomedically relevant information is essential for drug development. 2D cell culture has been conventionally used for drug candidate testing; however, it has been shown that the correlation between successful navigation of 2D tests and useful therapies is limited to none [1]. For this reason, many researchers suggest new methodologies for screening compounds be developed and tested.

Limitations of 2D culture include the lack of cell-cell and cell-extracellular matrix (ECM) signaling that occurs ubiquitously in 3D cultures and *in vivo*. The ECM is a collection of molecules secreted by living cells which provides

www.manaraa.com

mechanical support and biochemical influences fundamental to the organization of tissues. Such signals between neighboring cells and cells-and-ECM are essential to cell differentiation, proliferation and normal cellular functions [18, 19]. One element lacking in 2D environments important for cell function is integrin interactions. These integral membrane proteins help link the cells to their external environment through connections to actin, filamin and other proteins. Through messenger systems they relay external information and biochemical cues to the cell. As a result, it has been suggested that 3D *in vitro* systems such as MCTS may bridge-the-gap between 2D monolayer models and expensive *in vivo* testing [1].

Recent developments in 3D culture technology and analysis have highlighted potential key differences between 2D and 3D culture. When grown as monolayers, cells have been shown to have differences in cell morphology, polarity, receptor expression, oncogene expression, interactions with ECM and basement membrane, and overall different cellular architectures when compared to *in vivo* samples. Confining cells to grow in a 2D space on artificial surfaces leads to the lack of tissue hierarchy observed in monolayer cultures [4]. Such findings question the validity and significance of studies performed on 2D cultures. As a result, the field has shifted towards studying and improving 3D culture methodologies due to their superior physiological relevance [1].

www.manaraa.com

Additionally, 3D cultures histologically to represent *in vivo* microcarcinomas to a high degree [4]. *Figure 1* compares an *in vivo* tumor with a spheroid (MCTS) side by side. Notice the many similarities in functional architecture between the two tissues. One important difference is how they are perfused, the tumor from a central capillary, the spheroid by culture medium at its periphery.

www.manaraa.com

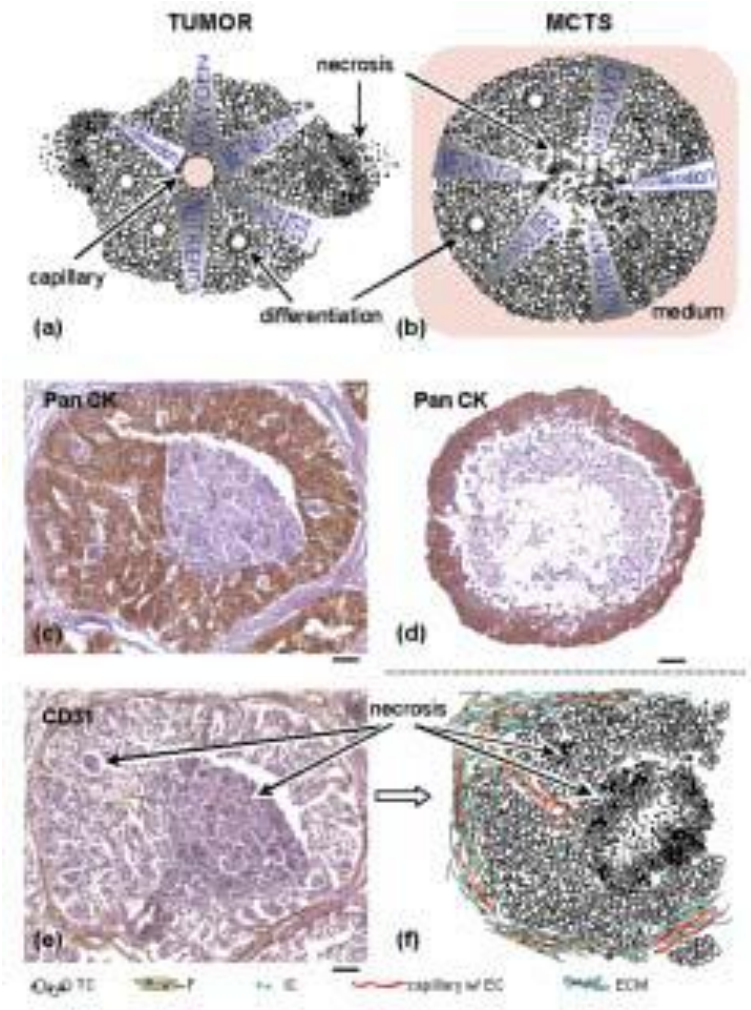

Figure 1. Immunohistochemical staining of spheroid sections (b,c,f) next to sections of biopsied tumor specimens (a,c,e). Reproduced from Kunz-Schughart (2004).

Another reason for the superiority of 3D culture is its ability to preserve the original phenotype and function of explanted cells. For example, both primary articular chondrocytes and hepatocytes rapidly lose morphology upon monolayer culture. In 3D, this loss may be attenuated or even reversed. Additionally, a study showed how multipotent mesenchymal stromal cell

www.manaraa.com

(MSC)-derived hepatocytes were better able to perform important functions such as albumin and urea synthesis, as well as ammonia and drug clearance in 3D [4]. This example is one of many providing evidence for 3D cultures as superior *in vitro* models to 2D monolayer culture.

2.4. The Mechanical and Chemical Properties of the *In Vitro* Microenvironment and their Influences on Cellular Biochemistry - Requirements for Improved 3D Models

The extracellular matrix (ECM) may be thought of as the foundation of tissues. It is constantly modified by cells to control mechanical and chemical properties of the microenvironment. Mechanical properties of the ECM are controlled by the composition, architecture and the degree of crosslinking between various proteins and biopolymers [7]. Cells are able to finely tune these properties of local ECM to suit the needs of a specific tissue. Accomplishing this requires the synthesis, secretion and incorporation of proteins like collagen into the ECM. Collagen is one protein the cell uses to resist tensional stresses. This protein, which is actually a heterodimer of interwoven proteins, acts as a molecular braided rope with a modulus of elasticity between 5 and 11.5 GPa at room temperature [20].

In order to resist compressional stresses using flexible and soluble organic molecules, the cell must be more creative. Structural integrity under compressive loading is accomplished with the use of heavily glycosylated

www.manaraa.com

proteins called proteoglycans. Glycosylation is the covalent bonding of sugar molecules to proteins, lipids or other organic molecules. In the case of proteoglycans, proteins are attached to glycosaminoglycans. They contain many carbohydrate residues, specifically sulfate and uronic acid groups which are negatively charged at physiological pH. The result of this negative charge is the attraction of partially positive hydrogen atoms present in water molecules. Ultimately, proteoglycans are heavily hydrated molecules which use the incompressible fluid, water, to resist compressional stresses. The high charge density of proteoglycans makes protein transport throughout the ECM difficult. Dynamic compressive forces have been shown to control the deposition patterns of proteoglycans and protease inhibitors in chondrocytes [21]. This principle has been exploited in tissue engineering through the mechanical stimulation of cultures to promote chondrogenesis with good results [22]. Additionally, basement membrane, secreted basally by epithelial and endothelial cells, also hinders protein transport and acts to increase mechanical stiffness [23].

Also incorporated into ECM are globular, or nonstructural, proteins which play important roles as enzymes and in chemical signaling. Globular proteins control cellular events such as adhesion, migration and ECM remodeling, a process which occurs constantly in response to the external environment. Remodeling of the ECM to increase strength is just one example of how

www.manaraa.com

mechanical stresses are coupled to chemical composition. Furthermore, globular proteins help control cell migration, proliferation, apoptosis and differentiation. The large number of growth factors, chemokines, and other morphogenetic and signaling proteins secreted and embedded into the ECM during its synthesis assist cells in accomplishing these tasks. Ultimately, the ECM controls the bulk and local mechanical environment and contributes to the tissue's microenvironment, a microenvironment which is preserved to a much higher degree in 3D culture compared to 2D.

Production of ECM in spheroids has been described in a number of studies [24-29] and has been shown to be far more extensive in the amount and assembly compared to corresponding 2D cultures. Production of ECM in tumor spheroids is different than in nonmalignant cells. In tumor cells, ECM is predominantly of tumor cell origin. *In vivo*, ECM is typically produced by non-tumorigenic, stromal cells. In MCTS, this is not the case. Therefore, it is important to monitor the origin of ECM as this may be a factor in tumor initiation [26].

2.4.1. Specific effects of external mechanical forces on cellular physiology. Basal cellular phenotype is determined by integrating the numerous mechanical and chemical cues strongly coupled in the 3D environment. The growth and regulation of connective tissues, such as muscle and bone, are

www.manaraa.com

strongly influenced by mechanical forces. Mechanical loads are transferred from the macro to the cellular level where they are transmitted to the ECM and cells integrated within. This is one example of how molecular signaling mechanisms are directly coupled to stretch and compression. These mechanisms may be easily lost in monolayer cultures adhering to a flat, rigid substrate. Molecules involved include those attached to the ECM, and all types of other extracellular signaling molecules which respond to the mechanical stimuli: endocrine, paracrine and autocrine messengers. For example, weight bearing exercises increase muscle mass and bone density; space travel has the opposing effects. These are physiological responses to external stresses, or lack thereof.

In addition to eliciting chemical responses, mechanical stresses physically change the spatial distribution of cells, ECM and effector molecules [7]. This occurs even in tissues without typical mechanical responsibilities. Many of these signals are well understood on an individual basis, but the field of tissue engineering still looks to discover how signals modulate each other to create the responses observed *in vivo*. The ECM also binds many growth factors and biological effector molecules. It further influences the cellular microenvironment by sequestering molecules which otherwise would diffuse, creating local regions of higher concentrations. The ECM can also act to slow diffusion of paracrine and autocrine factors due to its porosity. In this way, the mechanical and

www.manaraa.com

chemical structure of the ECM directly influences chemical signaling dynamics [7].

A more complete understanding of the coupling effects between mechanical forces and chemical signaling will have profound impacts on regenerative medicine. Additionally, since so many cues are present in the ECM, recreating this environment *in vitro* is difficult. Isolating individual factors and determining unique responses also has limitations due to the variable composition of ECM between synthetic batches. High-throughput analysis of multicellular spheroids composed of healthy human cells could be a key model for future studies on the coupled effects of numerous biological variables.

2.4.2. ECM stiffness and composition regulate cellular response and phenotype. Matrix stiffness plays a key role in certain cellular processes such as endothelial organization. During tissue remodeling, morphogenesis, and differentiation, cells exert stresses on the ECM. Cells can contract the matrix to varying degrees depending on the number of integrin-ligand bonds and the architecture of the ECM. Other factors such as cellular migration and intracellular tension may be affected as well. Stiffer matrix creates increased difficulty of contraction and greatens energy expenditure. A stiff matrix can promote endothelial organization while inhibiting other cellular processes [30].

www.manaraa.com

Two hallmark characteristics of cancer tumors are the lack of ECM organization and increased matrix stiffness. In cancer, the ECM network is often deregulated, leading to more malignant cellular phenotypes and metastases. The elasticity of the matrix is also closely intertwined with its biochemical properties; a stiff matrix is often an indicator of disease. Since sensing external forces involves the elasticity of the matrix, the ECM provides mechanical cues that influence cellular behaviors. The cytoskeleton along with focal adhesion components, the nuclear matrix, and the nuclear envelope and chromatin act as the biomechanical sensors that determine how cells react to forces from the ECM [31]. For example, researchers showed how changes in mechanical forces are correlated with differences in TGF-β signaling in mouse tendon [32]. Additionally, others showed how increasing the stiffness of mammary epithelia gels disrupted morphogenesis and enhanced proliferation through a mechanism of phosphorylation of focal adhesion kinases [33]. Matrix stiffness has also been shown to play a role in ECM contractions influencing healing and fibrosis [30]. ECM composition and stiffness are important regulators of cellular response.

Swartz and colleagues aimed to show how mechanical stress can be communicated from stressed to unstressed cells in the coordination of the cooperative tissue remodeling process [34]. The study showed how mechanical stress on human airway epithelial cells could elicit a matrix remodeling response

www.manaraa.com

in unstressed, co-cultured lung fibroblasts through soluble chemical signals. The results challenge the accepted mechanism of fibrosis in asthma, which has been attributed to the effects of the inflammatory response. However, it is now hypothesized that mechanical stresses also play a role in the fibrotic response. Results of the study concluded that epithelial-fibroblast interactions are complex, two-way cellular interactions where the presence of each cell type modulates the response of the other. Additionally, they noted that since the ECM is deformable and that interactions between it and cells contained are coupled, the communication which arises due to these mechanical stresses should studied be more closely. Since fibrosis and ECM stiffness are indicators of cancer, further studying these communication networks may be important to reveal the underlying mechanisms of the disease.

Another form of mechanical stress that influences the microarchitecture of tissues is shear stress from microvascular fluid flows. Microvascular endothelial cells sense an increased need for fluid flow to a specific region due to higher than normal shear stresses. Short term responses included increased recruitment of quiescent capillaries and if the situation persists, angiogenesis may result [35].

In vitro models which contain two or more cell types may respond in different ways to mechanical forces than single-cell cultures. First, cells may rebuild their local environment resulting in a new, shared micromechanical

www.manaraa.com

environment. For example, epithelial cells may stiffen the environment with the secretion of basement membrane. The rebuilding of the environment may be coordinated between the signals of the multiple cell types. Secondly, simply the presence of another cell type may modulate the expression of the other cell types present [36]. Spheroid co-culture studies have the potential to combine the power of typical co-culture studies, but in a more natural environment. Additionally, many cancer pathologies are a result of numerous cell types present in tumors leading to the observed pathophysiology.

Other molecules present in ECM such as adhesion molecules in the integrin and cadherin families are critical in determining a cell's fate with respect to proliferation, life and death. The apoptotic mechanism is closely related to contact with other cells, as are mechanisms associated with contact inhibition of proliferation [29]. An article published in the Oncology Review Editorial in emphasized the importance of using spheroids as a tool because "such a model of three-dimensional growth should bring a better understanding of the role of intercellular adhesion in dictating cellular fate" [29].

2.4.3. Molecular gradients in 3D culture. The composition of ECM and cells residing within is directly responsible for the accumulation of chemicals over time. Most gradients, such as oxygen and nutrient gradients, may be measured and analyzed. For some regulatory molecules such as epidermal

www.manaraa.com

growth factor (EGF) and other cytokines, concentration gradients are difficult to measure because good input data is lacking. Work in this area has progressed due to phenomenological observations in biology that require qualitative analysis. One important finding is the idea that paracrine loops, once thought to be a hallmark of cancer, are now understood to be a cells' probing mechanism into the local environment. A cell uses autocrine loops to probe the microenvironment by sending out an array of molecules locally and analyzing the fraction of the signal returned. It is hypothesized that this aids the cell in sensing tissue boundaries [37].

Other molecular gradients exist including those of oxygen, glucose and other nutrients. Tumor spheroids develop significant chemical gradients in cultures between 200 and 500 μm, with a secondary region of necrosis present in the center of spheroids greater than 500 μm. It would appear that low levels of oxygen and glucose present in the central region should be the lead cause of necrosis, as initially hypothesized. Experimental evidence suggests that these assumptions may not be true and that the concentration gradient for glucose itself is rather minimal [38]. However, another hypothesis is that the necrotic region develops naturally due to force balances and a gradual reduction of cell density occurring as a result of surface tension and stabilization factors [39]. Regardless, this functional hierarchy of cells closely reflects the *in vivo* situation

www.manaraa.com

of actively cycling tumor cells adjacent to capillaries while the inner region of cells become quiescent and die through apoptosis or necrosis [40], although quiescence is not a consequence of hypoxia [38]. There is no single, definitive factor leading to necrosis i.e. hypoxia, lack of nutrients, catabolites or hydronium ions creating a toxic environment.

One important feature of the spheroid model lies in its ability to metabolically adapt the central, necrotic cells to maintain intracellular homeostasis in response to stresses created from gradients [40]. Many features of cellular physiology are affected by these gradients such as proliferative and functional features, cellular RNA and protein expression, the distribution and function of biologically active molecules, and their penetration. All of these factors lead to response to treatment [4, 40-42].

In order to control the delivery of oxygen and reduce gradients, many different culture systems have been created. One design includes cell-culture dishes with a semipermeable membrane. The membrane elevates cells near the air-medium interface so they may be perfused in a region of higher oxygen concentration both from above and below. There are also many different bioreactors including membrane-based, hollow-fiber, rotating drum, and perfusion bioreactors designed to combat these problems. The pros and cons of each will be discussed further in section *2.6 3D Culture Techniques and Analytical*

www.manaraa.com

Challenges. However, most of these systems are designed for creating masses of cells instead of finely controlled and reproducible 3D spheroids such as those created in this study.

2.4.4. Mechanical and chemical properties unique to spheroids. Just as in any three dimensional tissue, concentration gradients can exist for any soluble molecule consumed or produced by a spheroid. The two main competing factors influencing gradients are diffusion and convection. Both mechanisms affect all types of molecules, but typically diffusion dominates in smaller molecules, and convection, or bulk transport, dominates the dispersion of larger biomolecules. There are two ways established concentration gradients may affect the cell or tissue. First, cells in different regions of the 3D tissue may behave differently due to unique conditions experienced by each microenvironment as the result of the summation of numerous concentration profiles. 3D spheroid cultures therefore become a convenient way to study the changes along these gradients because of their spherical geometry. Secondly, gradient dependent cell responses such as migration may occur which are important for modeling tissue organization and metastasis [7].

Concentration profiles may be modeled mathematically by Fickian diffusion. The mass transport equation, governing the relationship, is a balance

www.manaraa.com

of diffusive transport and tissue consumption. The resulting differential balance is

$$\boldsymbol{Q = D\frac{d^2C}{dx^2}}, \qquad \textit{(Equation 2.1)}$$

where C is the concentration of the molecule in question, x is the distance from point of interest to the tissue surface, and Q is the volumetric consumption rate by the tissue. Using zero order consumption, $\boldsymbol{rate = k[C]^0}$, the solution becomes:

$$\boldsymbol{\frac{C}{C_0} = 1 - \phi^2\left[\left(\frac{x}{L}\right) - \frac{1}{2}\left(\frac{x}{L}\right)^2\right]}, \qquad \textit{(Equation 2.2)}$$

where C_0 designates surface concentration, L is the distance of diffusion and ϕ is the Thiele modulus. The Thiele modulus is a dimensionless coefficient which describes how tissue thickness, cell density (i.e. nutrient consumption rate), and surface concentration affect the resulting concentration profile as follows:

$$\boldsymbol{\phi^2 = \frac{reaction\ rate}{diffusion\ rate} = \frac{L^2Q}{C_0D}}. \qquad \textit{(Equation 2.3)}$$

For $\phi = 1$, the solution is $\frac{C}{C_0} = \frac{1}{2}$, which means the concentration of the molecule in question at the surface of the tissue is half of what it was at the source (C_0, L=0). For $\phi > 1$, significant concentration profiles develop within the tissue [7].

The most important nutrient gradient to consider is oxygen, as it is rapidly depleted due to its low solubility in culture medium. It may also be depleted in areas of high cell density due to large consumption rates. Gradients of glucose

www.manaraa.com

and amino acids are close to negligible due to their high concentrations and solubilities [43]. Oxygen gradients affect cells in multiple ways. In addition to respiration, local oxygen concentrations regulate cellular redox states and affect signaling pathways. Under high oxygen concentrations, these signaling pathways may create reactive oxygen species linked directly to DNA damage [44].

High oxygen concentrations also are toxic to many cells [44]. Significant oxygen gradients develop in tissues with high cell density and aggregates greater than 250 μm in diameter. This may occur in aggregates of epithelial cells and islets behaving normally, but also in various tumor cells. However, in stromal tissues which are more loosely packed only small, relatively insignificant gradients occur. Additionally, it should be noted that even in a 2D monolayer culture, concentrations develop if the medium is unstirred. At a distance just 2 mm under the surface of the culture medium, the oxygen concentration drops between 50 and 90%, based on the density of culture and consequently the rate of oxygen consumption. Conversely, low oxygen concentrations may promote the differentiation of stem cells leading to further changes in the local microenvironment [45].

pH gradients also play a role in spheroid metabolism and are interrelated with oxygen gradients. Although, both types of gradients are heterogeneous in

www.manaraa.com

shape with respect to the radial axis of the spheroid, there is no direct relationship between pH and oxygen concentration at the local level. However, strong correlations were found between mean pH and pO2 profiles [46]. Other studies looked to find differences between spheroids of various cell lines. It was found that the quotient of ΔpO2/ΔpH was consistent across all spheroids of a given cell line. Faster growing spheroids tended to have higher quotients such as those formed with human colon carcinoma cells (HT29). Low quotient spheroids, such as those formed with grade IV glioblastoma cells (U-118 MG), were found to produce about 3 times as much lactate and consume 3 times less oxygen than HT29 spheroids. This result highlights differences in metabolism between types of spheroids [47].

One molecule known to create specific engineering challenges in 3D cultures is protein regulator molecules. Protein regulator molecules have a more difficult time diffusing through a 3D spheroid culture. For this reason, molecules such as epidermal growth factor (EGF) are often added to culture media in concentrations well above their dissociation constant, K_d [mol] [7]. This constant is a measure of a receptor's affinity for its ligand and is the concentration necessary to achieve 50% of receptor binding. Biochemically, this is important as a strong relationship between ligand concentration, dissociation constant and biochemical activation is present. EGF binds to epidermal growth factor receptor

www.manaraa.com

(EGFR) and the complex is internalized, removing the receptor from the membrane to inside the cell where it can no longer "sense" EGF. Therefore, in order to achieve a relevant concentration of EGF in the center of a 3D culture, one must create a higher than normal concentration (>K_d) at the periphery of the tissue causing many receptors to be bound and internalized. Consequences are still unclear, but likely outcomes are receptor downregulation and ligand depletion.

www.manaraa.com

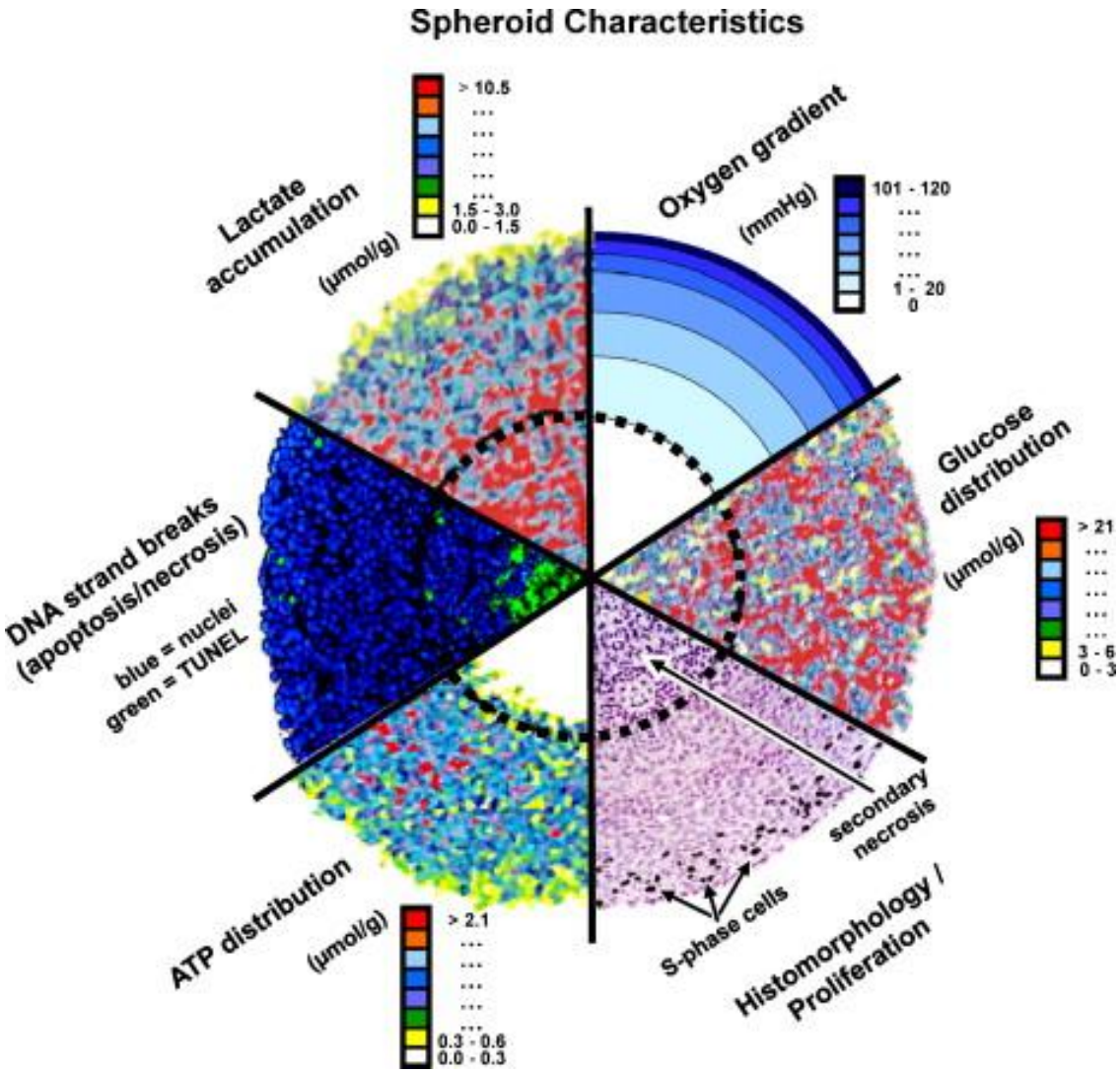

Figure 2. Spheroid gradient characteristics**.** The image reproduces a defined 3D structure and uniform geometry of a spheroid alongside multiple assays showing molecular gradients present. Reproduced from Hirschhaeuser et al. Multicellular tumor spheroids: An underestimated tool is catching up again (2010).

2.4.5. Thoughts for the future. Recreating identically the mechanical properties of the *in vivo* environment for testing purposes may not be necessary. In the case of scaffolds for wound-healing and regeneration, the job is simply to provide support and a reservoir of cells to facilitate natural processes. Often it is

www.manaraa.com

adequate to create scaffolds with geometries toleranced to tens or hundreds of microns, and then allow biology to do the rest [7]. In addition to the spatial distribution of cells on a scaffold, its chemical properties and composition may be controlled to more closely represent the natural environment.

When engineering the mechanical and chemical environment in a physiologically relevant way, what amount of precision is necessary? Is it adequate to simply create some of the structures found *in vivo*, couple them with the dominant cues, and to allow biology to do the rest? For example, cells secrete their own ECM and growth factors to impact and control tissue synthesis and organization. The tissue engineering *in vitro* model may only need to produce an environment suitable enough for deposited cells to take over and turn the artificial niche into a more natural one for studying biology. In this way, the power of biology is used for its own study. Only time and further research in tissue engineering and regenerative medicine may fully answer these questions.

2.5. Why 3D Culture?

"Keeping in mind the fundamental differences between monolayers and spheroids with regard to cellular sensitivity to various treatment modalities, tumor spheroids should be mandatory models in applied cancer research, for example in major programs for drug screening and development" [29]. Two dimensional monolayer culture appears to be an adequate environment for a

www.manaraa.com

very select few number of cell types accustomed to growing as multilayered sheets *in vivo*. Although, even in this scenario, cellular adherence to artificial substrates fails to reproduce the native environment. A true basement membrane, along with vasculature, is lacking. For example, epithelial cells such as keratinocytes and corneal epithelial cells may be adequately modeled *in vitro* in this manner [48]. Almost all other cell types should benefit from a culture and study in a more realistic environment.

Scientists have long understood how removing cells from the *in vivo* environment changes many important variables while also inducing atypical conditions. Even though the cell is the most fundamental repeating structure in biology, the functional unit of tissue is recognized as cells plus ECM [19]. Unique properties emerge from the synergistic effects of cells interacting with the ECM to form tissues, as discussed in *2.4*. For this reason, improving drug development requires studying the effect of compounds on tissues as a system, a methodology proven to be more indicative of the *in vivo* response. Properties such as specialized cell-cell contacts, polarized morphology and attachment to underlying basement membrane help comprise the normal functions of a tissue. These functions are essential for proliferation, differentiation, survival and secretion, and may aid in drug resistance [49]. The goal of 3D culture is to produce the most *in vivo*-like structures possible to more accurately predict drug

www.manaraa.com

response. By including 3D culture into the drug development process, this technique can bridge-the-gap between simplistic *in vitro* 2D analysis and more complex animal models of disease. Implications include rapidly increasing the speed of drug screening to potentially save large sums of money, and the ability to create more effective, less toxic therapeutic regimens [1].

Experts in cell biology believe that 3D culture is a basic necessity for the development of therapeutics, a natural stepping stone before turning to whole-animal studies [4]. Unfortunately, the use of rodent models is driven not by predictive capacity and scientific reasoning, but by regulatory and legal requirements, as well as strong clinical tradition. By maintaining a large number of rodent models, the overall predictive power is increased. No single model has substantial predictive power alone. Since the cost of drug development increases significantly at the rodent model stage, screening out poor candidates with cell-based models early in the process has been a long-standing strategy. Improving the power and capacity of these cell-based models to eliminate toxic and nonfunctional compounds could effectively streamline the entire process. Cell-based approaches will remain an important part of the process as they are low cost, take less time and use intact cells as a good representation of living patients. Cell-based approaches are important because they capture responses not observed in rodent models. Multicellular tumor spheroid cultures are an ideal

www.manaraa.com

testing platform of intermediate complexity, fitting logically between monolayer culture and *in vivo* animal systems.

Testing potential drug candidates should involve the most natural *in vivo* representation possible with respect to the spatial arrangement between cells and ECM, the resulting interactions, and other biological factors which influence the microenvironment. Three dimensional culture techniques have been used by the biomedical community in studying organogenesis and tumor progression since the first half of the 20th century. Today, it is well known that 3D culture is highly superior because it can restore biochemical and morphological features lost through 2D monolayer and suspension techniques. Unfortunately, the full potential of 3D culture has been ignored until recently. Supporting research in 3D culture technology, the National Cancer Institute has developed a program called Signatures of the Cancer Cell and its Microenvironment. It awards $40 million per year for research aiming to increase understanding of the relationship between microenvironment and tumor pathology. During this program, 3D culture will be emphasized in hopes of making its use more widespread in the scientific community [4]. Seemingly, it does not make sense to study organs and tissues using a homogenous cell population as is often employed in 2D culture. 3D tissues do a better job of mimicking the complex structures and relationships of vessels, nerves and stroma, and can do so while incorporating the numerous

www.manaraa.com

cell types present to the *in vivo* situation which are known to modulate each other.

2.5.1. Elucidation power of spheroids through biological mechanisms.

Spheroids are widely used in biology for their ability to provide a 3D *in vitro* model to study proliferation, death, differentiation and metabolism of tumor cells in response to radiotherapy or chemotherapy. It is also believed that including spheroids in high-throughput analyses during the drug delivery pipeline could greatly expedite the process of developing new therapeutics. Generating spheroids takes 24-48 hours, potentially longer depending on cell line, and creates cultures with homogeneous sizes, morphologies, and a specific regionally based pattern of cells. This pattern includes cells at different points in the cell cycle with regards to growth and arrest. It consists of a stratification of proliferating cells at the rim of the spheroid, and hypoxic, necrotic cells in the core of the tissue, with a region in between of quiescent cells [50]. These differential cell cycle states are also realized when observing *in vivo* tumor pathology.

However, most cell types require cues from an environment that is similar enough to the native 3D arrangement in order to respond in a physiologically relevant way. Adding a third dimension to cell culture allows cells to receive external mechanical inputs for cell adhesion and attachment in all planes. This

www.manaraa.com

affects integrin ligation, cell contraction and intracellular signaling, all of which are important to the life of a tissue and rooted in the ECM [51]. Spheroids make a great tool for probing cell-cell and cell-matrix interactions through tissue-based mechanistic assays because they replicate a specific cellular niche. They have assisted the investigations of biologists in elucidating the roles played by adhesion molecules in tumor pathology [52].

The third dimension also allows chemical signals to affect the cell in a more natural way. For instance, the 3D matrix binds important molecules such as growth factors and enzymes. Normally in a tissue, these molecules occur in gradients which may not be present in 2D, eliciting specific cellular responses. Evidence has also shown that the 3D environment may be necessary to study remodeling events, such as epithelial acinar duct formation, occurring over longer-length time scales [19].

Just like with nutrients such as oxygen, treating cultures with a chemotherapeutic drug creates a concentration gradient between the central and peripheral regions of the spheroid [53]. *In vivo* tumors develop similar gradients due to poor drug uptake by the tumor or poor distribution within the tumor. The rate of diffusion into tumors is a clinically significant factor with respect to the efficacy of treatment [54]. As a result, basic pharmacokinetic features should be replicated in cell-based assays for optimal relevance.

www.manaraa.com

Spheroids have also been used as a tool to investigate cell-matrix interactions. Spheroids have played an important role in investigating a new immune-activation phenomenon called nemosis. Nemosis is programmed cell death in activated fibroblast spheroids without the normal apoptotic markers, but accompanied by the production of cyclooxygenase (COX) 2, proteinases and proinflammatory cyto- and chemokines [55]. Knockout studies, or those blocking fibronectin receptors, have shown that nemosis is initiated by integrin-fibronectin binding and regulates fibrocyte spheroid formation [52].

Other novel proteins, such as the gap junction proteins connexins and pannexins, have been studied using spheroids. Spheroid studies using the C6 glioma cell line have shown the ratio of Panx1 to Panx2 proteins determines the degree of packing of cell aggregates. In addition to recapitulating cell-cell interactions, spheroids also better represent morphogenetic movements such as tissue contraction and condensation [52].

2.5.2. Mechanism of drug action and culture environment have profound effect on resulting therapeutic capacity of drugs. There is a difference in resistance to apoptosis and chemotherapeutic drugs with spheroid cultures compared to monolayer cultures. This fact supports the hypothesis that differences in culture environment can affect how cells respond to drug treatments [1]. One specific study by Tung et al. [56] highlights how drug

www.manaraa.com

mechanism of action and the culture environment can have a profound effect on drug efficacy, and thus the resulting viability of remaining cultures. In the first study, 5-fluorouracil (5-FU) was applied to both 2D and 3D culture at the same concentration of 10 μM. 5-FU is a thymidylate synthase inhibitor which blocks the synthesis of pyrimidine and thymidine necessary for DNA replication. The overall effect is a reduction in cell proliferation. The drug reduced 2D cultures to only 5% viability after 96-hours of treatment while 3D cultures remained at 75% viability after identical treatment. It was concluded that the 3D spheroids were better able to resist the anti-proliferative effects of the 5-FU through multicellular tumor resistance. Multicellular tumor resistance reflects the intrinsic drug-resistant phenotype of most solid tumors, and it is the ability for a cluster of cells to better resist therapeutic attempts through limited drug penetration and a reduced number of proliferating cells as drug targets. Almost all conventional cytotoxic anticancer drugs are less effective at killing MTSC than monolayers of tumor cells [9].

Tirapazamine (TPZ), a hypoxia activated cytotoxin, was tested in an identical manner. In 2D culture, cell viability was reduced to 72% after 96-hours while in corresponding 3D cultures, viability was reduced to 40%. The opposite effect compared to 5-FU was observed as 2D cultures were more resistant to the drug. Since 3D spheroids generally have hypoxic cores due to limited oxygen

www.manaraa.com

diffusion, the finding of increased therapeutic efficacy in spheroid culture supports the mechanism of action. Up to 60% of *in vivo* solid tumors have hypoxic regions within their structure, further supporting the use 3D spheroid models as testing platforms in drug development, and showing how this region can be used as a drug target. The study highlights how culture methods can drastically alter the effect of a drug on cells. It also shows that 3D cultures are not necessarily more resistant to all drugs, and drug resistance is a combination of the specific drug and the cellular environment where its effects take place [56]. Furthermore, the study highlights how a potential drug candidate may be screened out early in the development process if only tested in 2D, thus emphasizing the importance of testing drugs in the more realistic 3D environment.

Differences between 2D and 3D culture were noted in SKBR-3 cells which overexpress the oncogene HER2 [57]. Cells grown as spheroids using the forced-floating p-HEMA-coated plate method had HER2 homodimers form [58]. In 2D culture, the same cells formed HER2 heterodimers with HER3. Further differences in 3D culture included reduced epidermal growth factor receptor (EGFR); enhanced phosphorylation of HER2, HER3 and EGFR; and the downregulation of activated protein kinase B, an important protein in metabolism, apoptosis, proliferation, transcription and migration. Additionally,

www.manaraa.com

it was shown that trastuzumab has a significantly differing effect on cells grown in 2D versus 3D. Trastuzumab is a monoclonal antibody used to treat breast cancer which binds the overexpressed HER2 receptor. The drug leads to cell arrest during the G1 phase of mitosis and reduces cell proliferation. The study showed that proliferation was reduced by 48% in spheroids but only 16% in monolayer culture, suggesting differences in signaling patterns between the two tissue architectures, specifically, altered phosphoinositide 3-kinase (PI3K) and mitogen-activated protein kinase (MAPK) signaling [40].

Further examples of differing results in 2D versus 3D have been noted. Li et al. showed that MCF10A cells (fibrocystic, non-malignant breast cells) cultured in 3D exhibited a higher resistance to doxorubicin, a drug which inhibits the unwinding of DNA for transcription, compared to those grown in 2D. Cell lines SA87 (brain derived, metastatic breast cancer), NCI-H460 (large cell lung cancer) and H460M (metastatically derived from pleural effusion, large cell lung cancer) grown in 3D all have higher resistance to 5-FU and doxorubicin than those in 2D [59]. Finally, 3D cultured MCF-7 cells (breast cancer) treated with tamoxifen are more viable than those grown in 2D and treated with the same drug concentrations [60].

Culture environment also strongly influences the resulting cellular physiology. One study showed that culturing breast-epithelial cells on ECM

www.manaraa.com

restored some mammary-specific gene expression not observed during culture on standard polystyrene plates [33]. Another study [19] showed how the organization of the microenvironment could contribute to different cellular responses due to the same biological factor. In the study, both non-malignant and malignant HMT-3522 breast cells were grown in 3D using Matrigel. The non-malignant cells organized normally, forming polarized acini as observed *in vivo*. The cancerous cells formed disorganized, loose aggregates. Both populations were then treated with antibodies against β-integrin, an overexpressed surface receptor in the malignant cells. β-integrin caused apoptosis in the healthy cells; however, it caused an apparent reversal of phenotype in the cancerous cells back to the normal cell type. This occurred to the point that the two cell populations became indistinguishable. The experiment was repeated in 2D and this result was not observed. This showed how extracellular cues can affect cellular phenotype. It was hypothesized that cellular phenotype was dominant over genotype in this situation [18].

2.5.3. Additional applications of MCTS cultures. Spheroids are often spoken of in terms of developing cancer therapeutic drugs; however, the technology is applicable to other disease states and treatment modalities. Spheroids have been employed as models for a myriad of other therapeutic techniques including radiotherapy, chemotherapy, radioimmunotherapy, cell-

www.manaraa.com

and antibody-based immunotherapy, hyperthermia, gene therapy, and photodynamic treatment. Additionally, MTSC have been routinely employed in studies regarding the microenvironmental regulation of proliferation, viability, energy metabolism, nutrient metabolism, invasion, cell-cell interactions, and ECM composition [61].

Further uses for spheroids include the investigation of specific host-tumor cell interactions including evasion as well as evaluations of normal cell injury due to tumor cell presence. A technique used to study this involves growing spheroids and placing them on monolayers of confluent fibroblasts or endothelial cells with an underlying ECM. Conversely, fibroblast spheroids may be cultured in tumor cell suspensions to study tumor cell invasion/migration. This technique also allows for the study of tumor cells which do not form spheroids on their own. Incubating tumor or stromal spheroids with immune cell suspensions likewise allows the study of immunological response *in vitro* such as migration, differentiation and activation. These co-culture systems have been employed to study the interactions between cancer cells and their cellular environment, and have the potential to be applied to study simplified versions of any biological system. It may be ideal to use these advanced types of systems to gain a fuller understanding of drug sensitivity as well as to screen for agents that affect the host-tumor interaction.

www.manaraa.com

2.5.4. The rationale for MCTS in HTS approaches. While generating and maintaining 3D cultures may be more labor-intensive than 2D, the tradeoff is that incorporating spheroids into *in vitro* drug efficacy and toxicity testing will probably yield more accurate versus monolayer culture alone. 3D culture will allow the more rapid selection of lead compounds worth pursuing [1].

The rationale for using spheroids can be lumped into four specific points. The first is that spheroids recreate the morphological, functional and mass transport phenomena of similar tissues *in vivo*. Specifically, cells in spheroids restore the observed *in vivo* differentiation pattern for several weeks of culture. This recapitulation of *in vivo* function is not only relevant for modeling the pathophysiology, but also is useful for studying penetration, binding, and bioactivity of drugs. The morphology of spheroids is close to that of experimental tumors in mice and natural tumors in humans, before neovascularization occurs [3].

Secondly, MCTS approximate the growth kinetics and microenvironment of avascular tumor nodules, micrometastases and intervascular regions of large solid tumors. The Gompertz equation is used to predict tumor growth *in vivo* [4]. It has been shown, along with multiple other biologically based mathematical models, to analogously predict spheroid growth *in vitro*. MCTS exhibit two to three distinct morphologies, depending on the diameter of the culture. A

www.manaraa.com

proliferation gradient is observed which begins with a layer of proliferating cells at the periphery, a layer of cell-cycle-arrested cells stuck in the G0 phase in the middle, and in cultures larger than 400-500 μm a hypoxic, necrotic core. As previously discussed, oxygen and nutrient gradients develop inward, while catabolite gradients outward, just as observed in tumors *in vivo*. These play important roles in how tumors respond to drugs.

The third benefit of using spheroids is that their spherical symmetry allows for a direct comparison between structure and function. Specifically, microenvironmental gradients, biomarkers and cell morphologies can be spatially correlated to changes in cellular physiology. There are three ways that this can be very useful. The first advantage is that assays can be directly related to a specific region of the spheroid either through *in situ* histological analysis or by harvesting cell subpopulations for further analysis. Additionally, the spherical symmetry allows for simplistic, theoretical predictions to radiation response, drug penetration and binding, or the interpretation of typical studies such as cell viability and proliferation. The third advantage is the ability to create large groups of individual, identical cultures as long as a homogenous cell population is used with constant external culture conditions [4].

Finally, spheroid culture can be adapted to allow for the coculture of multiple types of cells. Of most interest is the coculture of cancer cells along with

www.manaraa.com

one or more noncancerous stromal cell types such as fibroblasts, endothelial cells or hematopoietic cells. Co-culture systems have not been extensively characterized but have the potential to be even more relevant than single-cell-line systems. Understanding the relationship between healthy and cancerous cell populations is necessary in the study of disease progression, as these relationships play important roles in tumor pathology.

The chief scientific officer of a major pharmaceutical company was quoted saying, "In 10 years, anyone trying to use 2D analyses to get relevant and novel biological information will find it difficult to get funded." A paper published in Critical Reviews of Oncology in 2000 stated, "Notably, spheroids seem to be the appropriate model to study novel hypoxic markers, targeted therapy, multicellular mediated drug resistance, and heavy ion irradiation" [3]. Researchers and academics at the precipice of new technology have been waiting patiently for this technology to become widely adopted, and now is finally the time where we are beginning to see such shifts in biomedical research take place.

www.manaraa.com

2.6. Three Dimensional Culture Techniques

MCTS were originally adapted to cancer diagnostics in the early 1970s by Sutherland and associates [62]. This model is still used throughout research labs and has the most potential for application to HTS systems in anticancer drug development. MCTS have greatly contributed to our knowledge of cellular response and, possibly more profoundly, have allowed researchers to understand the "microenvironmental regulation of tumor cell physiology" [63]. Initial methodologies for generating spheroids involved placing a drop of cell suspension on the lid of a standard Petri dish and then inverting it. The lid, with up to a few individual drops, was placed back on the dish containing a liquid such as media or PBS to keep the environment humid during culture. Since the 1970s, methodologies have rapidly improved alongside developments in electronics and control systems, micro manufacturing, and chemical engineering.

2.6.1. Forced-floating methods. Spheroid formation may be induced by preventing a solution of cells from attaching to the culture vessel surface leading to self-adherence. Forced-floating methods prevent this by modifying the surface, thus promoting cell-cell contacts and spheroid organization [64]. Some coatings used to prevent attachment include 0.5% poly-2-hydroxyethyl methacrylate (poly-HEMA) and 1.5% agarose. The benefits of this method are reproducibility, uniform spheroid size as a result of identical initial cell

www.manaraa.com

concentrations, compatibility with high-throughput testing, and the ability for long-term culture. However, some drawbacks include the time it takes to coat the plates, costs of purchasing pre-coated plates, and difficulties with media changes [42, 50, 65].

2.6.2. Agitation-based approaches. There are two main types of agitation-based approaches: (i) spinner flask bioreactors [65, 66] and (ii) rotational culture systems [67]. Both systems involve placing a cell suspension in a large vessel which is kept in motion through stirring or rotation of the vessel walls. In this way, cells do not adhere to the vessel walls, but come together through cell-cell interactions [68].

Spinner flask bioreactors are employed as a simple technique which can create many spheroids very rapidly. This technique excels in long-term growth of cultures requiring media changes. The motion of the flask is also thought to aid in mass transport of nutrients and wastes. One particular drawback of this culture technique includes the exertion of shear forces on aggregates due to constant stirring. This may elicit mechanochemical responses and affect the natural physiology of the cells. Additionally, spinner flasks use large amounts of media and produce a broad range of spheroid sizes requiring the difficult task of sorting the resulting tissues for drug screening assays [64]. To combat this issue, spheroids may be initially formed using a forced floating or hanging drop

www.manaraa.com

technique and then placed in the spinner flask for long term culture [69]. This method ensures a more uniform spheroid size and allows for environmental control over nutrient and oxygen exchange during extended culture. However, the spheroids still must be replated into 96- or 384-well plates for assay, creating many extra steps in the process.

Instead of using a stirring mechanism, rotating cell culture bioreactors function by rotating the culture container itself. These were initially developed by NASA in 1992 to mimic microgravity and exert low shear forces in culture. The culture chamber, which screws onto a rotator, is slowly rotated along its horizontal axis. The result is the ability to keep cultures in the center of the vessel, preventing attachment to walls. Low shear forces are the main advantage of this system. The speed of rotation can be increased over time as spheroids become larger and fall through the medium faster. Further advantages and limitations are the same as in spinner flask bioreactors; rotating bioreactors use simple methods, enable the production of a large number of spheroids, and allow for long-term culture with easy media changes with little ability to control the size of spheroids generated.

2.6.3. Microfluidic cell culture platforms. Most microfluidic culture systems only support 2D culture which is arguably no longer relevant [70]. However, some researchers described a system allowing 3D culture with

www.manaraa.com

collagen-matrix interactions and imaging in three spatial dimensions. The system works by passing a cell suspension through an array of micropillars. Cells aggregate inside the pillars and the spheroids are perfused by the passing culture medium. Once a certain level of 3D structure is achieved, collagen is passed through the system fixing the cell structures and allowing for cell-matrix interactions [71]. The benefits of this system include the ability to work with high-throughput testing, high content analysis due to imaging capabilities, and minimizing reagent volume. Limitations of the system include the lack of opportunity to retrieve and extensively characterize the spheroids formed [71]. Other similar systems like this exist and may ultimately challenge currently employed systems as they allow for a finer degree of control over nutrient and drug administration while allowing for imaging without intermediate steps.

2.6.4. Matrices, scaffolds and the tumor fragment model. Since cells naturally interact with ECM *in vivo*, it stands to reason that 3D culturing methods allowing cell-ECM interactions would better reproduce the natural cellular environment. Matrigel is a commercially available ECM derived from Engelbreth-Holm-Swarm (EHS) mouse tumor cell basement membrane proteins. EHS is composed of collagen IV, laminin, perlecan, entactin, matrix metalloproteinase-2 and growth factors [72]. Cells growing in ECM interact with

www.manaraa.com

each other in a natural, three dimensional way and develop similar structures to those observed *in vivo*.

There are two notable ways to apply extracted ECM into the generation of spheroid cultures. The first method involves incorporating ECM into a gel and embedding the cells within the gel for growth. The second method involves creating a similar gel, but instead growing the cells on top of it after micropatterning the surface of the gel with an array of shallow wells [73]. Although generating spheroids in this manner does take comparatively more work, it is still relatively easy and thus commonly employed. Some additional drawbacks include differences in composition between batches of ECM, costs of purchasing the ECM itself, non-uniform spheroid sizes generated, and the fact that the spheroids end up unevenly distributed throughout the ECM if grown within. The micropatterning technique works to alleviate this problem by creating spheroids at specified locations [74].

Biodegradable materials such as collagen, laminin and alginate may be fabricated into scaffolds with optimal chemistries and geometries for cell growth and metabolism. Engineering scaffolds is a hybrid field of chemical and tissue engineering. Cells seeded onto scaffolds may migrate between fibers, attach to fibers, and form 3D cellular structures in the interstitial spaces between fibers [75]. These materials may be designed to incorporate ECM molecules that can be

www.manaraa.com

released to the cells over the degradation life of the scaffold, creating *in vivo*-like cues [76]. The most important parameter to control is the scaffold's porosity as it dictates cellular attachment and mass transfer properties [77, 78]. Ultimately, the scaffold facilitates the growth of the cells into 3D structures which resemble the geometry of the scaffold after it has degraded and been eliminated . Therefore, scaffolds are not typically used to make spheroids, but other three-dimensional shapes.

The tumor fragment spheroid model involves mechanically dissociating tumor specimens and using the resulting fragments to generate spheroids. The cellular components of the resulting fragment spheroids often vary greatly. Some spheroids may contain predominantly tumor cells while others are comprised of a majority of stromal elements (i.e. fibroblasts, pericytes, etc.) [79].

2.6.5. Hanging drop method. The hanging drop method uses a small aliquot (40 μL for the Insphero system) of cell suspension pipetted into 96 bottomless wells in a three-part culture plate. The wells allow the droplets to attach via surface tension and hang from the central of the three plates (*Figure 3*).

www.manaraa.com

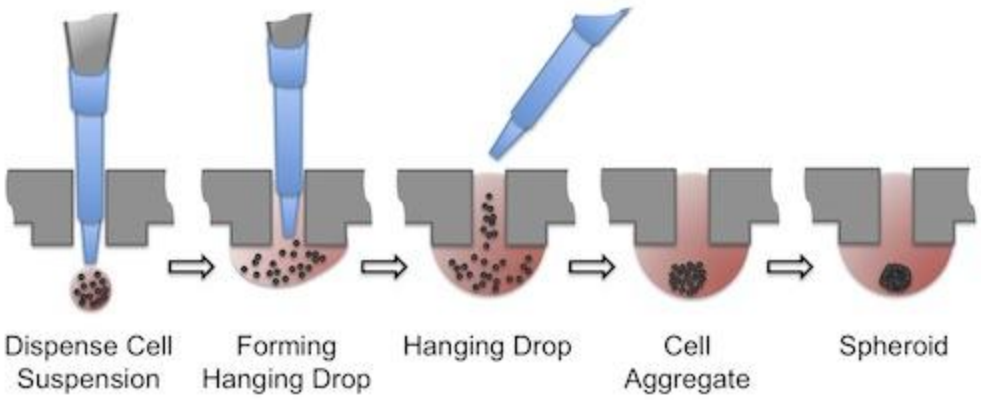

Figure 3. Spheroid formation in hanging drop plate (3D biomatrix https://3dbiomatrix.com/features/)

The cells eventually collect and form a dense, tightly-packed spheroid in the bottom of the droplet near the air-liquid interface. If allowed to culture for long enough, the cells may even proliferate after forming a spheroid. Droplets are kept moist by an absorbent pad hydrated with sterile water housed in the bottom part of the plate. The third piece is a top plate, covering the apparatus and keeping the system moist. The InSphero Gravity-PLUS system may then be wrapped in parafilm to further prevent droplet evaporation. In addition to losing water, droplet evaporation creates a dangerous hypertonic environment for the cells. The InSphero system also comes with a non-adhesive Gravity-TRAP plate used to transfer spheroids from hanging drop to standard 96-well culture. This plate allows for further cultures or assays to be performed.

www.manaraa.com

Hanging drop culture is relatively simple and has been reported to generate uniform spheroids at a rate close to 100% for many different cell lines. Further benefits of the system include easy media changes and uniform 3D tissues with low variability in sizes. Klem et al [80] reported that the tissues created were patho- and physiologically relevant because spheroids created their own ECM and displayed high levels of tissue organization characterized through histology. The major drawback of this technology is the droplet size is limited to approximately 50 μL and creating tissues larger than 1000 μm in diameter proves difficult.

2.6.6. Limitations of spheroids. One limit of spheroids is the time necessary to expand cells, form spheroids, and have them grow to sufficient size to develop the three typical morphological regions as observed *in vivo*. Typically, it takes 2 to 4 weeks for an aggregation of a few cells to reach the point of usefulness. This process may be expedited by forcing a large number of cells to aggregate; however, this technique will still require a few days to one week for proliferative and viability gradients to develop. There are many ways available that can expedite this process including 3D culturing with other reagents such as methylcellulose and collagen. This has reduced spheroid formation from one week to as low as two days in our lab. However, the exact roles of these components are unknown. One paper reported that collagen and agarose

www.manaraa.com

networks may reduce natural cellular motility through steric forces in spheroid models, but this occurred with increased agarose concentration, not collagen concentration alone [81]. Fortunately, time to complete assays on 3D cultures would be similar to assays involving monolayers as the screening of drugs can be done once spheroids are formed. It would appear that the limitation of added setup time would be outweighed significantly by superior and more relevant resulting information. Another limitation of spheroids is the lack of standardized, well characterized tumor models for use in conducting studies.

Finally, the 3D spheroid model will never replace animal testing in the drug-development process. Even though tumor, and even normal cell models made with spheroids provide a myriad of new information, the system lacks the complexity necessary for complete study and understanding of absorption, distribution, metabolism, elimination and toxicity [4]. The use of 3D models for studying toxicity of potential compounds is speculative and there is no current way to extrapolate data from spheroids to *in vivo* systems; animal testing is not going away. Microfluidic devices which incorporate and link spheroids and other three dimensional tissues made from cells of different organs may help to elucidate the relationships between such organs that are not possible in today's 3D culture.

www.manaraa.com

2.7. Analytical Challenges of Spheroids

A major reason that promising 3D culture systems used in basic and applied tumor biology are not used for drug screening and other HTS systems is the lack of simple, controlled techniques for rapid, standardized assays. The current trend in 3D culture technology has emphasized increasing the throughput of simple culture systems without regard for *in vivo* relevance of the resulting cultures or their ability to be easily analyzed. Increasing throughput without regard to the resulting *in vitro* biological data recreates flawed logic in a similar way that monolayer culture hoped to replicate the *in vivo* environment.

Analytical protocols for high-throughput analysis of 2D cell-based screens are well-established and documented. Unfortunately, translating methods directly to 3D setups is not straightforward as new analytical challenges are created in these systems [52]. For example, in the lactate dehydrogenase (LDH) cell viability assay, the volume of culture causes a linger in fluorescent signal making the data unreliable [82]. Additionally, the necrotic core of 3D cultures naturally creates an increase in lactate dehydrogenase enzyme which is not necessarily indicative of the viability of cultures. Analyses such as screening for cell viability and spheroid size can be done using automated processes. But beyond screening for clinically relevant drugs, limitations are encountered when testing for drug toxicity as drug penetration, contact-dependent multidrug

www.manaraa.com

resistance, and oxygen deficiency create difficulties with the cultures themselves. These are the mechanisms we hope to capture with HTS 3D spheroid histological analysis. Furthermore, mechanistic assays which explain differences between 2D and 3D are not readily available, and the ones that work in 2D do not always work when analyzing 3D cultures. For example, researchers had difficulty determining the therapeutic range of irinotecan, a new anticancer drug, on colorectal cancer spheroids because the proper assays were not available [42]. Others hypothesized that showing increased osteogenic properties of human MSC/HUVEC spheroid cocultures would not be possible with current assay technology [52]. As previously mentioned, controlling spheroid size, and therefore the presence of hypoxia in the core, can create additional variables which become essential parts of the assay. In addition to researching 3D culture methodologies, the field must tune the respective 2D assays into the third dimension to make the technology truly useful for drug development.

Confocal microscopy is a technique that can be successfully applied to imaging spheroids. Its benefits include imaging spheroids up to 320 μm in depth and the ability to apply live/dead and some other fluorescent stains [83]. As early as 1995, the potential for imaging spheroids was realized, and the ability to image and separate spheroids based on the three standard regions of proliferation around the rim, quiescence in the center, and necrotic cells in the

www.manaraa.com

core was described [84]. The work showed how cells begin developing a necrotic core around 400 +/- 25 μm in size. However, this technique is not as easily as applicable to HTS as the different layers of cells may pose an analytical challenge as the structures interfere with chemiluminescent signals. Confocal microscopy is also tedious and expensive with a single unit costing over $500,000, and more if customized to suit HTS analysis. Therefore, this technology is not available in many standard biology research labs. Other researchers are currently developing confocal microscopy methods for rapidly measuring drug penetration into individual spheroids with optimism that the technique may be applied to HTS technologies [4]. This type of assay would show which compounds to have the ability to penetrate a tumor-like tissue.

Finally, should data be successfully collected in a HTS set up, such a large amount of information will require new dedicated systems for processing and analysis. Fenema et al. reported in 2013 that "to the best of our knowledge, high-throughput confocal structural analysis of 3D cultures has not yet been established" [52]. Some assays that have been reported to work include gene and protein analysis using multiplex PCR and multiplex ELISAs, respectively. Thus, the paramount future challenges of spheroid HTS are assay development and analysis of large quantities of data.

www.manaraa.com

Many assays that are currently used for 2D cultures could be easily adapted to 3D, such as those used for cytotoxicity, proliferation, drug binding, apoptosis, and ATP level [4]. However, the response would be an average of all cells in the aggregate and information on differential, regionally based responses would be lost. Standard phase-contrast microscopy in conjunction with computer image analysis could be used to acquire such information such as the growth and shrinkage of spheroids. Furthermore, commercial automated microscopy systems could be fitted to rapidly analyze the effects of drugs on spheroid growth. Again, these techniques would unfortunately sacrifice many of the advantages of the 3D spheroid model.

The creation of new methods to stain individual, intact spheroids and measure the extent of necrosis should be simple and straightforward from a histological perspective, but using common methods would be time consuming and inefficient due to processing only a handful of spheroids at a time. This data would provide information on the effects of drugs on the viability of the inner cells of the spheroid. Furthermore, other stains may be applied to measure apoptosis, proliferation and various metabolic markers that could be read by an image-screening system applicable to HTS format. Additionally, assays to measure differing responses of subpopulations of cells (proliferating, quiescent, hypoxic) would significantly enhance the usefulness of MCTS [85].

www.manaraa.com

MCTS may allow *in vitro* assays for penetration and binding of drugs in the 3D format. Assays done on monolayer cultures that were difficult to adapt to HTS, may now be performed in HTS format. By monitoring drug binding in individual tumor and host spheroids, a system may be developed to measure the differing binding properties of new compounds. Dosing spheroids at different times would allow for the kinetic analysis of drugs and even the calculation of their effective diffusion coefficients [4].

Horman et al showed how entire plates of spheroids could be quantified by optical imaging for rapid, multicolor, whole-well quantification. However, it still remains to be seen how spheroids can be analyzed through histology in high-throughput manners [86].

A recent method for toxicological and biomedical testing uses a bioelectrical microarray system to calculate the impedance of *in vitro* tissues. This method may be applicable to spheroid culture providing information on the drug activity in the spheroids. Unfortunately this test would calculate the average effect on the population of cells in the spheroid, losing any regionally based differential responses [87]. Regionally based information is the main advantage of sectioning and staining spheroids in a microarray system.

Clearly advancements in assay technology are necessary to bring spheroid systems into the HTS arena. Investing in these technologies should be seen as

www.manaraa.com

worthwhile as there are clear advantages to HTS spheroid systems. Screening protocols for measuring cytotoxicity, growth arrest and viability could be developed rather simply and applied to high-throughput systems. Assays that work in homogenous cell population spheroids would also be applicable to co-culture systems [4].

www.manaraa.com

Chapter 3

Methodology for the Creation of a 96-Spheroid Microarray for High-Throughput Analysis

3.1. Microarray Mold Creation

A positive, aluminum mold was designed in SolidWorks™ (*Figure 4*) and machined using a 5º, 1/32" tapered end mill (Ford) via a computer numeric controlled (CNC) process. An end mill with 5º tapers was selected in order to provide relief during mold release. The aluminum part was used to create a polydimethylsiloxane (PDMS) negative mold along with the Slygard ® 184 Silicone Elastomer Kit. A 10:1 base to curing agent ratio was used per the kit's instruction manual. This mixture was poured over the positive mold into a Petri dish and allowed to cure in the oven at 65ºC for a period of 24 hours. *Figure 4a* is a three view drawing of the positive mold. *Figure 4b* shows the final PDMS negative mold created from the aluminum part.

www.manaraa.com

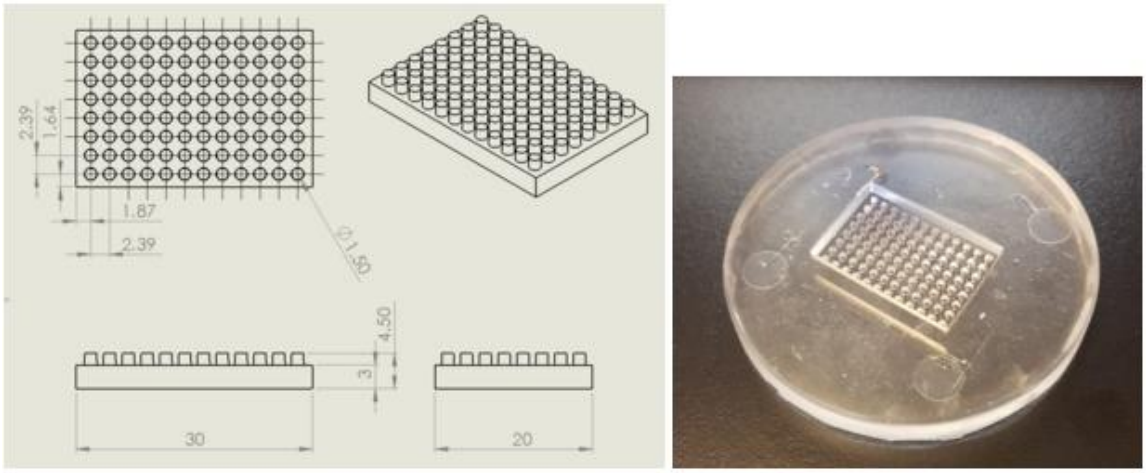

Figure 4. Microarray PDMS mold fabrication. (a) Three-view CAD drawing of negative mold in millimeters (left). (b) Final PDMS mold to be used in microarray formation (right).

3.2. Culture of HTB-126 Breast Cancer Spheroids

Breast cancer cell line Hs 578T (ATCC® HTB-126™) was cultured with the following media: Dulbecco's Modified Eagle's Medium (Gibco) supplemented with 10% fetal bovine serum (Gibco), 1% Penicillin-Streptomycin (Gibco), and 0.01 mg/mL insulin isolated from bovine pancreas (Sigma-Aldrich). Cells were incubated at 37ºC with 5% CO_2 and grown in 75 cm^2 adherent bottom culture flasks (Sarstedt) until confluence. Media changes were made every other day. Cell harvesting began with aspiration of the entire culture medium volume followed by the addition of 5 mL of 0.25% Trypsin-ETDA (Gibco) which was incubated for 5 minutes at standard cell growth conditions. The trypsinized cell solution was collected, combined with 5 mL of fresh culture media, and

www.manaraa.com

centrifuged at 1500 rpm for 5 min. The supernatant was discarded and the cell pellet was washed twice with 1 mL fresh culture media. Breast cancer cells were resuspended in fresh media supplemented with 0.24% methylcellulose prepared as described in [88] and seeded at densities of 20,000 to 35,000 cells/spheroid using the GravityPLUS™ hanging drop system (InSphero). Cell densities were verified using manual hemocytometry (Hausser Scientific). The densities are equivalent to cell concentrations of 5.00×10^5 to 8.75×10^5 cells/mL for 40 μL drops. The cell suspension was allowed a period of 3 days for 3D spheroid formation with one media change after 48 hours. Culture plates were wrapped in parafilm to prevent media evaporation. Additionally, 15 mL deionized water was added to the bottom chamber of the GravityPLUS™ system along with the humidifying pad provided by Insphero. To change the media, a 12-channel multipipettor (Fisherbrand Elite) was used. 15 μm of media was removed, discarded, and replaced with 17 μm of fresh media containing methylcellulose. A slight excess was added to make up for evaporated media. The spheroids were then transferred into GravityTRAP™ plates (InSphero) as follows. Each well of the GravityTRAP™ plate was pre wetted with 70 μL of 4% paraformaldehyde (PFA) (Electron Microscopy Sciences). The bottom piece of the 96-well hanging drop GravityPLUS™ plate was removed and replaced with a GravityTRAP™ plate. Once attached, 70 μL of PBS (Gibco) was added to each

www.manaraa.com

well of the GravityPLUS™ plate using the multipipettor causing spheroid cultures to fall into the GravityTRAP™ plate below. After allowing 2 hours for fixation, spheroids were embedded in the microarray or stored long-term at room temperature.

3.3. 3D Microarray Formation

The microarray mold (F*igure 4b & Figure 5*) was filled with deionized water. Microbubbles were removed using a 1 mL pipette and the microjetting technique as described in *Figure 5a*. Removal of all microbubbles in microwells is imperative for successful microarray formation. Breast cancer cell spheroids were then placed individually into the microwells using a 1 mL pipette and the gravitational transfer technique described in *Figure 5b*. Arrays of 24- (4x6) and 96-spheroids (8x12) were created using the 96-well mold. Arrays of 24-spheroids were created using the central wells of the mold. Spheroid placement was verified using inverted light microscopy (Carl Zeiss Axio Vert.A1). For each 24-spheroid microarray created, 10 random spheroids were imaged and their diameters were measured using the Zen 2 Imaging Suite (Zeiss) prior to agarose infiltration for the study of processing effects.

Verified arrays were ready for agarose infiltration. This commenced with the removal of water from the top, rectangular portion of the mold, leaving water only in the micropillars (*Figure 5c*). UltraPure™ agarose (Invitrogen) was added

www.manaraa.com

to DI H_2O at 3% (w/v) and boiled in the microwave until completely dissolved. The molten agarose was then allowed to cool to 80ºC on the lab bench. The mold was infiltrated with agarose by pipette into the corner of the mold at a rate of approximately 0.1 mL/sec (*Figure 5d*). Larger flow rates may disturb spheroids in microwells, causing them to become displaced. Enough agarose should be added to form a slight meniscus above the height of the open mold. A tissue cassette (Symport) was then mounted as shown in *Figure 6* and additional agarose was added to the top. The infiltrated mold was placed in the oven at 65ºC for 5 minutes to allow complete diffusion of water and agarose. The microarray assembly was then removed and cooled at room temperature for 30-60 minutes. The agarose transitions from a clear liquid to a slightly translucent, cloudy white, firm gel when solidification is finished. The cassette may now be removed carefully from the PDMS mold, bringing with it the spheroids embedded in the micropillars of the array. Removal must be done slowly, carefully and in a straight and even manner away from the mold so as to limit pillar fracture.

www.manaraa.com

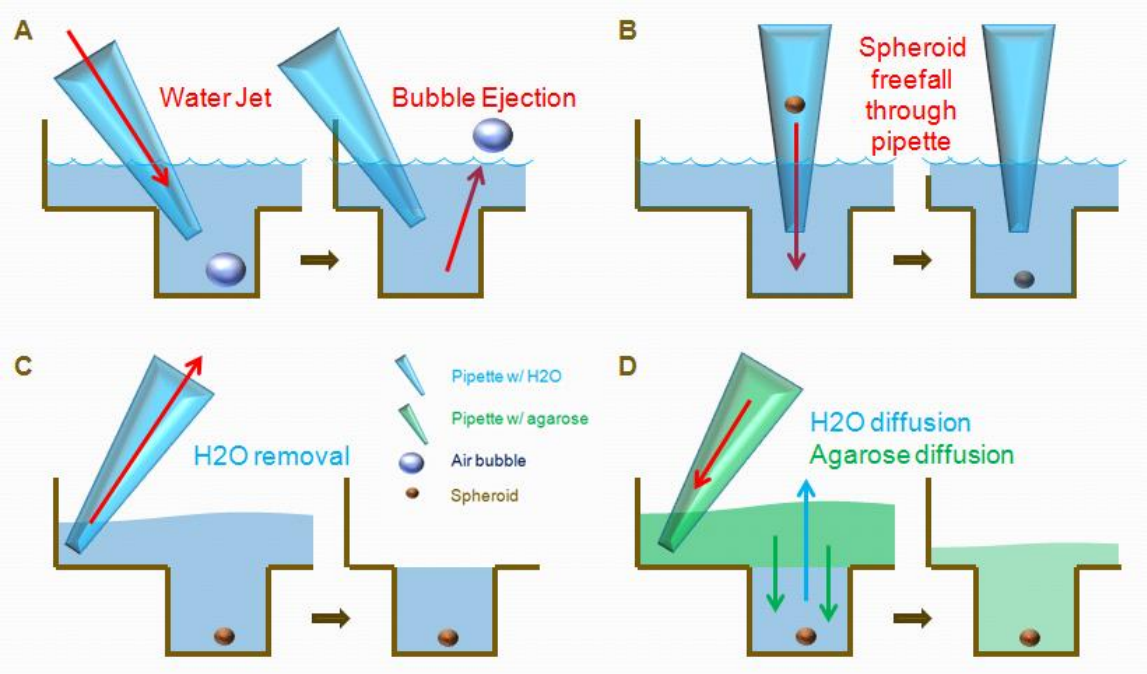

Figure 5. Microarray fabrication (with spheroids). Once the mold is completely filled with deionized water, the pipette push button is fully depressed, and then the tip of the pipette is submerged into the water in the mold. Once submerged, the push button is released, bringing up water into the pipette tip. The pushbutton is then depressed and released repeatedly while the tip is aimed at submerged microbubbles. The resulting microjets will cause the successful ejection of all microbubbles. (b) After successful removal of all microbubbles, spheroids are ready to be transferred into individual wells. Note, the pipette tip should be trimmed down approximately 1mm to increase its working diameter for spheroid transfer. Spheroids are pipetted from GravityTRAP plates into a 1 mL pipette tip at a working volume of 0.1 mL. The spheroid is visually located in the pipette tip, which is held horizontally. Once visualized, the pipette tip is touched to the bottom of a single well of the mold and turned vertically, allowing the spheroid to sink, due to gravity, through the volume of water in the pipette tip. The spheroid finally comes to rest in the bottom of the well after 10-20 seconds, depending on the spheroid diameter and density. After successful placement of all spheroids, the microarray is then centrifuged at 500 rpm for 5 minutes to remove any microbubbles created during spheroid placement. Additionally, this centrifugation step makes sure all spheroids are in contact with the bottom of the wells and in the same plane. (c) Water is removed from the top, rectangular portion of the mold by placing the pipette tip in the corner, and slowly pipetting water at a rate of approximately 0.1 mL/sec. Water is now present only in cylindrical microwells. (d) Agarose is slowly and carefully pipetted into the corner of the PDMS mold so as to not disturb the spheroids in the microwells. The agarose and water slowly diffuse together. This is enhanced by placing the assembly in the oven at 65ºC for 5 minutes, after addition of the tissue cassette. This is a critical step because it is very hard to work with the spheroids in

www.manaraa.com

agarose directly. Beginning with water and later adding the agarose allowed assembly of the arrays in an aqueous environment.

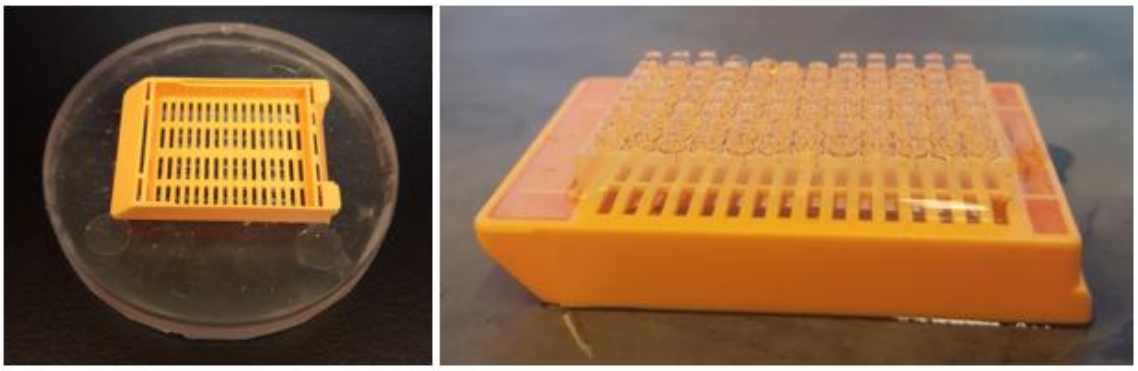

Figure 6. Cassette and completed microarray. (a) Cassette (orange) placement over microarray which occurs after agarose addition. Once placed, more agarose was added on top of the cassette to surround it with a continuous layer, securing the array for removal from the mold. (b) After the agarose has been allowed to cool, it is carefully removed from the mold, showing the finally assembly of the spheroids embedded in the microarray. Care must be taken to ensure no pillars become fractured as apparent in the top row of the image.

3.4. Paraffin Infiltration

The spheroid array, stabilized in agarose and physically fixed to a tissue cassette, was placed in a graded series of 100 mL ethanol, HistoClear (National Diagnostics) and paraffin (Fisher Histoplast LP) washes for 3 hours each on the shaker at 65ºC as follows in *Table 1*:

www.manaraa.com

Table 1

Paraffin infiltration procedure

	Solution	# of washes X duration
1	50% ethanol	1 X 3 hours
2	70% ethanol	1 X 3 hours
3	85% ethanol	1 X 3 hours
4	95% ethanol	1 X 3 hours
5	100% ethanol	3 X 3 hours
6	HistoClear (National Diagnostics)	3 X 3 hours
7	Paraffin (Fisher Histoplast LP)	5 X 3 hours

After processing, the array was placed in a cassette receiver filled with molten paraffin and allowed to cool to room temperature for solidification.

3.5. Histology of Spheroid Microarrays

Successful alignment of the mounted cassette with respect to the microtome blade is absolutely crucial so that all spheroids may appear on the same section. The alignment procedure used was as follows. First, it was assumed that previous steps used to create the microarray resulted in an array of spheroids that were parallel to the front surface of the tissue cassette. Now, the tissue cassette had to be aligned normally to the axis of forward translation in

www.manaraa.com

both the vertical and horizontal directions. Vertical alignment was done using the bubble level attached to the cassette receiver. This was completed first before horizontal alignment. For the horizontal alignment, a blank cassette was placed into the cassette receiver and the microtome blade was installed. The receiver was then adjusted using an iterative process which involved setting the angle, and using the wheel which allows for forward translation (without the slicing motion), to match the blade up to the blank cassette. The blade position was verified against the blank cassette at the cassette's superior and inferior edges as well as in between. Successful positioning was achieved when the blank cassette came into contact with the blade at exactly the same time during forward translation of the receiver. Visual verification of this contact was limited in exactness to approximately 50 um, which proved adequate for the study. After successful alignment of the blank cassette, the receiver was translated away from the blade, and the cassette containing the microarray was mounted. For the sake of the study, it was assumed that all cassettes were manufactured identically.

Slices were taken using a manual microtome (KEDEE KD-2258) at 20 um beginning at the tip of the microarray pillars and through the distance of the spheroids. The number of sections taken per block varied depending on spheroid diameter; however, generally a number of sections spanning a distance of [spheroid diameter]*150% were taken to insure that no spheroid samples were

www.manaraa.com

left unsliced. Sections were mounted onto adhesive microscope slides (Tru Scientific - TruBond 380) starting at the first appearance of agarose wells and concluded at the predetermined distance or once no more spheroids could be observed visually. The paraffin sections were then placed in the oven at 60ºC overnight to increase adherence to slides before the staining procedure.

Slides were deparaffinized, hydrated and stained with Hematoxylin and Eosin (H&E) as follows:

www.manaraa.com

Table 2

Slide deparaffinization and H&E staining procedure

	Solution	# of washes X duration
1	HistoClear	n X 15 minutes (until compete removal by visual inspection)
2	100% ethanol	2 X 5 minutes
3	95% ethanol	2 X 5 minutes
4	DI H_2O	2 X 5 minutes
5	Hematoxylin	1 X 10 seconds
6	DI H_2O	1 X 4 minutes
7	Bluing agent (VWR Bluing Agent RTU)	1 X 1 minute
8	DI H_2O	2 X 1 minutes
9	95% ethanol	1 X 30 seconds
10	Eosin	1 X 10 seconds
11	100% ethanol	1 X 1 minute
12	DI H_2O	1 X 1 minute
13	Coverslip with aqueous slide mount	indefinite

Fluoro-Gel with TES Buffer (Electron Microscopy Sciences) was used as the aqueous coverslipping agent.

www.manaraa.com

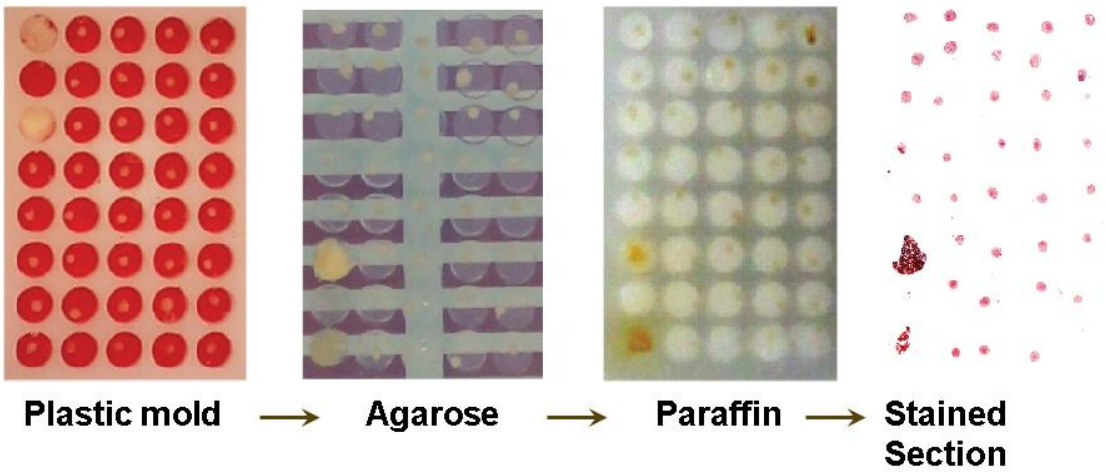

Figure 7. Process overview.

3.6. Results and Discussion

3.6.1. Optimization of methodologies. Each step of the process underwent iterative design beginning with mold creation. The first iteration of the positive mold (*Figure 4a*) was machined using an end mill with 1º of relief. It was soon realized that regardless of agarose concentration, it was difficult to remove the agarose/spheroid/cassette assembly from the mold without fracturing pillars. The part was re-machined with 5º of relief, greatly improving micropillar pullout to 90-95%.

Even though the literature contains some resources on breast cancer spheroid formation with cell line HTB-126, there were numerous engineering challenges associated with achieving successful culture and fixation in our

www.manaraa.com

laboratory. The first major problem was drop evaporation during 3D culture. This occurred predominantly in the drops along the outer rim of the culture plate even though it did effect all drops to a degree. To combat this problem, 2% agarose solution was placed in the top rim of the middle dish of the GravityPLUS™ system. Ultimately, this was not a great solution. When InSphero changed the design of the GravityPLUS™ in the summer of 2015, this approach was no longer feasible. Another attempt included hydrating the pad with sterile deionized water instead of PBS to increase the partial pressure of water in the chamber as the ions in the PBS act to trap the water to its liquid state. Water reduced drop evaporation but further improvement was necessary. Simply adding more culture medium to deficient drops was not adequate as this created a hypertonic cellular environment. The final solution was to use deionized water in the bottom hydration chamber and to wrap the culture dish in parafilm. This combination prevented drop evaporation and actually increased the size of the drops at times. Regardless, this was a key step in the successful culturing of spheroids.

Once drop volume was stabilized, the next difficulty was getting cells to consistently form dense spheroids instead of loose aggregates. We hypothesized aggregates did not fully come together because (a) over confluence during 2D culture created significant numbers of necrotic cells or (b) improper culture

www.manaraa.com

conditions did not promote aggregation. Now, some changes were made. Cells were consistently washed with PBS during each media change to remove dead or loosely adherent cells, and hanging-drop culture was performed with the addition of 0.24% methylcellulose. Additionally, cells were only cultured to approximately 90% confluence to avoid necrosis. These changes allowed for consistent spheroid production of over 80% (>75/96 spheroids), and on occasion >95%, per culture plate.

As previously mentioned, agarose concentrations were varied to determine the optimal concentration for maximizing the pullout of micropillars. As agarose concentration was increased, pillars formed more rigidly and were fractured less often. The competing mechanism was that increasing agarose concentration increased the viscosity of the gel. High viscosity agarose was difficult to work with especially as it cooled rapidly. The optimal concentration was experimentally determined using molds with no spheroids. It was found that at concentrations of 0.25, 0.50 and 0.75% the resulting gel was unable to properly harden for pullout. At concentrations of 1.0 and 1.5%, the gel was able to harden in many wells, but did not pull out consistently. Additionally, the water in wells around the outer rim of the mold did not mix sufficiently with incoming agarose, leading to increased fracture of edge micropillars during pullout. This was due to water accumulating around the outer rim of the mold

www.manaraa.com

as a result of surface tension. As agarose was added to the mold with spheroids, its effective concentration around the rim was reduced due to the presence of water. All concentrations above 1.5% tested (2.0, 3.0, 4.0%) consistently pulled out over 90% of pillars, with some successfully pulling out 100%. As a result we elected to begin using 2% agarose with molds housing spheroids.

The results of embedding spheroid microarrays with 2% agarose were hit-or-miss. Occasionally, pullout of >90% pillars was achieved. Often, as many as 50% of pillars failed to be removed. We hypothesized that a boundary layer of water was being created around the spheroid contributing to pillar fracture (*Figure 8*).

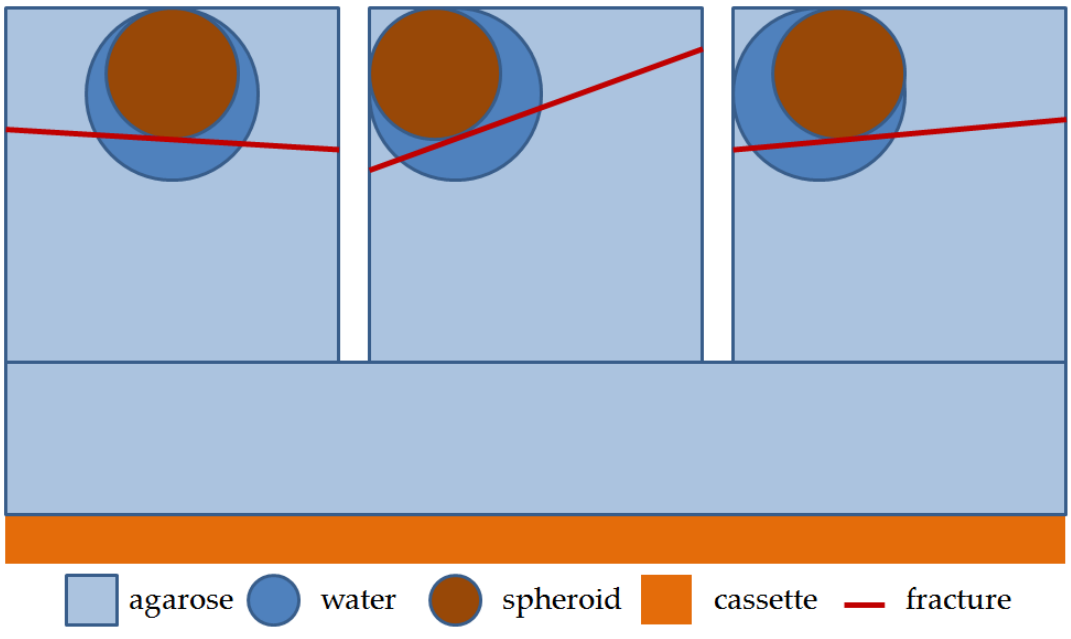

Figure 8. Hypothesized pillar fracturing mechanism.

www.manaraa.com

Evidence for this was seen in spheroids left behind in the mold as a result of fractured pillars. The agarose around these spheroids seemed unusually hydrated. Additionally, histology confirmed that agarose was not completely surrounding the spheroids. We also noted that this finding may have been due to spheroid shrinkage during the dehydration process. A gap could often be seen between the boundary layer of the spheroid and the agarose in successfully removed micropillars (*Figure 9*). To combat this, agarose concentration was increased to 3%. Additionally, after the addition of agarose and placement of the cassette, the assembly was incubated for 5 minutes in the oven at 65ºC to promote diffusion and slow cooling of the gel. These two changes allowed for consistent pullout of greater than 90% of micropillars. After successfully solving the problems of culture and microarray fabrication, processing and sectioning of the array was generally straightforward.

www.manaraa.com

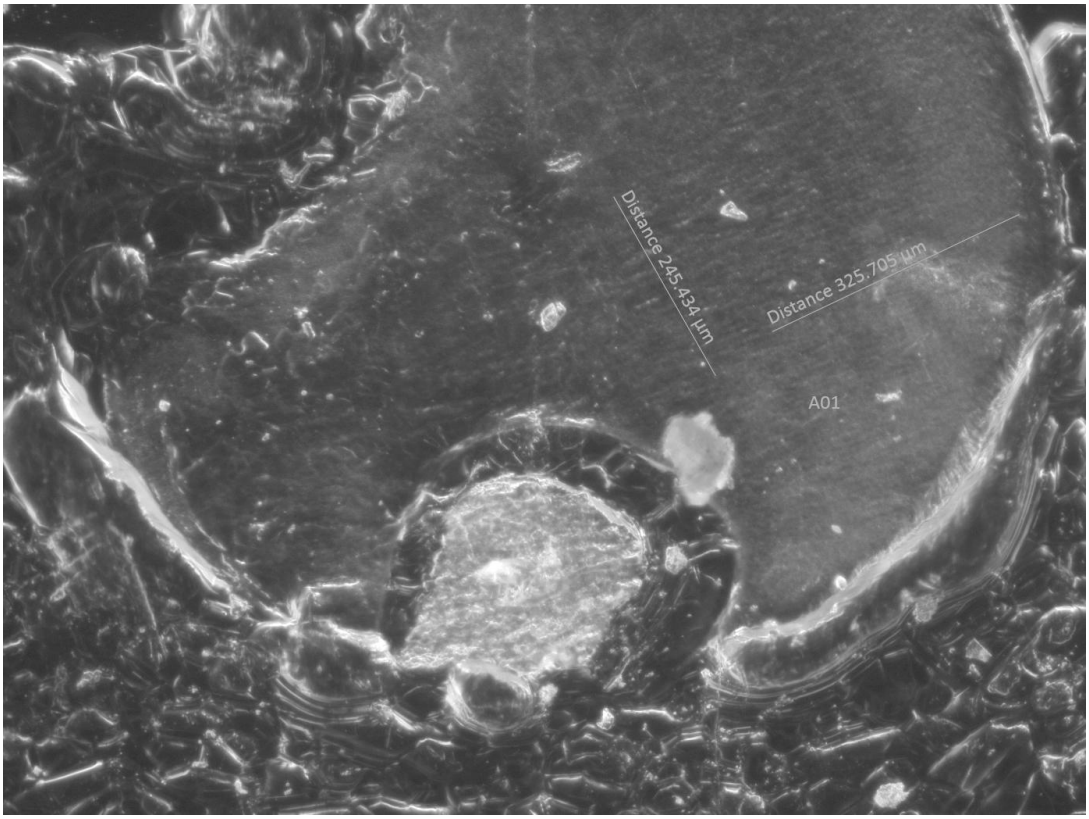

Figure 9. Image of sectioned spheroid showing a gap between the boundary layer of a spheroid and that of the agarose well.

3.6.2. Quantifying the effectiveness of the 24-spheroid block system.

The effectiveness of the system was first studied on array's of 24 spheroids (4x6). After sectioning each array, the best five slides were chosen for analysis. "Best" was experimentally determined to be as follows. First, ten random spheroids were imaged and measured before processing. Each spheroid was approximated as an ellipse with measurements taken for both the long and short axis of the spheroid. These were used to determine the "pre-processing average maximum area" of the spheroids for a given block. Maximum in this case refers to the

www.manaraa.com

section of a given spheroid having the largest cross-sectional area, as there could be 10 or more sections of an individual spheroid. After sectioning, each spheroid on each section was measured. Only spheroids with areas >25% of the pre-processing maximum average were considered successfully processed. The five sections with the greatest number of spheroids processed were considered the "best" and chosen for analysis. *Table 3* shows the results by block.

Table 3

24-block study overview

Block	Pre-processing average maximum area (stdev)	% recovered per section (out of 24)	Post-processing maximum area (stdev)
B12	1.855E5 μm² (2.213E4)	80.8% (19.4)	1.319E5 μm² (5.434E4)
B13	1.698E5 (2.014E4)	90.0% (21.6)	1.152E5 (3.869E4)
B15	1.299E5 (1.764E4)	79.2% (19.0)	9.416E4 (2.298E4)
B17	1.959E5 (1.418E4)	86.7% (20.8)	7.900E4 (2.025E4)

Statistical analysis was performed between the pre-processing average maximum area (n=40) and the post-processing average maximum area (n=37). The null hypothesis was that processing has no effect on the spheroid maximum area. The standard deviation of the post-processing group was determined to be

www.manaraa.com

7.021E3. Since the sample means were 1.728E5 (pre) and 1.312E5 (post), the Z-score was calculated to be 5.924 standard deviations away from the pre-processing mean. This correlates to p=1.594E-9 ≈ 0. Therefore, the null hypothesis must be rejected and we conclude that processing has a direct effect on spheroid area.

Leading hypotheses on the mechanisms effecting the system include spheroid shrinkage during dehydration through ethanol, and compression during sectioning. Shrinkage during dehydration is straightforward. As water is forced from cells in the spheroid and replaced with a less dense liquid, the structure naturally tends to contract, even after fixation. This mechanism may also account for the separation between the boundary layers of the spheroid and agarose as seen in *Figure 9*, as the spheroid and agarose may initially share a boundary layer until the spheroid is shrunk by dehydration and ripped away from the agarose. This theory would tend to discount the pillar fracturing mechanism hypothesis.

Compression during sectioning is less intuitive to a non-histologist. As a wax section is sliced very thin, on occasion the ribbon retrieved is shorter in distance than the width of the block (distance of the edge normal to the edge of the blade is under consideration). This results in shrinkage along the y-axis of the block as much as 5 or 10%. A finite element analysis results in each element

www.manaraa.com

being compressed this percentage along the y-axis, including the bits of tissue embedded within.

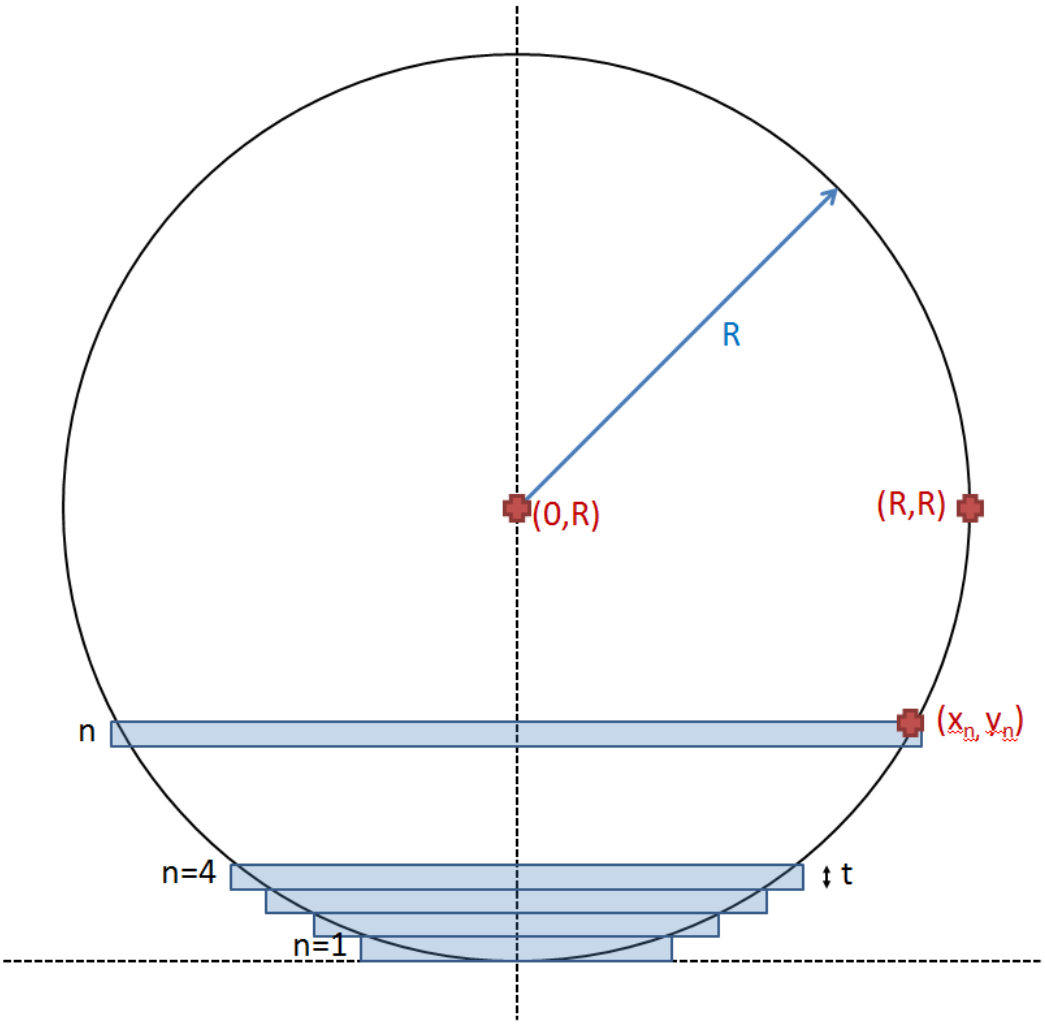

Figure 10. Spheroid sectioning geometry.

www.manaraa.com

Figure 10 is a diagram which represents n consecutive sections of a spheroid with radius, R at a section thickness, t. The equation along the edge of the circle between (0,0) and (R,R) is

$$\boldsymbol{x_n{}^2 + (y_n + R)^2 = R^2,} \quad \textbf{(Eq. 1)}$$

where

$$\boldsymbol{y_n = n\,t\,.} \quad \textbf{(Eq. 2)}$$

which simplifies to

$$\boldsymbol{x_n = \sqrt{R^2 - (n\,t + R)^2}\,.} \quad \textbf{(Eq. 3)}$$

The area of the resulting spheroid with radius $\boldsymbol{x_n}$ is

$$\boldsymbol{A_n = \pi\, x_n^2\,.} \quad \textbf{(Eq. 4)}$$

Equations 3 and 4 were used to calculate the radii and areas of optimal spheroids with a known radius, R, on consecutive sections. Note that combining *Equations 3 and 4* and eliminating constants results in the relationship,

$$\boldsymbol{A_n \propto x^2,} \quad \textbf{(Eq. 5)}$$

which will be important in figures displaying results of sectioning (*Figures 3.11-14*).

Figure 11 shows imaging of a single spheroid before processing (A) and on seven consecutive sections after histology (B-H) at 10x (scale bar, 100 μm). *Figure 12* shows 11 consecutive sections of a spheroid after histology in color at 20x.

www.manaraa.com

The scale bar is 50 μm. *Figure 13* shows eight sections from block 15 as viewed by the naked eye.

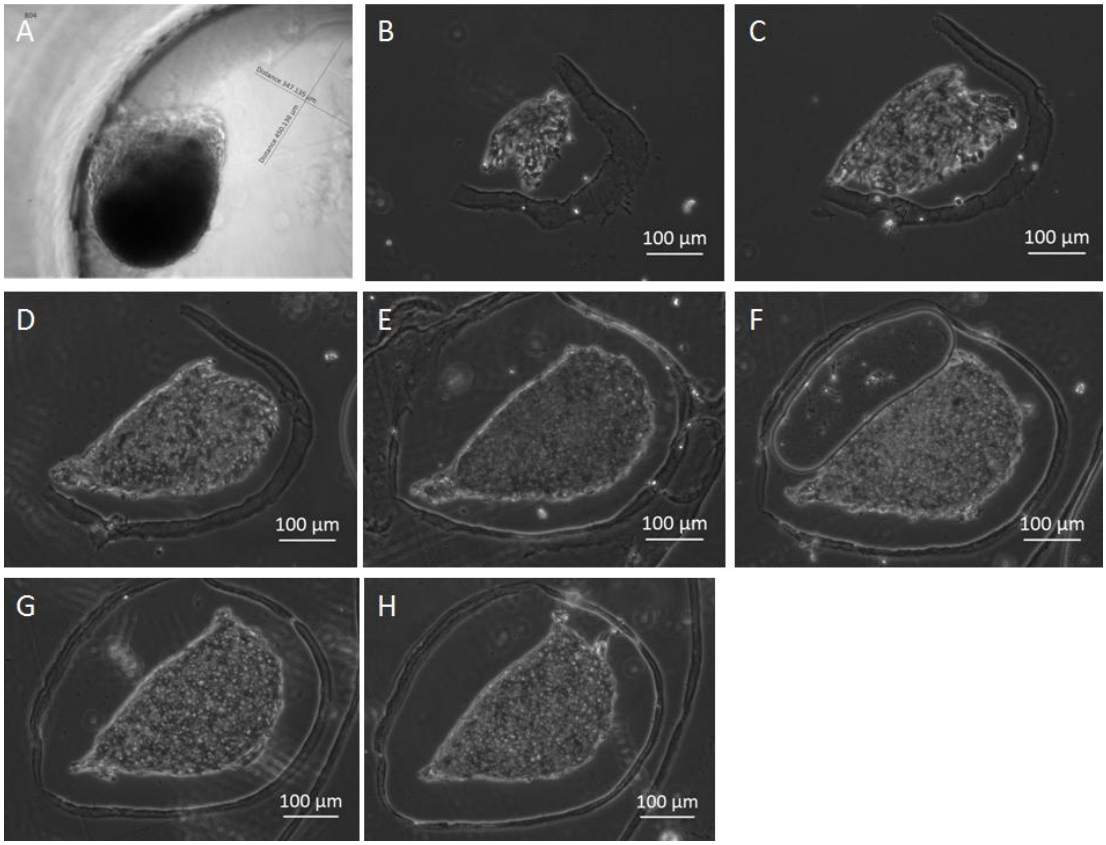

Figure 11. Spheroid pre- (A) and post-processing (B-H).

www.manaraa.com

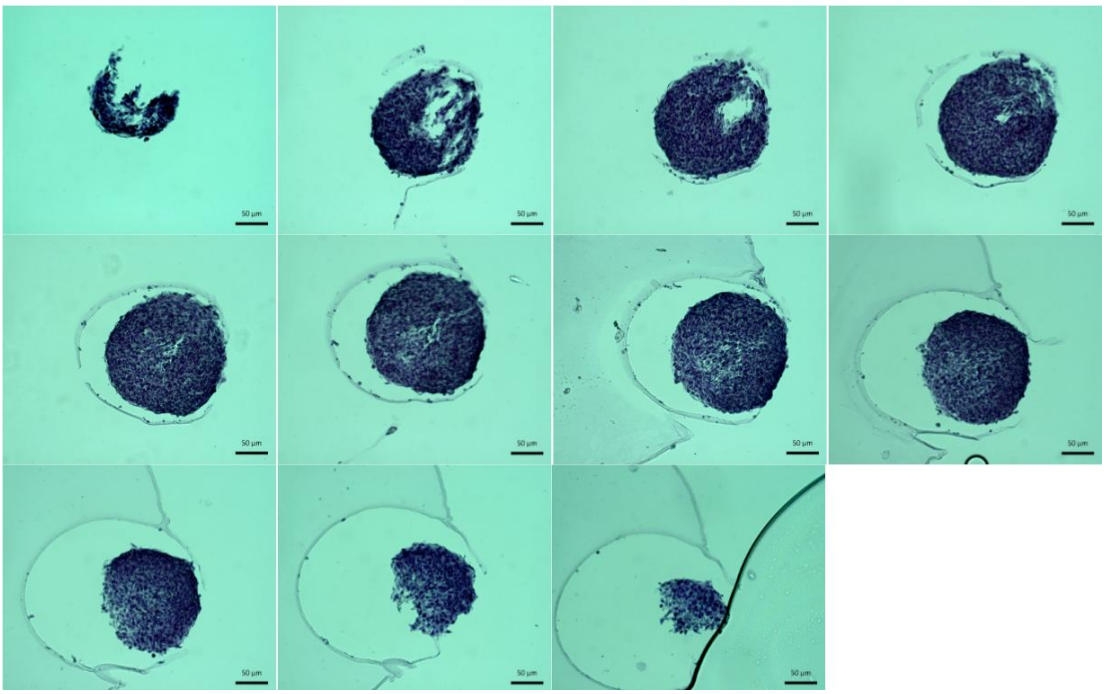

Figure 12. Eleven consecutive sections of a single spheroid after H&E staining at 20x.

www.manaraa.com

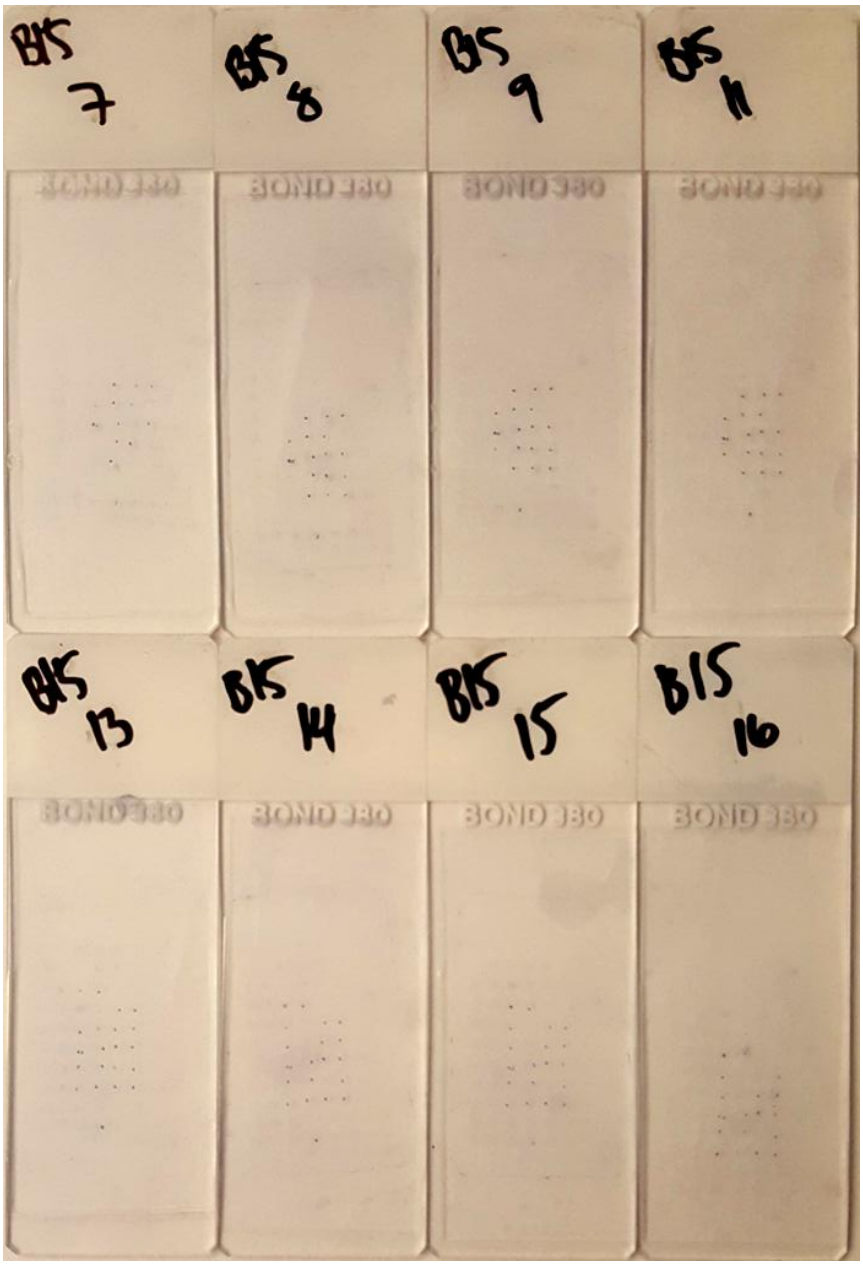

Figure 13. Eight sections from block 15 as viewed by the naked eye.

The same ten random spheroids were imaged and measured on each section as done for pre-processing measurements. Measurements taken were used to calculate the spheroid's area approximated as an ellipse. These areas

www.manaraa.com

were plotted against the section numbers. For block 15, the spheroids with largest area were centered to section number 9 in *Figure 14*. The other spheroids were normalized around section number 9 keeping intact the relative number of sections apart. The post-processing maximum areas were used for calculating column 4 of *Table 1*. The area of an optimal, spherical spheroid with diameter 350 μm was plotted for reference.

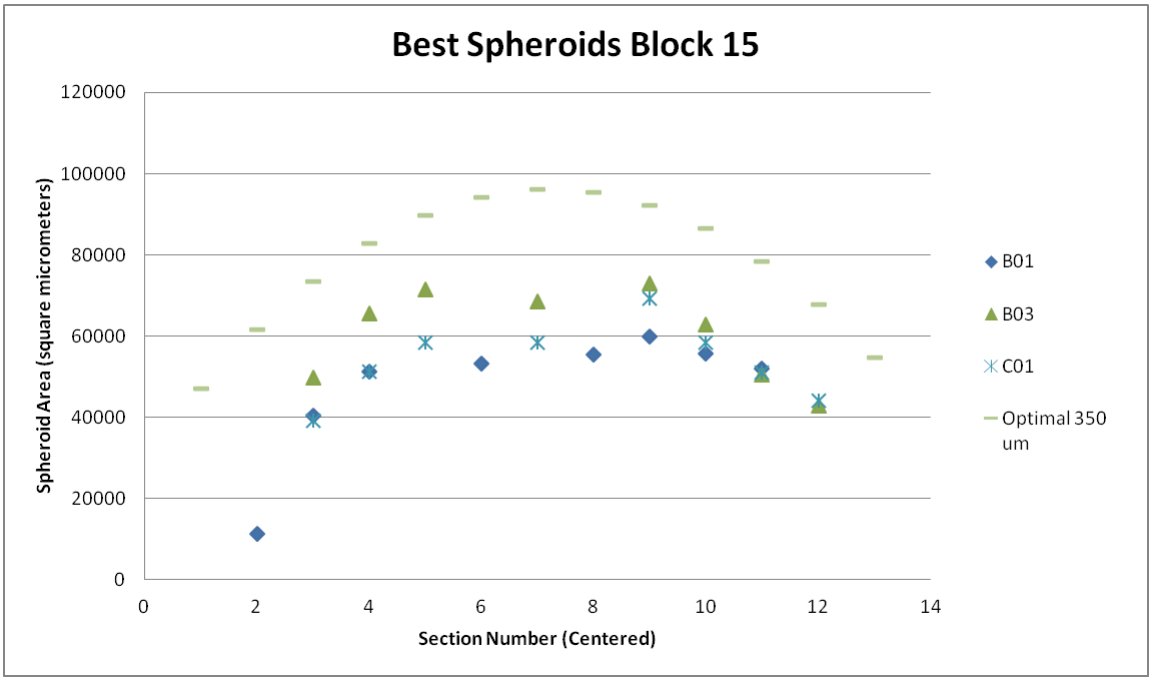

Figure 14. Three of the best spheroids from Block 15.

Figure 14 shows that spheroid area correlates well to the shape of the optimal spheroid curve for three different spheroids from block 15. Spheroid area increases as the center of the spheroid is approached during sectioning.

www.manaraa.com

Each section was taken at 20 μm; therefore, the total amount sectioned is equivalent to the product of section number and 20 μm. The eleven sections taken from number 2 to number 12 in *Figure 13* span a distance of 220 μm. The rationale for centering the maximum area secretions to section number 9 was to account for tilt and inconsistencies in spheroid diameter, allowing for better visualization of the trend across different spheroids in the group. In order to achieve all maximum spheroid diameters on a single section, the user is required to section the block with perfect 0º tilt[5] on both x- and y-axes. Additionally, initial spheroid diameters would have to be uniform with perfectly round geometries. Further complications include spheroids all evenly touching the bottom of the mold during agarose embedding; often some become dislodged by the incoming agarose and rest a short distance away from the tip of the micropillar. Due to these factors, it is unreasonable at this time to anticipate maximum area sections occurring on the same histological section as the variance in spheroid diameter is relatively high due to the nature of culturing biological samples. To combat this, the maximum area of each spheroid was determined by section number, and the rest of the data was normalized (shifted) to the this section. *Figure 15* shows 8 different spheroids processed from Block 15

[5] Tilt is further discussed in section 3.6.3 Tilt analysis.

www.manaraa.com

which appeared on at least 7 of 8 sections. The dashed line represents the polynomial order 2 fit of the optimal 350 μm spheroid scatter plot.

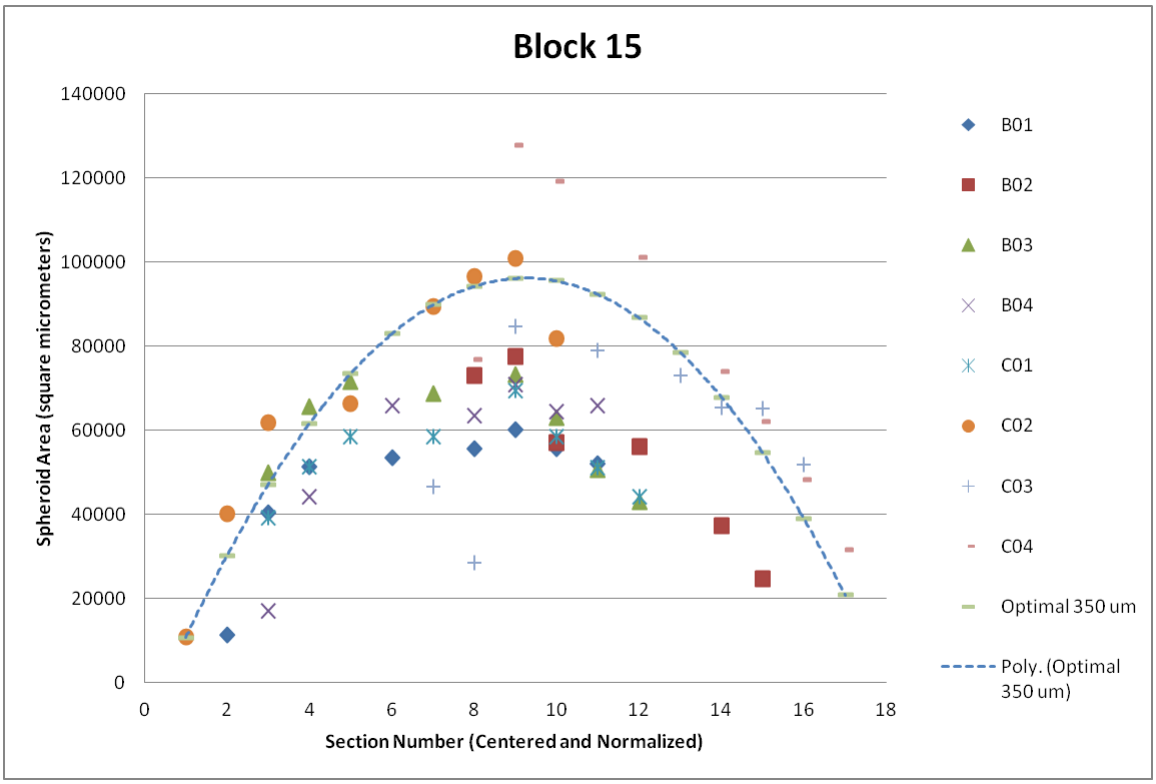

Figure 15. All spheroids from Block 15. Only spheroids appearing in at least 7/8 blocks shown.

Figure 16 is identical to *Figure 15* but contains additional polynomial curve fits of order two. R^2 values are displayed for reference. Of the eight spheroids tested from Block 15, only one showed a low correlation fit (C03, R^2=0.5281).

www.manaraa.com

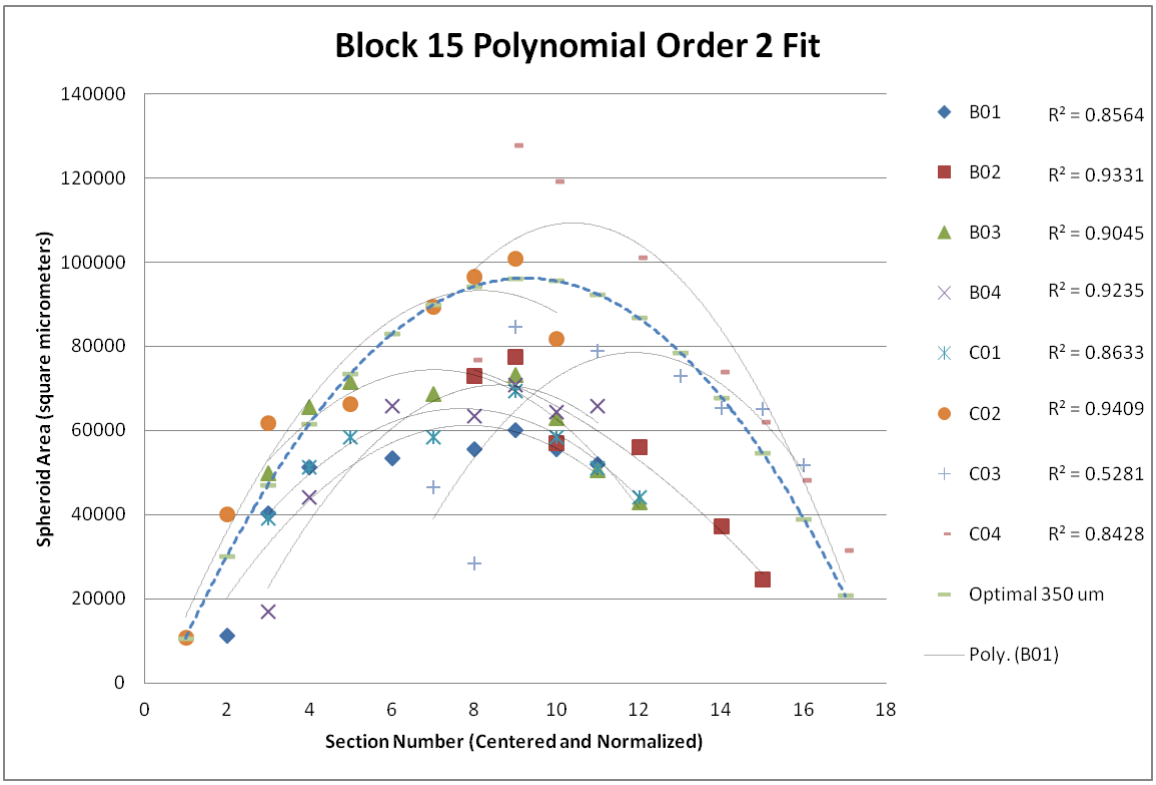

Figure 16. Spheroids from Block 15 with curve fitting data.

Curves were fit with a polynomial function of order 2 to match the geometrical relationship derived in *Equation 3.1*. This was done similarly in *Figure 17* for block 17.

www.manaraa.com

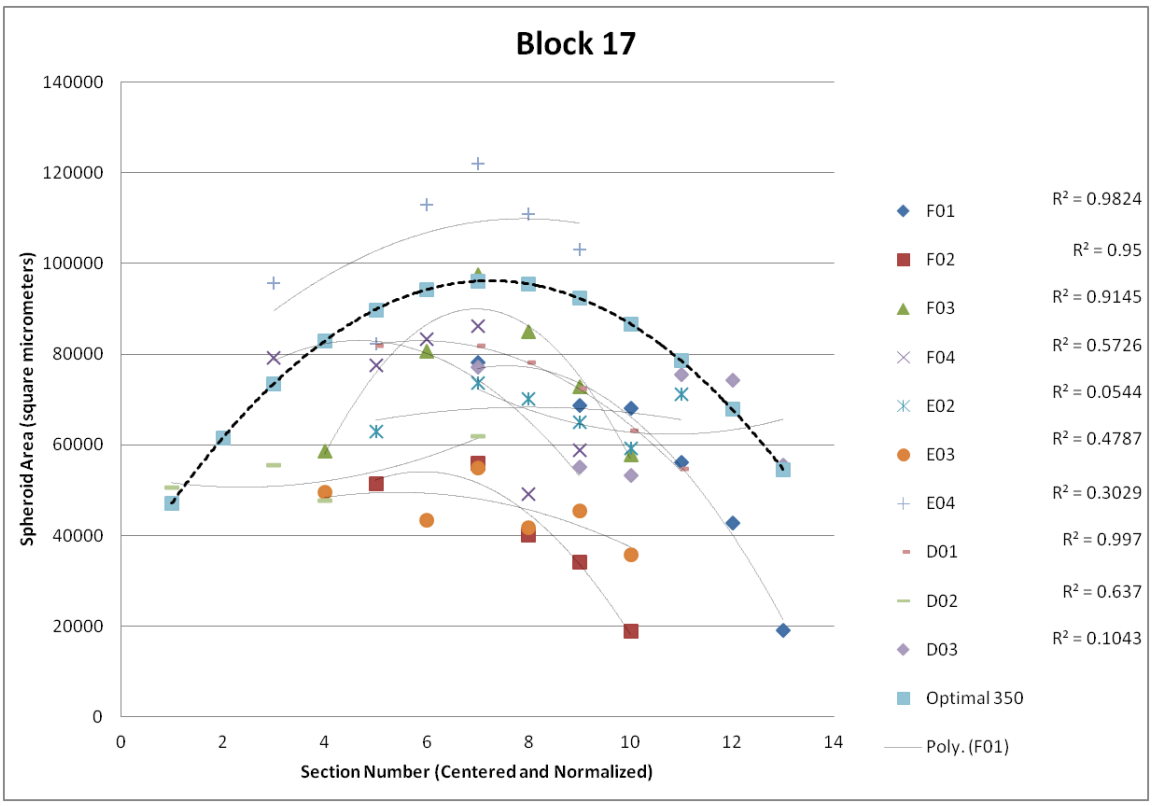

Figure 17. Spheroids from Block 17 with curve fitting data.

Table 4 shows a heat map of the best five sections from each of the four blocks summed together for a total of 20 sections. It would appear there is no direct trend for the successful processing of spheroids; although columns A-C were significantly more successful than D-F. This is likely an artifact of random error accumulating from the following factors: sectioning beginning past the center of the spheroid, ellipsoidal spheroid geometry with odd orientation, or systematic error arising as a result of the mold, microtome or operator.

www.manaraa.com

Table 4

Heat map for all sections of 24-spheroid blocks

	A	B	C	D	E	F
1	18	17	16	14	16	14
2	18	17	18	17	15	15
3	19	19	19	13	13	17
4	18	20	20	15	16	18

3.6.3. 96-spheroid blocks. Blocks of 96 spheroids were not analyzed as in depth as those of 24 spheroids. However, the resulting histological sections were analyzed to determine the average recovery rate of spheroids between three different blocks. *Table 5* contains data for 96-spheroid blocks. Slides counted had >25% of spheroids successfully processed (24/96). The blocks are listed in chronological order. Note improvements between early and later blocks showing evolution of the process. *Figure 18* shows four of the best sections from block A3.

www.manaraa.com

Table 5

96-spheroid block data

Block	# of Sections (distance)	Sections with >50% recovery	Sections with >75% recovery	Sections with >90% recovery	5-best average (percentage)
A17	7 (140 µm)	4/7	0/7	0/7	56.6/96 (59.0%)
A2	9 (180 µm)	0/9	0/9	0/9	36.4/96 (37.9%)
A3	14 (280 µm)	13/14	7/14	0/14	82.8/96 (86.3%)
A4	13 (260 µm)	9/13	0/13	0/13	60.4/96 (62.9%)

www.manaraa.com

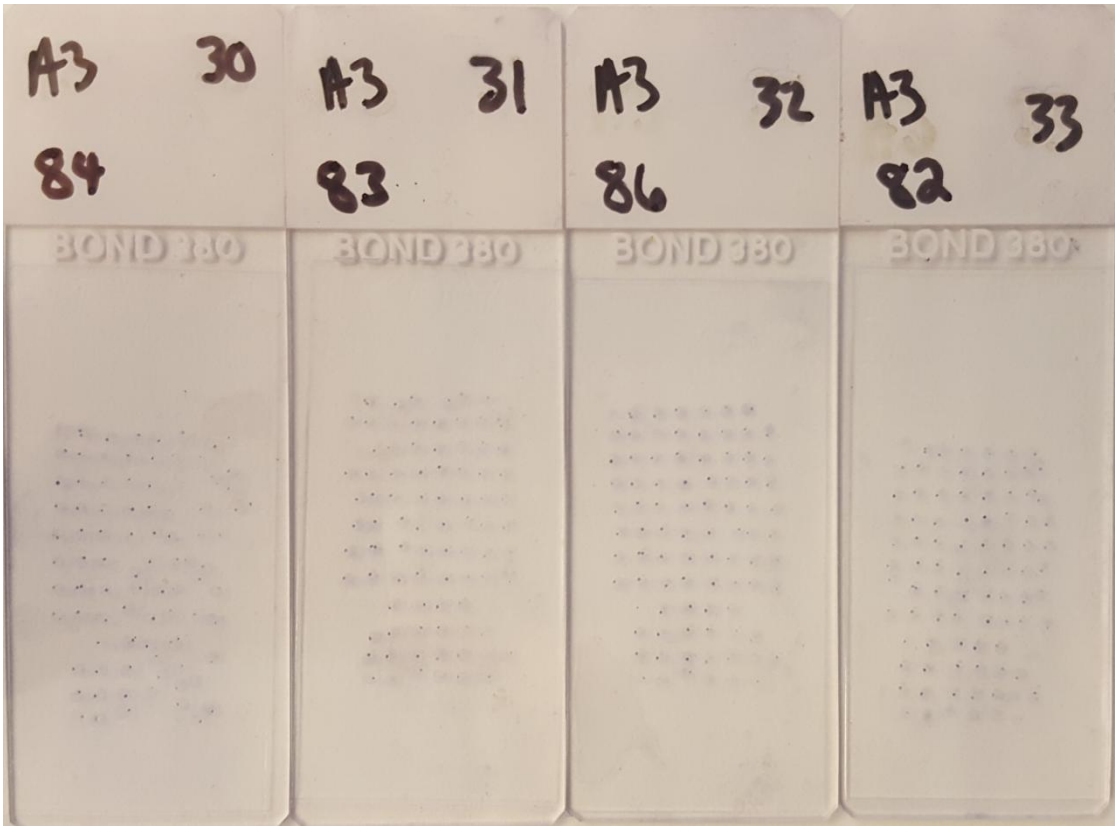

Figure 18. The four best sections from a 96-spheroid block, A3.

3.6.4 Tilt analysis. Analysis of tilt began with deriving an equation for the length of chord AB in *Figure 19*.

www.manaraa.com

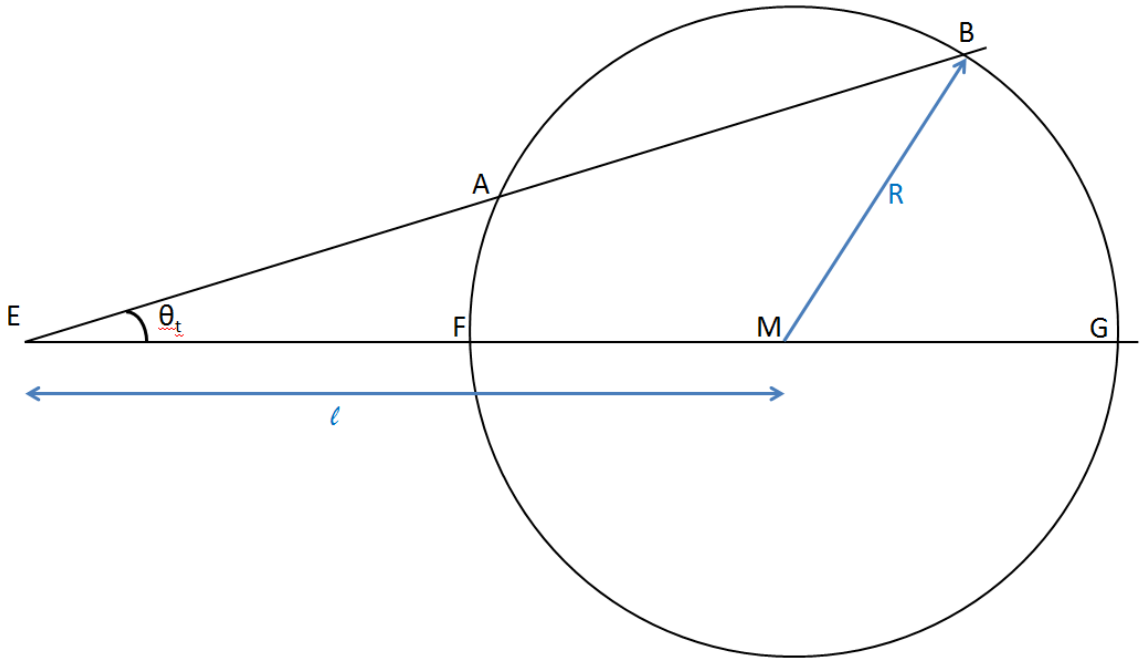

Figure 19. Geometrical setup for the derivation of the tilt equation.

From the law of cosines we have the relationship,

$$|AM|^2 = |AE|^2 + |EM|^2 - 2|AE||EM|\cos\theta_t, \quad \textbf{(Eq. 6)}$$

and from the power of a point theorem we have,

$$|EF||FG| = |AB||AE|, \quad \textbf{(Eq. 7)}$$

remembering that

$$|EF| = l - R \quad \textbf{and} \quad |EG| = l + R, \quad \textbf{(Eqs. 8 \& 9)}$$

the resulting length of chord **AB** is

$$|AB| = \frac{l^2 - R^2}{l\cos\theta_t \pm \sqrt{l^2\cos^2\theta_t - l^2 + R^2}}. \quad \textbf{(Eq. 10).}$$

www.manaraa.com

The relationship was expanded to solve for three cases: tilt in a 24-, 48- and 96-block. This was done using SolidWorks™ to setup the geometry and measure the relevant chords while driving the dimension of the angle. The data tables are available in Appendix A. The intersection of the zero tilt line and the cutting edge line was considered the "focal point of tilt." As the angle of tilt, θ_t (the angle between the zero tilt line and the cutting edge line) is increased, the resulting maximum spheroid diameter recovered is reduced. This new maximum diameter is pictured as chord **AB** in the *Figure 19*. In larger arrays, spheroids further from the "focal point of tilt" diameter's rapidly become shorter. The scenario was simplified to account for only the long axis, the axis requiring more precision to successfully cut all spheroids in plane. It was assumed that the tilt along the short axis would be similar, and thus have a less profound effect overall. *Figure 20* shows the long axis, focal point of tilt, and resulting diameters for a row of spheroids sectioned at three different angles (green=0, yellow=low tilt, red=high tilt). The lines below the spheroids represent the diameter of a spheroid sectioned using the given angle of cut (represented by color). Notice how spheroids furthest from the focal point of tilt are most affected.

www.manaraa.com

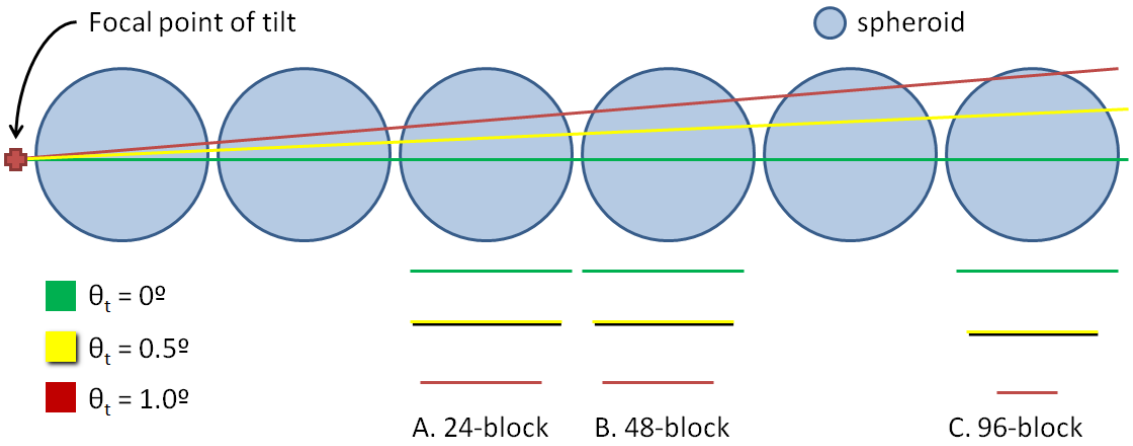

Figure 20. Cuts of tilt=0º, 0.5º and 1.0º (green, yellow, red) and the resulting maximum spheroid diameters (below as the length of colored lines). Lengths are for a 24-block (A), a 48- block (B), and a 96-block (C) with ideal spheroids.

The ratio of the shortened diameter (yellow and red) to the maximum diameter (green) was called the area reduction fraction. This decimal was subtracted from 1 to get the percentage area lost and plotted in *Figure 21* versus the angle of tilt, Θ_t. The percent area lost was calculated for Θ_t values between 0º and 2.25º.

www.manaraa.com

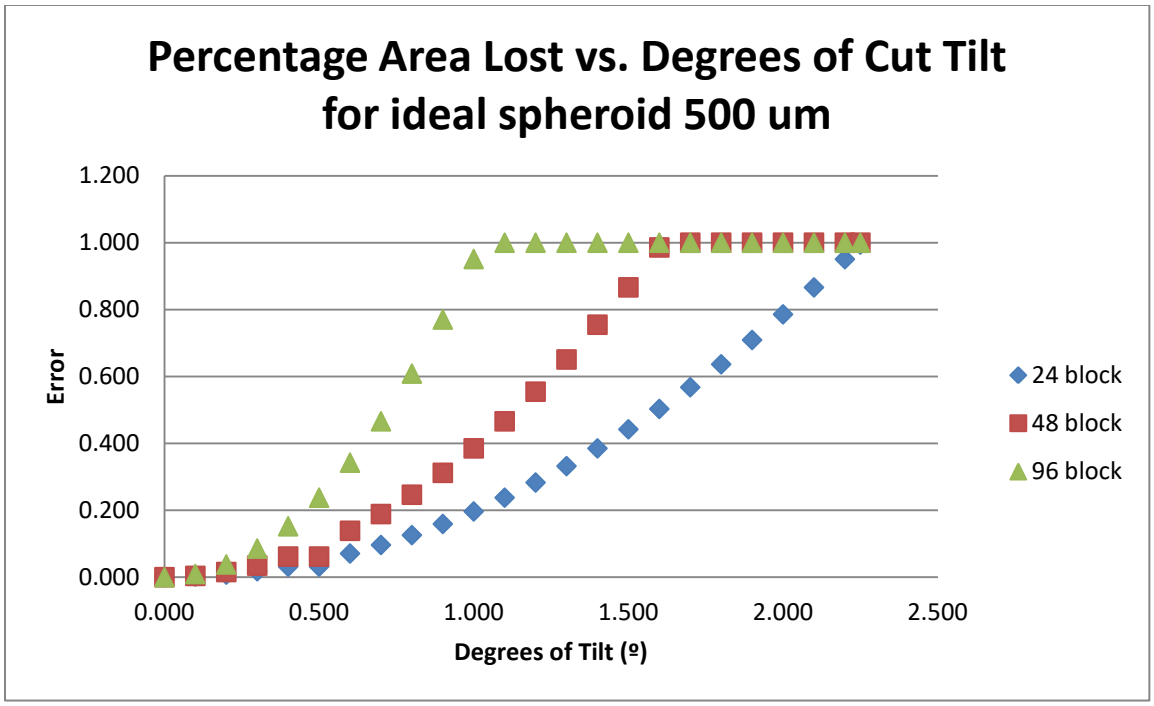

Figure 21. Percentage of area lost as a result of increasing tilt values.

Unsurprisingly, the spheroid furthest from the focal point in 96-spheroid blocks increased in error the fastest; error in 24-spheroid blocks increased the slowest. For 500 μm diameter spheroids in 96-blocks, Θ_t values greater than 1.0º completely missed the outermost spheroid. This angle is equivalent to missing the mark by 255 μm on each end of the block. Angle for 100% error in the most distant spheroid first occurred at 1.6º for 48-spheroid blocks and 2.25º for 24-spheroid blocks. These angles do not correlate with acceptable results. In order to keep sectioning error below 10%, angles of 0.70, 0.55 and 0.30º must be achieved for blocks of 24-, 48- and 96-spheroids, respectively.

www.manaraa.com

Next, tilt was quantified experimentally. During sectioning, it was observed that pillars did not always show up uniformly. Often, one side of the block would show micropillar wells before another side. Within a few sections, all pillars would usually become present. Assuming all pillars remained flat through processing, the tilt could be calculated based on vertical displacement (quantified by number of sections) and horizontal displacement (number of new pillars present). This pattern can be observed in *Figure 22* which shows the pattern of appearance of new micropillars across sections A-E for a given angle of tilt.

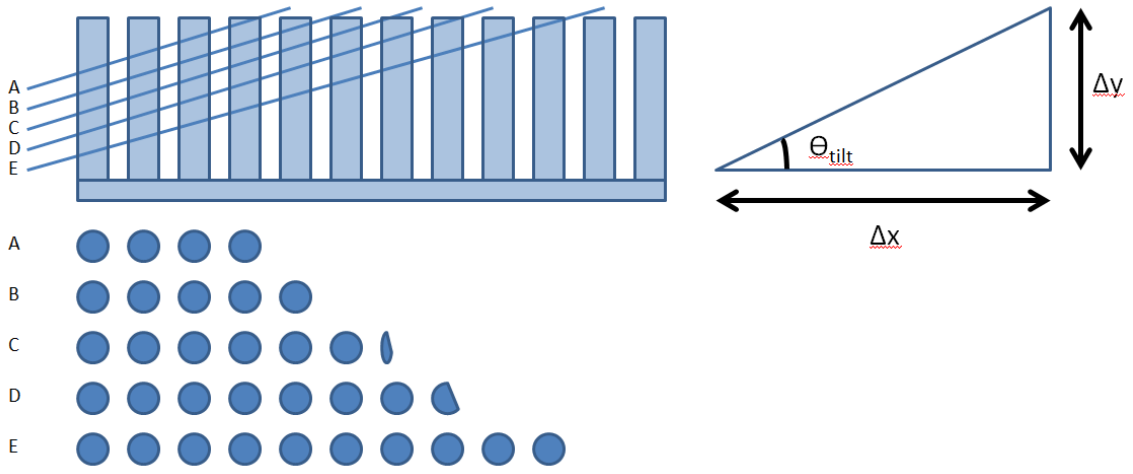

Figure 22. Method of quantification and calculation of experimental tilt.

Table 6 shows the experimentally determined tilt values for 4 different blocks. Not all blocks showed such an obvious pattern, and others contained

www.manaraa.com

pillars which clearly did not stay flat through processing. Incomplete dehydration of the agarose microarray during initial ethanol washing steps often leads to swelling and the formation of a concave meniscus along the tips of the micropillars.

Table 6

Experimentally determined tilt

Block	**X-tilt**	**Y-tilt**
B17	0.112º	0.315º
A1	0.116	0.0749
B5	0.0499	0.103
B7	0.180	0.124
Mean	**0.115º**	**0.154º**
Std. Dev.	**0.0530º**	**0.109º**

Average X-tilt (the long length of the block as described in the tilt section) was 0.115º correlating to about 0.2% error for a 24-spheroid block, a very low finding. The Y-tilt was slightly greater at 0.154º. This error was not theoretically determined but is less than its equivalent 24-block X-error of 0.5%. The reason for increased error is the alignment mechanism. The methodology of alignment

www.manaraa.com

correlating to X-tilt error involved placing a blank cassette in the microtome and comparing its orientation visually against the blade across its whole length. This method allowed for very accurate alignment. There was no way to replicate this alignment strategy for Y-tilt. Y-tilt was done strictly using the bubble level attached to the microtome and visual inspection. This explains the larger average error and standard deviation. Overall, tilt values were very low and could not alone account for reductions in the percentage of spheroids recovered.

3.6.5. Average time and costs saved to a user versus conventional methods. Conventional methods for histology of MCTS involve embedding one or a few spheroids in a wax block using no microarray. The greatly increases the number of blocks to be cut to perform the identical study using a microarray. Additionally, it requires the histologist to search for spheroids during cutting and staining. We propose a value proposition of using our microarray technique based on time and materials saved for an experiment involving 108 samples per patient. The sample number is based on an experiment which explants a patient's primary cancer cells, creates spheroids and subjects them to 12 treatment combinations, 3 treatment durations with a minimum of 3 replicates per group for statistical significance.

www.manaraa.com

Table 7

Comparison of conventional and microarray methods

Item	**Conventional Methods**	**96-spheroid microarray**
Processing and embedding	$3/specimen	$100/microarray
Unstained slides from paraffin block	$3 for first slide, $1/slide additional (10 slides)	$3 for first slide, $1/slide additional (10 slides)
IHC stain from slide	$18/slide x 10 slides	$18/slide x10 slides
Digital slide scanning 20x	$6/slide x 10 slides	$6 x 10 slides
Total	**$255/spheroid**	**$3.67/spheroid**

The conventional group would need to fabricate, section and stain 108 individual blocks, while the 96-spheroid microarray group would only need to fabricate 2 blocks (assuming 85% recovery, resulting in excess data). It is unsurprising to see that processing 96 spheroids at a time versus one spheroid is 98.6% cheaper per spheroid. All pricing is directly from the CHOP Pathology Core except for microarray processing and embedding. This was assumed to be $100 (~$50/hour for two hours of labor). The additional cost in preparing a 96-spheroid block is more than made up for in terms of cost of raw materials and time. Even if as many as five spheroids were processed in parallel bringing the

www.manaraa.com

conventional methods' cost to $51 each, the value proposition would still be 92.8%

3.6.6. Failure mode analysis. There were numerous failure modes at each point in the process which could ultimately result in the lack of spheroid recovery. After spheroid placement, a common occurrence was disturbance of a spheroid in one well due to the placement of a spheroid in an adjacent well. This problem could often be corrected, but on occasion the error was uncorrectable. This resulted in a well with no spheroid due to dislodging. This spheroid may have come to rest in no well, or more often, in another well causing a double spheroid well. This failure mode was also common during agarose infiltration. During agarose infiltration, other modes of spheroid dislodging included disturbances during water removal and disturbances while placing the cassette and adding agarose on top. As previously discussed, removal of the microarray from the mold almost always resulted in the loss of >5% of micropillars.

Processing had the potential for great effects on the agarose/spheroid microarray. Serious care was taking to mitigate these all too common failure modes. The first failure mode during processing was too rapid dehydration. This failure was caused by subjecting the array to too high initial ethanol concentrations during the dehydration steps. The result of this failure was curling of the agarose array resulting in a concave shape across the micropillars.

www.manaraa.com

Ultimately, this lead to the inability of the array to be sectioned in-plane. A similar failure involved incomplete dehydration. This allowed water to remain in the microarray through future processing steps, also causing warping and difficulty during sectioning.

Similar problems were encountered during the transition between HistoClear and paraffin wax. Many blocks were processed through paraffin wax that were contaminated with HistoClear from previous blocks. The result was solid blocks containing significant HistoClear. Sections of these blocks curled up or fractured, and thus were not able to be mounted to slides.

A few additional failure modes presented during sectioning of the microarray itself. The first of these, tilt, was previously discussed in depth. Other errors included the fracture of sections perpendicular to the blade as a result of a chip, dent, or a bit of wax stuck on the blade from cutting a previous section. Although possible, it was difficult piece these types of sections back together on a single microscope slide. Generally, these sections were lost.

Another failure mode occurred during transfer of the section into the water bath for mounting to a slide. On occasion a section would stick to a tool, the user's glove, or become folded during placement into the bath. These all resulted in the loss of a whole section.

www.manaraa.com

After baking slides, they were ready for staining. Very few losses occurred during staining; although, with very low frequency, some spheroid sections fell off into the staining solutions. Coverslipping occurred with no losses. *Table 8* summarized the compounding errors encountered during the experiment.

www.manaraa.com

Table 8

Errors incurred throughout microarray fabrication and processing optimization

Error	**Cause**	**Result**
spheroid displacement	disturbance due to adjacent spheroid placement, water removal, or agarose additon	wells with two or zero spheroids
fractured micropillar	incomplete agarose diffusion, lack of removal from mold	no micropillar and therefore no spheroid in a single well
too rapid/incomplete dehydration	poor dehydration sequence	swelling and warping of microarray
HistoClear diluting paraffin wax	failure to properly change HistoClear solution	inability to section block
tilt	improper microtome blade/block alignment	out of plane sectioning
fracture of wax section during cutting	chip, dent or wax bit on blade	wax section split horizontally in two
wax section folding or becoming deformed	section stuck to tool, glove or folded during placement in bath	irreversible loss of section

www.manaraa.com

Chapter 4

Validation of Tissue Microarray - Iron Oxide Nanoparticle Penetration Study

4.1. Experimental Procedure

The following procedure was used to determine the penetration and potential chemotherapeutic potential of 5k Da-polyethylene glycol coated superparamagnetic iron-oxide nanoparticles (5k-PEG SPIONs) on HTB-126 breast cancer cell spheroids. Both 2D and 3D culture systems were tested for comparison.

4.1.1. 2D culture and histology. Cells were collected from one confluent T75 flask and resuspended in 40 mL of fresh culture medium. In one 24-well, flat-bottom, adherent culture plate, 1 mL of cell suspension was added to each of 16 wells. Similarly, 1 mL of cell suspension was added to all 24-wells of a separate 24-well culture plate. In total, 40 separate monolayers of HTB-126 breast cancer cells were cultured. Plates were incubated until cells reached confluence. Media was changed every other day. Four wells were fixed with 4% paraformaldehyde and without incubation with SPIONs (negative control). Fixation was performed for two hours. Cells were washed with PBS and left to sit at room temperature in fresh PBS awaiting staining.

The remaining 36-wells contained 12 experimental groups of n=3 consisting of three dosages (1 μg/mL, 10 μg/mL, 100 μg/mL) and four time points

www.manaraa.com

(1d, 2d, 3d, 7d). After incubation for the prescribed duration, cell monolayers were fixed for two hours in 4% PFA, washed with PBS, and hydrated with PBS until staining.

2D cultures were not embedded and sectioned, but instead stained directly in culture plates following fixation. Preparation of the stain involved creating 20% aqueous solution of hydrochloric acid (20 mL concentrated hydrochloric acid added to 80 mL distilled water) and 10% aqueous solution of potassium ferrocyanide, trihydrate ($K_4Fe(CN)_6 \cdot 3H_2O$ (10 g potassium ferrocyanide Sigma Cat# P-3289, dissolved in 100 mL distilled water). The two solutions were mixed immediately before staining. 1mL of the solution was added to each well of the fixed 2D cultures and allowed to incubate for 30 minutes. The wells were then washed three times with distilled water and counterstained with 1 mL nuclear fast red stain for five minutes. After two more washes with distilled water, plates were imaged and photographed using the Zeiss AX10 microscope and Zen Imaging Suite.

4.1.2. 3D spheroid formation and incubation. Breast cancer spheroids with an initial density of 30,000 cells per 40 µL droplet were formed as described in *3.2 Culture of HTB-126 Breast Cancer Spheroids*. Spheroids were transferred with PBS to a sterile GravityTRAP™ plate without fixation using the same transfer technique that was used for placing spheroids into microwells (*Figure*

www.manaraa.com

5b). Due to normal losses during culture, two full plates of spheroids were necessary to fill one 96-well GravityTRAP™ plate with a single spheroid in each well.

The spheroids were then incubated with culture medium (DMEM supplemented with 10x FBS and 1x penicillin/streptomycin) containing 5k-PEG SPIONs received from Auburn University via Dr. Alan David's lab as described in [89]. Twelve experimental groups were created using two SPION dosages (1 μg/mL, 10 μg/mL) and six incubation lengths (1 hr., 4 hrs., 12 hrs., 24 hrs., 3 days, 7 days) for n=8 of each. Unfortunately, not enough particles were provided for a third dosage group of 100 μg/mL. Negative control spheroids were fixed without incubation (n=8). Calf's liver was dehydrated, infiltrated and embedded with paraffin for use as a positive control in the Pearl's Prussian Blue staining protocol. Upon completion of SPION incubation, each spheroid was transferred to a new GravityTRAP™ plate containing 4% paraformaldehyde (PFA) for fixation. Fixation proceeded for 2 hours followed by removal of PFA, one PBS wash, and the addition of PBS for long-term storage at room temperature until remaining spheroids were ready for embedding into a microarray.

4.1.3. Microarray fabrication and histology. Spheroid groups of n=8 began the incubation process. However, some spheroids disassembled and others were lost leaving groups of n=5 to n=8. The remaining spheroids were

www.manaraa.com

assembled into two separate microarrays using the center 48-wells (6x8) of each. Control spheroids were placed in the first four wells of the top row (wells A1-A4). After processing, spheroids were sectioned at 20 μm. The best six slides were chosen for analysis[6]. Slides #1, 3 and 5 were sent to the Children's Hospital of Philadelphia Pathology Core for Prussian blue staining (nuclear fast red counterstain) and digital slide scanning at 20x. Slides #2, 4, and 6 were stained using an identical Prussian blue stain/nuclear fast fed counterstain protocol in our own lab. The staining protocol from [90] begins with deparaffinization and hydration of sections to water. The protocol proceeds with creating and combining the same two reagents (20% hydrochloric acid, 10% potassium ferrocyanide) as discussed in *4.1.1 2D Culture and Histology*. Hydrated sections resulting from sectioning of the 3D spheroid microarray were incubated in the mixed solution for 30 minutes. Slides were then washed three times with distilled water and counterstained with nuclear fast red for five minutes. After two more washes in distilled water, sections were coverslipped with aqueous mounting medium and imaged using the AX10 microscope and software.

[6] Slides were chosen so that a minimum of n=3 for each spheroid experimental group as not all spheroids were on each slide.

www.manaraa.com

4.2. Data Collection

2D and 3D culture images were analyzed using ImageJ. Specifically, images were loaded into ImageJ, converted to 32-bit/grayscale, and threshold analysis was used to determine the percent area stained.

2D culture images were analyzed using the following thresholding values to specifically highlight the Prussian blue stain: hue 85-128, saturation 44-134, brightness 0-255. The software was used to measure the percentage of area stained.

Before analysis, 3D spheroid images were separated into four specific cores using Paint.net, an image editing program, as shown in *Figure 23*. Core 1 was the central region of the spheroid ranging from the center to a distance of 0.25r. The other cores 2, 3, and 4 were rings covering consecutive area ranges between 0.25r and 0.50r, 0.50r and 0.75r, and 0.75r and 1.00r, respectively.

www.manaraa.com

Figure 23. Core 4 through 1 shown from left to right for n=3 spheroids of a single group.

No analysis was performed for Prussian blue staining. Thresholding analysis between values of 67.5 and 184.5 were used to determine the degree of the nuclear fast red staining. Nuclear fast red stains nuclei red and the cytoplasm pink. As evident from the pictures, no positive Prussian blue staining was observed. The area enclosed and percentage stained was measured for each core. These percentages, along with standard deviations in the experimental groups, are reported in *Table 9*. Averages and standard deviations across single

www.manaraa.com

time points, individual cores, and for all samples were calculated. These values were used to collect information on the density of cells by region in the spheroid.

Table 9

Percentage of staining by cores and time points for all dosages

	Core 1	**Core 2**	**Core 3**	**Core 4**	**Time Averages**
Day 0	77.7 (12.8)	80.1 (10.4)	84.3 (9.44)	79.9 (5.94)	80.5 (8.85)
Day 0.5	71.5 (2.58)	68.9 (2.96)	70.6 (3.71)	82.4 (7.35)	73.3 (6.77)
Day 1	98.9 (0.806)	98.6 (0.417)	97.9 (2.23)	93.3 (3.04)	97.2 (2.86)
Day 3	74.6 (36.9)	63.2 (30.6)	65.3 (32.2)	55.2 (40.2)	64.6 (30.8)
Day 7	72.1 (32.6)	76.4 (17.7)	64.6 (17.0)	44.3 (12.8)	64.3 (22.3)
Core Averages	79.0 (22.0)	77.4 (18.7)	76.5 (19.5)	71.0 (25.0)	75.98 (21.1)

www.manaraa.com

4.3. Results and Discussion

The following images were taken of 2D monolayer cultures after Prussian blue staining. The negative control is not pictured. Dosages increase from left to right while incubation times increase from top to bottom.

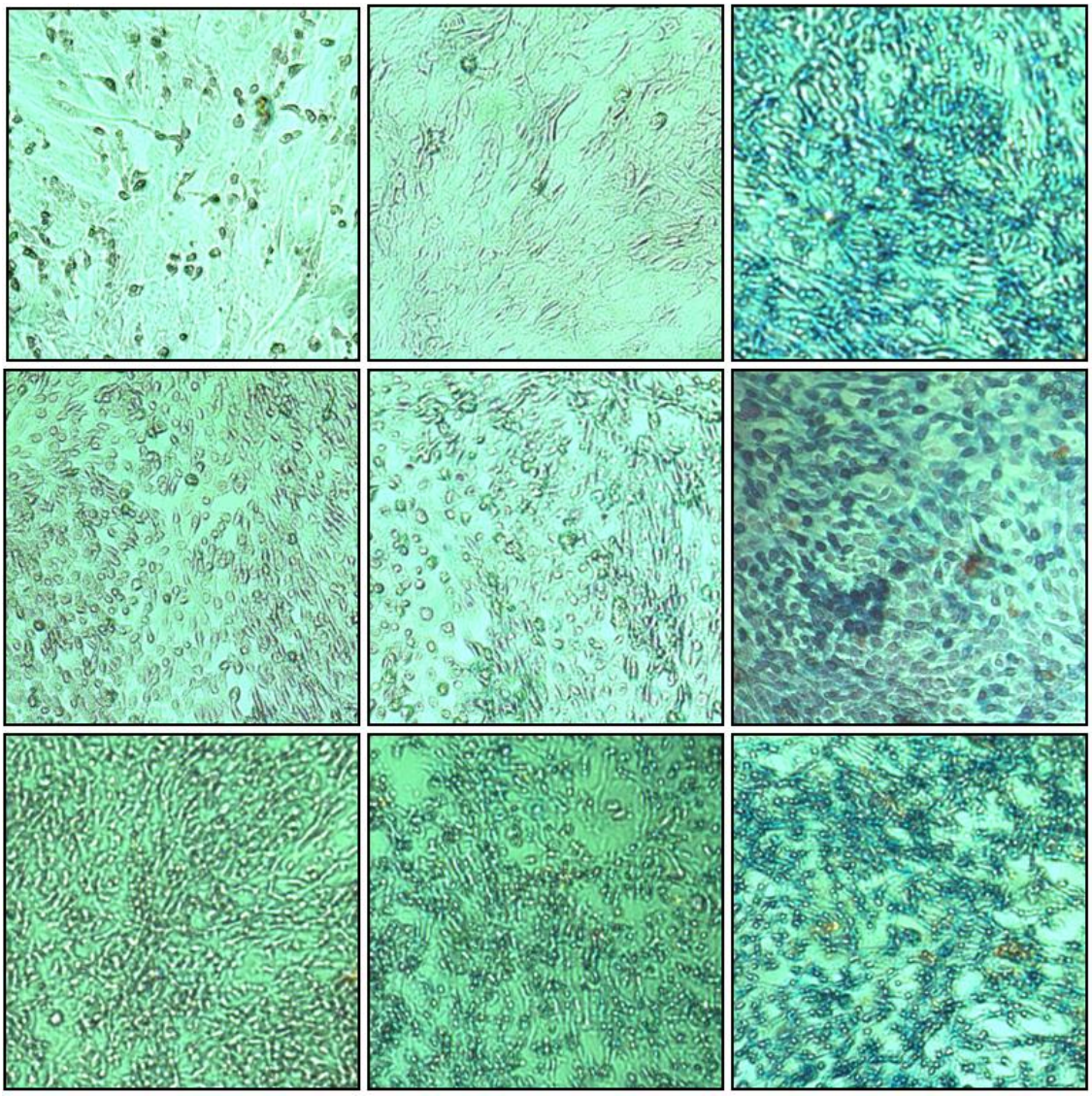

Figure 24. Staining of 2D cultures. Rows from top to bottom are days 1-3, dosages from left to right are 1, 10, 100 µg/mL.

www.manaraa.com

Thresholding values were used to calculate the percentages stained by Prussian blue. Error bars bracket one standard deviation from each experimental group (n=3).

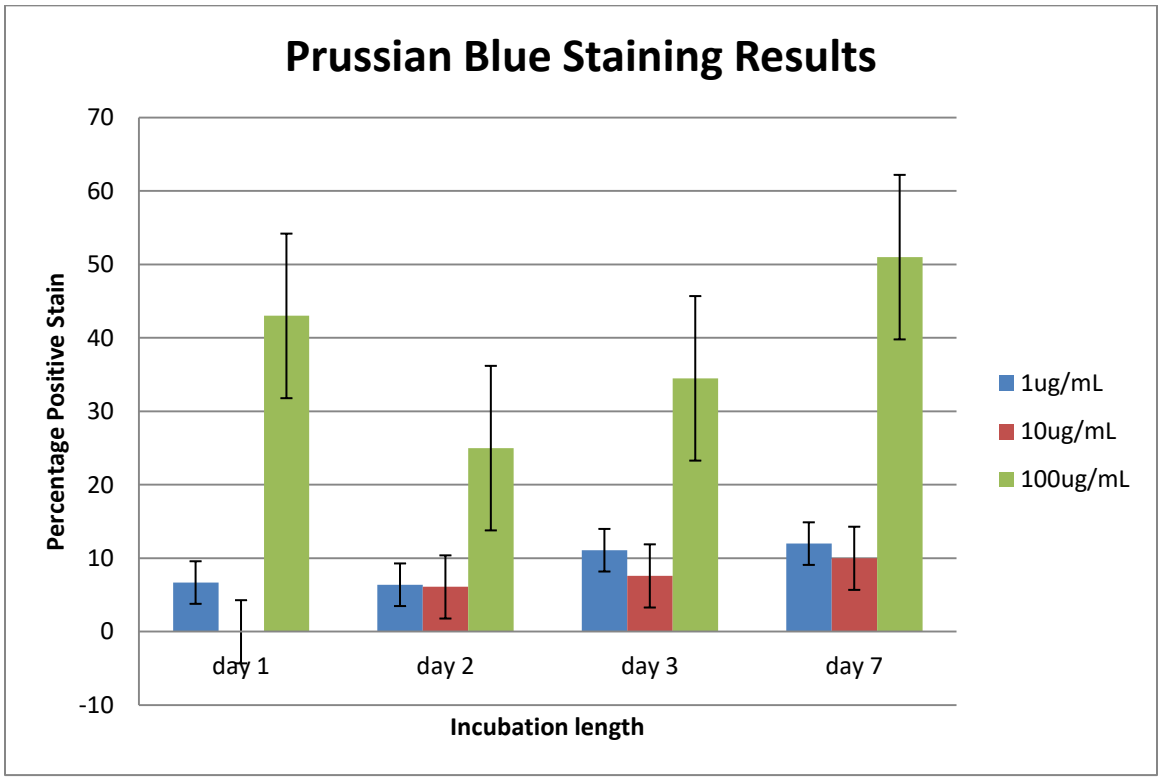

Figure 25. Percentage staining by dosage and incubation time. Error bars denote one standard deviation of the sample mean.

The results show that there was no significant difference between staining for dosages of 1μg/mL and 10 μg/mL. Significant differences in staining were observed between both 1 μg/mL and 100 μg/mL, and 10 μg/mL and 100 μg/mL dosages. It would appear that between 10 μg/mL and 100 μg/mL there exists a

www.manaraa.com

specific concentration which promotes increased uptake of SPIONs into cell monolayers. This is an interesting result moving forward as it helps explain what may have been observed in 3D culture experimentation.

The following images (*Figure 26 & 27*) show a lack of positive Prussian blue staining across all 3D spheroid cultures, regardless of dosage or incubation time. Note that between removal of the microarray from the mold, sectioning and slide mounting, the orientation is effectively mirrored over the y-axis as a result of the process. This leaves the control spheroids (n=3 pictured in this section) in the top right corner of the figure. Experimental groups begin on the right and move left across a single row. It is unfortunate that not enough particles were provided to study the dosage of 100 μg/mL on spheroid cultures. It is recommended that this is the starting dosage for future experiments.

www.manaraa.com

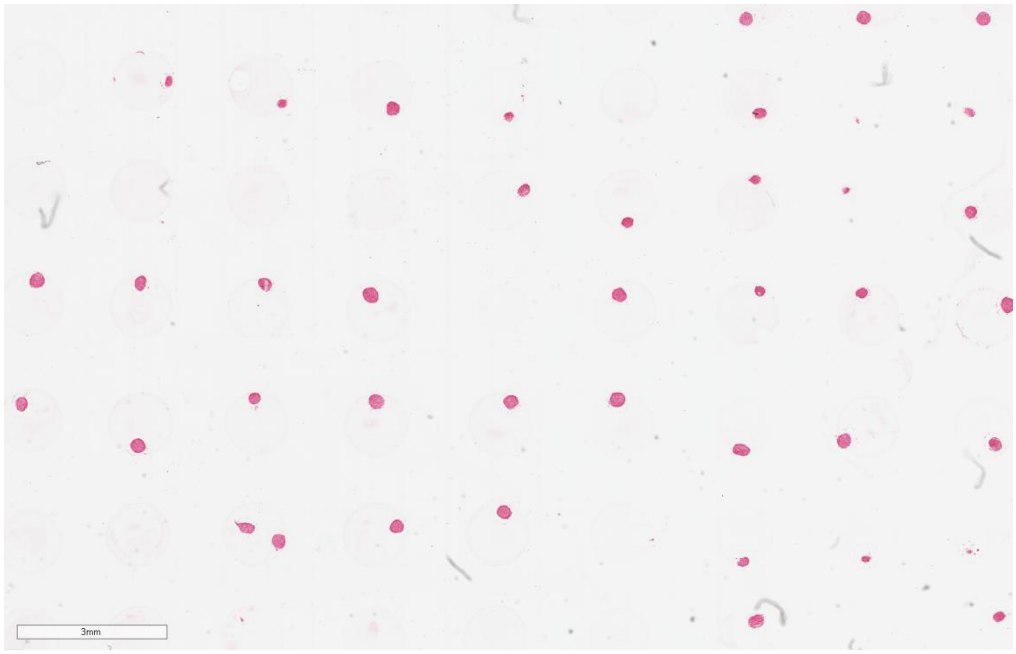

Figure 26. Block T1 Prussian blue stain (nuclear fast red counterstain).

www.manaraa.com

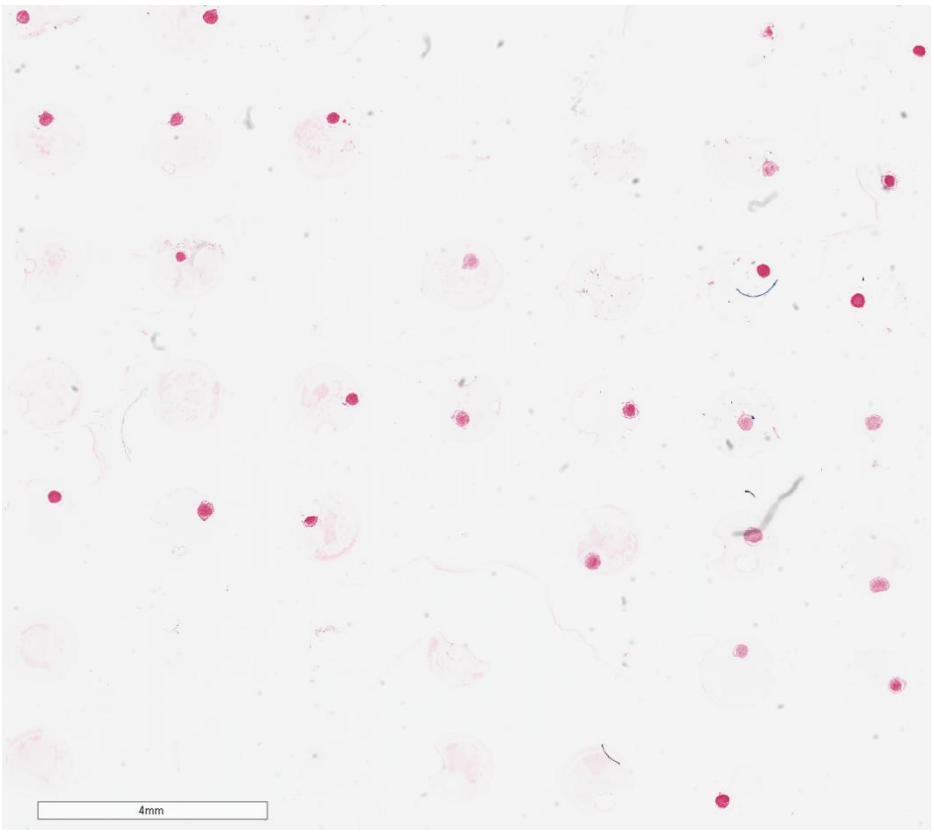

Figure 27. Block T2 Prussian blue stain (nuclear fast red counterstain).

The lack of positive Prussian blue staining in 3D culture could be indicative of multiple results. One obvious cause is experimental error arising from improper staining technique. This is relatively unlikely due to successful staining of 5k-PEG SPIONs in similar spheroids of a different cell line using an identical procedure. However, we should note that these spheroids were slightly larger, not as densely packed, and incubated for a period of 3 days. *Figure 24* shows positive staining for ferric ion in a rhabdomyosarcoma sarcoma (CRL-2061) spheroid at 20x indicating procedural success.

www.manaraa.com

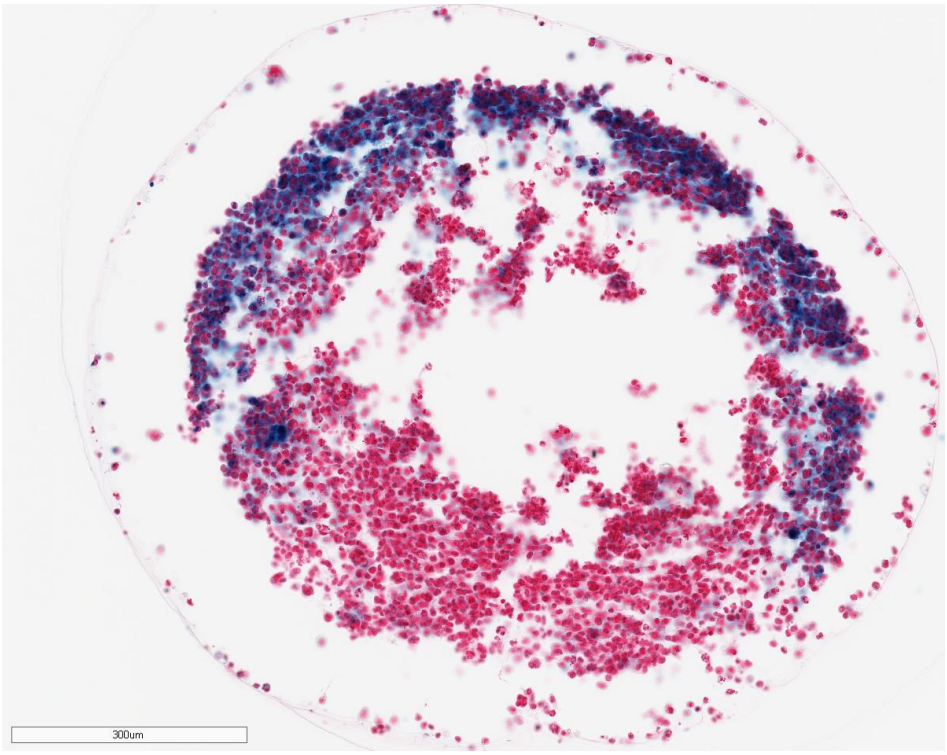

Figure 28 . Prussian blue stain (nuclear fast red counterstain) of a CRL-2061 spheroid of approximate diameter of 1.2 mm.

Unfortunately, no breast cancer spheroids contained a similar pattern of SPION penetration around the periphery of the tissue. The goal of this experiment was to determine penetration of these particles into different regions of the spheroid over time; however, this was not successful.

Another hypothesis for the lack of staining is particle removal through diffusion during microarray processing. This would explain the presence of

www.manaraa.com

particles in 2D and the lack of particles in 3D, as only 3D cultures were subjected to extended immersion in various reagents before staining.

Other hypotheses which explain the lack of positive ferric ion staining include multicellular tumor resistance. Discussed in *Chapter 2*, this resistance is the result of many cells becoming densely packed and working together to resist foreign agents, including chemotherapeutic drugs. Additionally, it is possible that breast cancer cell line HTB-126 does not have proteins with the ability to internalize SPIONs, while cells in the rhabdomyosarcoma cell line CRL-2061 are fully capable. Although, this is unlikely due to positive staining in 2D and the fact that all human (and eukaryote cells for that matter) cells possess similar integral membrane proteins. Previous research has shown successful penetration into cell monolayers [89]. Further experimentation needs to be performed before ruling out SPION penetration in 3D tissues. On occasion, nonspecific, positive ferric ion staining was observed which may be attributed to contamination at some point along the process, processing effects, or actual particle penetration.

One result noted was that spheroids seemed to go through three distinct phases of assembly, growth and disassembly across all four cores. The assembly phase can be described as the time between initiation of hanging drop culture and Day 0 of nanoparticle incubation. Once spheroids were assembled, they were incubated with particles. The next day saw a steady increase in spheroid

www.manaraa.com

counterstaining density indicating cellular growth and compaction. The next two staining time points, day 3 and 7, saw progressive deterioration of area stained in the spheroids attributed to disassembly of microtissues. This deterioration was not observed in any control spheroids; therefore, this result may likely be attributed to the chemotherapeutic effects of iron in the drug.

www.manaraa.com

Chapter 5

A Mechanical Solution for Automated Spheroid Transfer

5.1. Mechanical Transfer Ideation

The idea to automate the placement of spheroids into microwells was a natural technological advancement in the design of the system. Additionally, it was recommended by grant reviewers as a prospective way to increase the innovation potential and utility of the technology. The current system of spheroid transfer, although precise and with 100% success rate, is slow and very tedious. An ideal system would transfer spheroids directly from hanging-drop culture plates and into the microarray mold with low or zero losses. In this case, spheroids would need to be fixed either while in hanging-drops, or in the mold after transfer. Upon successful development of mechanical transfer technology, such decisions could be properly tested and made. There is a need to efficiently collect and transfer spheroids from culture into the microarray mold in an automated or mechanical fashion in order to improve the speed of the process by 100%. The current system takes between 1.5 and 2.5 hours to place 96 individual spheroids (~60-90 seconds each). Reducing this time would greatly reduce the labor cost associated with microarray fabrication (*Table 4*).

Design of the system began with the consideration of three different transfer mechanisms. The first design considered was a simple system to house a

www.manaraa.com

96-well plate and connect it to the microarray mold using a series of small plastic tubes. It would operate on the principle of spheroid transfer through gravitational fluid flow. The unknown aspect of this design was whether the enough force could be generated to move a spheroid through a thin tube with water and gravity alone. It was hypothesized that the surface tension of water may act to inhibit water and spheroid movement through a vertical tube due to the geometrical constraints of spheroid size, hanging-drop plate dimensions, and microarray mold geometry. The second design considered was similar to the first, but would incorporate a vacuum to assist in overcoming frictional forces or those arising due to water tension.

Design number three involved building a system that would operate with the assistance of a centrifuge. The governing design principle behind this device was to use the centrifugal force to transfer spheroids; the design would be required to mechanically connect hanging drop plates to the mold in a compact format so as to fit in the centrifuge's plate holder attachment. The design would then use the force of the centrifuge to overcome other forces present and one place the spheroid into the bottom of each microwell. Ultimately, it was determined to proceed with design one for simplicity and avoid over engineering. Future iterations would consider the use of other sources of force for spheroid transfer.

www.manaraa.com

5.2. Mechanical Design

In order to achieve the design goals discussed for design one in *5.1 Mechanical Transfer Ideation*, it was decided that the first prototype would consist of 4 fundamental parts: a rigid piece that fits existing pins of GravityTRAP™ 96-well plates to collect spheroids directly from culture; a rigid piece that fits the existing geometry of the microarray mold, containing a channel for each spheroid to flow downward into the mold; a series of 96 narrow, polymer tubes that connect the two parts; and a water vat on top to increase the pressure head of the system.

5.2.1. Microarray base connector. The microarray base connector was designed using the geometry of the microarray mold. *Figure 29a* is a SolidWorks™ isometric view of the mold which serves as the starting point for the design of the microarray base connector, *Figure 29b*. *Figure 30* shows two larger isometric views of the microarray base connector. Notable design features include counter bored holes which allow for the press fitting of tubes, a "clover leafed" geometry to mate the bottom of the part to the mold while creating ample open surface area for outlet water flow, pins which secure the piece directly into the four corner wells of the 96-well microarray mold, and a 200 μm cross shaped spacer at the bottom which allows for the outflow of water, but does not provide ample space for spheroids to jump between wells. The base connector was

www.manaraa.com

designed to incorporate transfer for only the center 24 wells of the hanging-drop plate at first. Future iterations will incorporate all 96 wells.

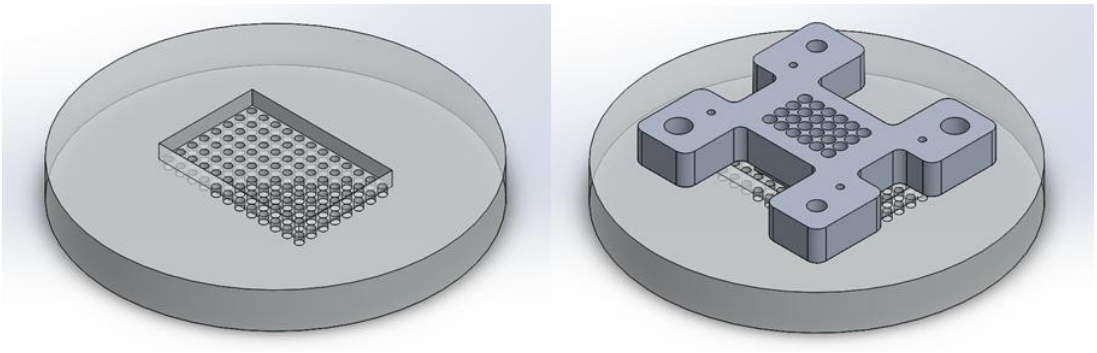

Figure 29. Microarray base connector. (a) SolidWorks isometric view of the microarray mold, the starting point for the design of the transfer device. (b) Assembly of the microarray base connector and the cell mold.

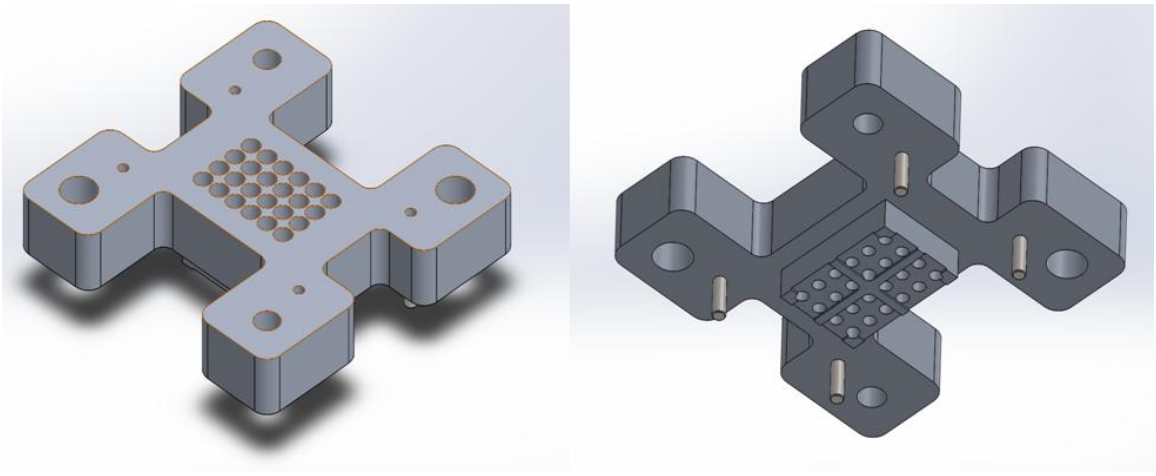

Figure 30. Isometric views of the microarray base connector.

www.manaraa.com

5.2.2. Hanging-drop plate interface. The next part was designed to interface a Insphero 96-well hanging drop plate to a series of tubes that would terminate into the microarray base connector. *Figure 32* depicts an isometric view of the part.

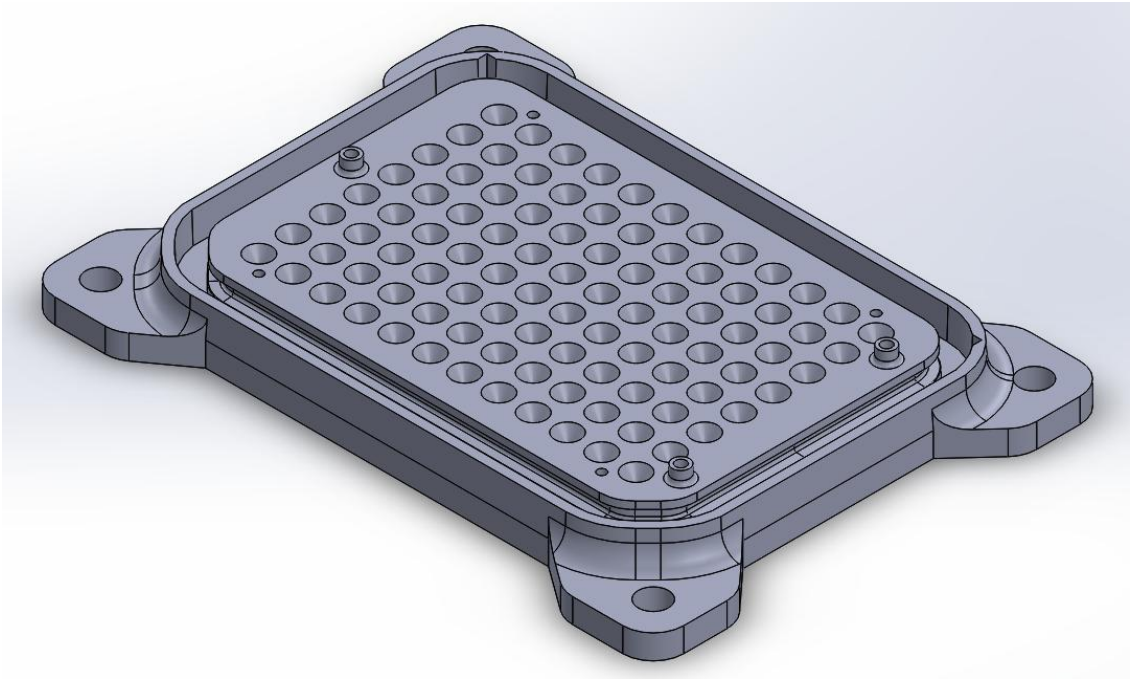

Figure 31. Hanging-drop plate interface.

The most important design feature of this part is the array of 96 countersunk holes and three pin holders (two bottom right side, one top left side) around the outside of the array for alignment. These were designed to work with preexisting pins of the GravityTRAP™ system. It was designed so that

www.manaraa.com

when interfacing with a GravityTRAP™ plate, hanging spherical drops of 40 μL would just slightly touch the hanging-drop plate interface, causing their transfer to the interface. Additionally, the geometry of the countersunk holes was designed to use water tension as an aid in transfer. The geometry of the holes is such that a 40 μL drop will not pass through the plate without additional water added on top. The countersunk holes traverse through the length of the part and on the bottom side are the appropriate size for press fitting the thin polymer tubes. This is extremely important for functionality of the complete system. Its operation will be discussed in *5.3 Automated Spheroid Transfer Operation*.

Other design features include a channel around the array of countersinks which allows the press fitting of the *5.2.4 Water vat*. This channel was designed to house an O-ring which keeps the connection between these two parts water tight. This plate also contains a hole in each corner for the addition of long threaded rods. These rods support the device and allow for the control of the interface's height, and thus the pressure head of the system.

At this time, only the center 24 wells of the hanging-drop plate interface were machined through the part. The remaining holes were not drilled, but the countersinks remain as placeholders for future design iterations.

5.2.3. PVC tubing. The system was designed to include clear PVC tubing with inside diameter of 1/32" and outside diameter of 3/32". Clear tubing was

www.manaraa.com

used for visualization of flow and spheroid transfer. The tubing was ordered from McMaster-Carr. Approximately 6" lengths of tubing were used. To install the tubing, the end was cut at a 45º angle to aid press fitting. *Figure 32* shows the fitting of the center 24 tubes into the system.

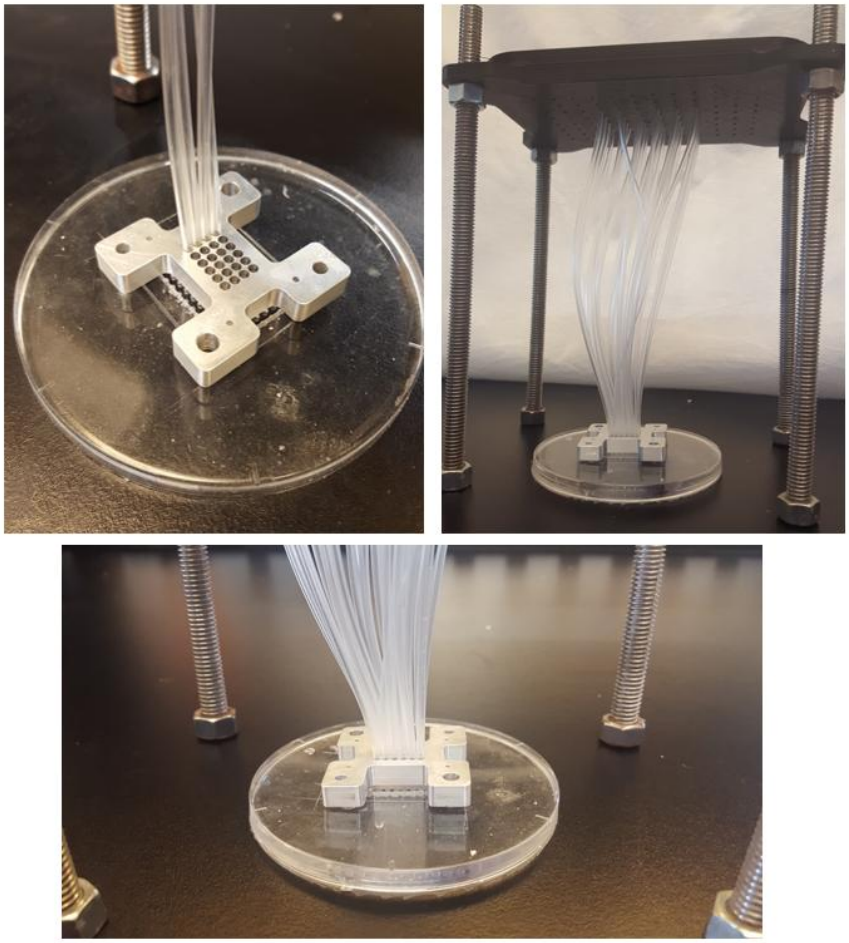

Figure 32. Three views showing the connection between the two main components of the design with tubes.

www.manaraa.com

5.2.4 Water vat. The water vat was a late design addition once testing had revealed that an additional pressure head would be necessary for spheroid transfer. The vat was designed to press fit to the hanging-drop interface (which needed slight modification), and form a water-tight seal with the help of two O-rings. *Figure 33* shows the system's full assembly, containing the water vat.

Figure 33. Mechanical transfer system completed assembly.

www.manaraa.com

5.3. Mechanical Spheroid Transfer Operation

The mechanical system was designed to operate as follows:

1. The microarray mold is prepared by filling its cavity with water and removing all microbubbles as described in *3.3 Microarray Formation*. It is then attached to the microarray base connector using four pins.
2. After placement of the Insphero hanging-drop plate to the hanging-drop interface, spheroids are transferred to the interface by contact with hanging-drops. Due to surface tension of the culture medium, spheroids and droplets remain in the counterbores of the hanging-drop interface part.
3. A piece of filter paper is applied, covering all counterbores of the array.
4. The water vat is then press-fitted into the hanging-drop interface. It is slowly filled with about one centimeter of water to increase the pressure head, flushing the spheroids through the tubes and into the microarray mold. Care is taken not to flush the interface too fast causing filter dislodging or flow rates too large for the system.

www.manaraa.com

Chapter 6

Conclusion

In this study, a novel process for the high-throughput analysis of multicellular tumor spheroids was designed, refined, and fully characterized. The system has full capabilities to increase the throughput, speed and effectiveness of biomedical research on spheroid cultures. Benefits of this system include increased power of study, side-by-side staining, and efficiency.

The system designed is not completely without error, and therefore comes with recommendations for the future. The most important error factors all have to do with pillar pull out and orientation through processing. Other errors, such as tilt during cutting, were shown to be acceptable, leading to a small amount of error, and thus should be considered for improvement only once permanent solutions to primary errors are reached.

The paramount issue with the system is the mold design which creates the geometry of the microarray. Pillars were designed to be cylindrical, but after thorough testing of all system parameters (gel composition, reagents, etc.) experimental pullout reached a maximum of 90/96 spheroids per microarray (n=2). After processing and sectioning, the maximum number of spheroids achieved on a single slide was 84/96 (n=1). Additionally, the cylindrical pillars allowed for a relatively large area for the spheroid to move and come to rest. The

www.manaraa.com

result were imperfect columns and rows of spheroids on slides after histology. To solve the issue of spheroid pullout and alignment, it is recommended that a positive mold of an array of square pyramids be used to replace the cylindrical pillars. This would allow for much larger angles of relief during pullout, and would also create geometry in the mold what would force spheroids to become centralized in each well. This design would also increase the surface area for diffusion during processing, potentially eliminating processing effects, while promoting better mixing during agarose infiltration.

The SPION study showed the potential power of using a microarray system to study spheroids and acquire regionally based information. Although no publishable results were obtained from the penetration of particles into spheroids, the power of the system was ascertained. A study which previously would have taken a lab months to assemble, process and section 96 individual spheroid blocks, was reduced to the processing of just two, while adding the ability for side-by-side comparison of multiple experimental groups (without normalization each to a stained and calibrated control).

The study did highlight a potential therapeutic dosage range between 10 μg/mL and 100 μg/mL for 5k-PEG SPIONs. Within this range, there appeared to exist a concentration which allowed the drug to penetrate the cell membrane. Furthermore, even without positive staining, dosage and time combinations of 3

www.manaraa.com

days and 10 μg/mL, 7 days and 1 μg/mL, and 7 days and 10 μg/mL all showed spheroids much less dense than their control counterparts which were disassembling and becoming necrotic. The dosage and time combination of 3 days and 1 μg/mL showed 67% normal spheroids and 33% necrotic spheroids. All other time points less than 3 days showed no signs of necrosis.

Finally, to improve the process of spheroid embedding, a design was successfully created that mechanically assisted spheroid transfer. The time to setup and use the system was ~5 seconds per spheroid, a large reduction in time compared with ~60-90 seconds per spheroid using the methods described in *3.3 3D Microarray Formation*.

www.manaraa.com

References

[1] S. Breslin, L. O'Driscoll, Three-dimensional cell culture: the missing link in drug discovery, Drug discovery today, 18 (2013) 240-249.

[2] J. Johnson, S. Decker, D. Zaharevitz, L. Rubinstein, J. Venditti, S. Schepartz, S. Kalyandrug, M. Christian, S. Arbuck, M. Hollingshead, Relationships between drug activity in NCI preclinical in vitro and in vivo models and early clinical trials, British journal of cancer, 84 (2001) 1424.

[3] E.A. Sausville, Overview. Cancer drug discovery: pathway promise or covalent certainty for drug effect--quo vadis?, Current opinion in investigational drugs (London, England : 2000), 1 (2000) 511-513.

[4] L.A. Kunz-Schughart, J.P. Freyer, F. Hofstaedter, R. Ebner, The use of 3-D cultures for high-throughput screening: the multicellular spheroid model, Journal of biomolecular screening, 9 (2004) 273-285.

[5] W.N. Hait, Anticancer drug development: the grand challenges, Nature reviews. Drug discovery, 9 (2010) 253-254.

[6] I.A. Cree, C.M. Kurbacher, M. Untch, L.A. Sutherland, E.M. Hunter, A.M. Subedi, E.A. James, J.A. Dewar, P.E. Preece, P.E. Andreotti, H.W. Bruckner, Correlation of the clinical response to chemotherapy in breast cancer with ex vivo chemosensitivity, Anti-cancer drugs, 7 (1996) 630-635.

[7] L.G. Griffith, M.A. Swartz, Capturing complex 3D tissue physiology in vitro, Nature reviews. Molecular cell biology, 7 (2006) 211-224.

[8] D. Barbone, T.M. Yang, J.R. Morgan, G. Gaudino, V.C. Broaddus, Mammalian target of rapamycin contributes to the acquired apoptotic resistance of human mesothelioma multicellular spheroids, The Journal of biological chemistry, 283 (2008) 13021-13030.

المنارة للاستشارات
www.manaraa.com

[9] A. Frankel, S. Man, P. Elliott, J. Adams, R.S. Kerbel, Lack of multicellular drug resistance observed in human ovarian and prostate carcinoma treated with the proteasome inhibitor PS-341, Clinical cancer research : an official journal of the American Association for Cancer Research, 6 (2000) 3719-3728.

[10] A.L. Howes, G.G. Chiang, E.S. Lang, C.B. Ho, G. Powis, K. Vuori, R.T. Abraham, The phosphatidylinositol 3-kinase inhibitor, PX-866, is a potent inhibitor of cancer cell motility and growth in three-dimensional cultures, Molecular cancer therapeutics, 6 (2007) 2505-2514.

[11] S. Jelic, Molecular basis of future patients-tailored treatment. Arch, Oncol, 13 (2005) 56-58.

[12] J. Poland, P. Sinha, A. Siegert, M. Schnölzer, U. Korf, S. Hauptmann, Comparison of protein expression profiles between monolayer and spheroid cell culture of HT-29 cells revealed fragmentation of CK18 in three-dimensional cell culture, Electrophoresis, 23 (2002) 1174-1184.

[13] F.M. Balis, Evolution of anticancer drug discovery and the role of cell-based screening, Journal of the National Cancer Institute, 94 (2002) 78-79.

[14] O. Pelkonen, A.R. Boobis, U. Gundert-Remy, In vitro prediction of gastrointestinal absorption and bioavailability: an experts' meeting report, European journal of clinical pharmacology, 57 (2001) 621-629.

[15] A. Rangarajan, S.J. Hong, A. Gifford, R.A. Weinberg, Species- and cell type-specific requirements for cellular transformation, Cancer cell, 6 (2004) 171-183.

[16] R. Ito, T. Takahashi, I. Katano, M. Ito, Current advances in humanized mouse models, Cellular & molecular immunology, 9 (2012) 208-214.

المنارة للاستشارات
www.manaraa.com

[17] K. Bhadriraju, C.S. Chen, Engineering cellular microenvironments to improve cell-based drug testing, Drug discovery today, 7 (2002) 612-620.

[18] V.M. Weaver, O.W. Petersen, F. Wang, C.A. Larabell, P. Briand, C. Damsky, M.J. Bissell, Reversion of the malignant phenotype of human breast cells in three-dimensional culture and in vivo by integrin blocking antibodies, The Journal of cell biology, 137 (1997) 231-245.

[19] M.J. Bissell, A. Rizki, I.S. Mian, Tissue architecture: the ultimate regulator of breast epithelial function, Current opinion in cell biology, 15 (2003) 753-762.

[20] M.P. Wenger, L. Bozec, M.A. Horton, P. Mesquida, Mechanical properties of collagen fibrils, Biophysical journal, 93 (2007) 1255-1263.

[21] J.B. Gurdon, P.Y. Bourillot, Morphogen gradient interpretation, Nature, 413 (2001) 797-803.

[22] T.M. Quinn, A.J. Grodzinsky, M.D. Buschmann, Y.J. Kim, E.B. Hunziker, Mechanical compression alters proteoglycan deposition and matrix deformation around individual cells in cartilage explants, Journal of cell science, 111 (Pt 5) (1998) 573-583.

[23] M.A. Swartz, Signaling in morphogenesis: transport cues in morphogenesis, Current opinion in biotechnology, 14 (2003) 547-550.

[24] T.M. Achilli, J. Meyer, J.R. Morgan, Advances in the formation, use and understanding of multi-cellular spheroids, Expert opinion on biological therapy, 12 (2012) 1347-1360.

[25] G. Hamilton, Multicellular spheroids as an in vitro tumor model, Cancer letters, 131 (1998) 29-34.

[26] J.B. Kim, Three-dimensional tissue culture models in cancer biology, Seminars in Cancer Biology, 15 (2005) 365-377.

www.manaraa.com

[27] J.B. Kim, R. Stein, M.J. O'Hare, Three-dimensional in vitro tissue culture models of breast cancer-- a review, Breast cancer research and treatment, 85 (2004) 281-291.

[28] T. Nederman, B. Norling, B. Glimelius, J. Carlsson, U. Brunk, Demonstration of an extracellular matrix in multicellular tumor spheroids, Cancer research, 44 (1984) 3090-3097.

[29] M.T. Santini, G. Rainaldi, P.L. Indovina, Apoptosis, cell adhesion and the extracellular matrix in the three-dimensional growth of multicellular tumor spheroids, Critical Reviews in Oncology/Hematology, 36 (2000) 75-87.

[30] F. Grinnell, C.H. Ho, Y.C. Lin, G. Skuta, Differences in the regulation of fibroblast contraction of floating versus stressed collagen matrices, The Journal of biological chemistry, 274 (1999) 918-923.

[31] P. Lu, V.M. Weaver, Z. Werb, The extracellular matrix: a dynamic niche in cancer progression, The Journal of cell biology, 196 (2012) 395-406.

[32] T. Maeda, T. Sakabe, A. Sunaga, K. Sakai, Alexander L. Rivera, Douglas R. Keene, T. Sasaki, E. Stavnezer, J. Iannotti, R. Schweitzer, D. Ilic, H. Baskaran, T. Sakai, Conversion of Mechanical Force into TGF-β-Mediated Biochemical Signals, Current Biology, 21 (2011) 933-941.

[33] M.J. Paszek, N. Zahir, K.R. Johnson, J.N. Lakins, G.I. Rozenberg, A. Gefen, C.A. Reinhart-King, S.S. Margulies, M. Dembo, D. Boettiger, D.A. Hammer, V.M. Weaver, Tensional homeostasis and the malignant phenotype, Cancer cell, 8 (2005) 241-254.

[34] M.M. Choe, P.H.S. Sporn, M.A. Swartz, An in vitro airway wall model of remodeling, American Journal of Physiology - Lung Cellular and Molecular Physiology, 285 (2003) L427-L433.

www.manaraa.com

[35] A.S. Popel, P.C. Johnson, Microcirculation and Hemorheology, Annual review of fluid mechanics, 37 (2005) 43-69.

[36] M.A. Swartz, D.J. Tschumperlin, R.D. Kamm, J.M. Drazen, Mechanical stress is communicated between different cell types to elicit matrix remodeling, Proceedings of the National Academy of Sciences of the United States of America, 98 (2001) 6180-6185.

[37] A. Janowska-Wieczorek, M. Majka, J. Ratajczak, M.Z. Ratajczak, Autocrine/paracrine mechanisms in human hematopoiesis, Stem cells, 19 (2001) 99-107.

[38] W. Mueller-Klieser, Three-dimensional cell cultures: from molecular mechanisms to clinical applications, American Journal of Physiology - Cell Physiology, 273 (1997) C1109-C1123.

[39] K.A. Landman, C.P. Please, Tumour dynamics and necrosis: surface tension and stability, IMA journal of mathematics applied in medicine and biology, 18 (2001) 131-158.

[40] F. Hirschhaeuser, H. Menne, C. Dittfeld, J. West, W. Mueller-Klieser, L.A. Kunz-Schughart, Multicellular tumor spheroids: An underestimated tool is catching up again, Journal of Biotechnology, 148 (2010) 3-15.

[41] J. Friedrich, R. Ebner, L.A. Kunz-Schughart, Experimental anti-tumor therapy in 3-D: Spheroids – old hat or new challenge?, International Journal of Radiation Biology, 83 (2007) 849-871.

[42] J. Friedrich, C. Seidel, R. Ebner, L.A. Kunz-Schughart, Spheroid-based drug screen: considerations and practical approach, Nat. Protocols, 4 (2009) 309-324.

www.manaraa.com

[43] K. Kellner, G. Liebsch, I. Klimant, O.S. Wolfbeis, T. Blunk, M.B. Schulz, A. Gopferich, Determination of oxygen gradients in engineered tissue using a fluorescent sensor, Biotechnology and bioengineering, 80 (2002) 73-83.

[44] D.C. Radisky, D.D. Levy, L.E. Littlepage, H. Liu, C.M. Nelson, J.E. Fata, D. Leake, E.L. Godden, D.G. Albertson, M.A. Nieto, Z. Werb, M.J. Bissell, Rac1b and reactive oxygen species mediate MMP-3-induced EMT and genomic instability, Nature, 436 (2005) 123-127.

[45] F. Hermitte, P. Brunet de la Grange, F. Belloc, V. Praloran, Z. Ivanovic, Very low O2 concentration (0.1%) favors G0 return of dividing CD34+ cells, Stem cells, 24 (2006) 65-73.

[46] G. Helmlinger, F. Yuan, M. Dellian, R.K. Jain, Interstitial pH and pO2 gradients in solid tumors in vivo: high-resolution measurements reveal a lack of correlation, Nature medicine, 3 (1997) 177-182.

[47] J. Carlsson, H. Acker, Relations between ph, oxygen partial pressure and growth in cultured cell spheroids, International Journal of Cancer, 42 (1988) 715-720.

[48] E.J. Suuronen, H. Sheardown, K.D. Newman, C.R. McLaughlin, M. Griffith, Building in vitro models of organs, International review of cytology, 244 (2005) 137-173.

[49] L.E. O'Brien, M.M.P. Zegers, K.E. Mostov, Building epithelial architecture: insights from three-dimensional culture models, Nature reviews. Molecular cell biology, 3 (2002) 531-537.

[50] A. Ivascu, M. Kubbies, Rapid generation of single-tumor spheroids for high-throughput cell function and toxicity analysis, Journal of biomolecular screening, 11 (2006) 922-932.

www.manaraa.com

[51] C.D. Roskelley, P.Y. Desprez, M.J. Bissell, Extracellular matrix-dependent tissue-specific gene expression in mammary epithelial cells requires both physical and biochemical signal transduction, Proceedings of the National Academy of Sciences of the United States of America, 91 (1994) 12378-12382.

[52] E. Fennema, N. Rivron, J. Rouwkema, C. van Blitterswijk, J. de Boer, Spheroid culture as a tool for creating 3D complex tissues, Trends in biotechnology, 31 (2013) 108-115.

[53] A. Ivascu, M. Kubbies, Diversity of cell-mediated adhesions in breast cancer spheroids, International journal of oncology, 31 (2007) 1403-1413.

[54] G.M. Thurber, K.D. Wittrup, Quantitative spatiotemporal analysis of antibody fragment diffusion and endocytic consumption in tumor spheroids, Cancer research, 68 (2008) 3334-3341.

[55] A. Vaheri, A. Enzerink, K. Rasanen, P. Salmenpera, Nemosis, a novel way of fibroblast activation, in inflammation and cancer, Experimental cell research, 315 (2009) 1633-1638.

[56] Y.-C. Tung, A.Y. Hsiao, S.G. Allen, Y.-s. Torisawa, M. Ho, S. Takayama, High-throughput 3D spheroid culture and drug testing using a 384 hanging drop array, The Analyst, 136 (2011) 473-478.

[57] D.J. Slamon, W. Godolphin, L.A. Jones, J.A. Holt, S.G. Wong, D.E. Keith, W.J. Levin, S.G. Stuart, J. Udove, A. Ullrich, et al., Studies of the HER-2/neu proto-oncogene in human breast and ovarian cancer, Science (New York, N.Y.), 244 (1989) 707-712.

[58] M. Pickl, C.H. Ries, Comparison of 3D and 2D tumor models reveals enhanced HER2 activation in 3D associated with an increased response to trastuzumab, Oncogene, 28 (2009) 461-468.

www.manaraa.com

[59] D. Huh, G.A. Hamilton, D.E. Ingber, From 3D cell culture to organs-on-chips, Trends in cell biology, 21 (2011) 745-754.

[60] S.Y. Chen, P.J. Hung, P.J. Lee, Microfluidic array for three-dimensional perfusion culture of human mammary epithelial cells, Biomedical microdevices, 13 (2011) 753-758.

[61] M.T. Santini, G. Rainaldi, Three-dimensional spheroid model in tumor biology, Pathobiology : journal of immunopathology, molecular and cellular biology, 67 (1999) 148-157.

[62] W.R. Inch, J.A. McCredie, R.M. Sutherland, Growth of nodular carcinomas in rodents compared with multi-cell spheroids in tissue culture, Growth, 34 (1970) 271-282.

[63] R.M. Sutherland, J.A. McCredie, W.R. Inch, Growth of multicell spheroids in tissue culture as a model of nodular carcinomas, Journal of the National Cancer Institute, 46 (1971) 113-120.

[64] R.Z. Lin, H.Y. Chang, Recent advances in three-dimensional multicellular spheroid culture for biomedical research, Biotechnology journal, 3 (2008) 1172-1184.

[65] Q. Li, C. Chen, A. Kapadia, Q. Zhou, M.K. Harper, J. Schaack, D.V. LaBarbera, 3D models of epithelial-mesenchymal transition in breast cancer metastasis: high-throughput screening assay development, validation, and pilot screen, Journal of biomolecular screening, 16 (2011) 141-154.

[66] J.B. Kim, Three-dimensional tissue culture models in cancer biology, Semin Cancer Biol, 15 (2005) 365-377.

[67] T.J. Goodwin, T.L. Prewett, D.A. Wolf, G.F. Spaulding, Reduced shear stress: a major component in the ability of mammalian tissues to form three-dimensional assemblies in simulated microgravity, Journal of cellular biochemistry, 51 (1993) 301-311.

www.manaraa.com

[68] B. Rodday, F. Hirschhaeuser, S. Walenta, W. Mueller-Klieser, Semiautomatic growth analysis of multicellular tumor spheroids, Journal of biomolecular screening, 16 (2011) 1119-1124.

[69] F. Hirschhaeuser, T. Leidig, B. Rodday, C. Lindemann, W. Mueller-Klieser, Test system for trifunctional antibodies in 3D MCTS culture, Journal of biomolecular screening, 14 (2009) 980-990.

[70] M.H. Wu, S.B. Huang, G.B. Lee, Microfluidic cell culture systems for drug research, Lab on a chip, 10 (2010) 939-956.

[71] Y.C. Toh, C. Zhang, J. Zhang, Y.M. Khong, S. Chang, V.D. Samper, D. van Noort, D.W. Hutmacher, H. Yu, A novel 3D mammalian cell perfusion-culture system in microfluidic channels, Lab on a chip, 7 (2007) 302-309.

[72] H.K. Kleinman, G.R. Martin, Matrigel: basement membrane matrix with biological activity, Semin Cancer Biol, 15 (2005) 378-386.

[73] G.Y. Lee, P.A. Kenny, E.H. Lee, M.J. Bissell, Three-dimensional culture models of normal and malignant breast epithelial cells, Nature methods, 4 (2007) 359-365.

[74] T.R. Sodunke, K.K. Turner, S.A. Caldwell, K.W. McBride, M.J. Reginato, H.M. Noh, Micropatterns of Matrigel for three-dimensional epithelial cultures, Biomaterials, 28 (2007) 4006-4016.

[75] A. Sourla, C. Doillon, M. Koutsilieris, Three-dimensional type I collagen gel system containing MG-63 osteoblasts-like cells as a model for studying local bone reaction caused by metastatic cancer cells, Anticancer research, 16 (1996) 2773-2780.

[76] B.A. Justice, N.A. Badr, R.A. Felder, 3D cell culture opens new dimensions in cell-based assays, Drug discovery today, 14 (2009) 102-107.

www.manaraa.com

[77] J.J. Schmidt, J. Rowley, H.J. Kong, Hydrogels used for cell-based drug delivery, Journal of biomedical materials research. Part A, 87 (2008) 1113-1122.

[78] C. Ji, A. Khademhosseini, F. Dehghani, Enhancing cell penetration and proliferation in chitosan hydrogels for tissue engineering applications, Biomaterials, 32 (2011) 9719-9729.

[79] L. Fjellbirkeland, R. Bjerkvig, O.D. Laerum, Tumour fragment spheroids from human non-small-cell lung cancer maintained in organ culture, Virchows Archiv : an international journal of pathology, 426 (1995) 169-178.

[80] J.M. Kelm, N.E. Timmins, C.J. Brown, M. Fussenegger, L.K. Nielsen, Method for generation of homogeneous multicellular tumor spheroids applicable to a wide variety of cell types, Biotechnology and bioengineering, 83 (2003) 173-180.

[81] T.A. Ulrich, A. Jain, K. Tanner, J.L. MacKay, S. Kumar, Probing cellular mechanobiology in three-dimensional culture with collagen-agarose matrices, Biomaterials, 31 (2010) 1875-1884.

[82] J. Friedrich, W. Eder, J. Castaneda, M. Doss, E. Huber, R. Ebner, L.A. Kunz-Schughart, A reliable tool to determine cell viability in complex 3-d culture: the acid phosphatase assay, Journal of biomolecular screening, 12 (2007) 925-937.

[83] L. le Roux, A. Volgin, D. Maxwell, K. Ishihara, J. Gelovani, D. Schellingerhout, Optimizing imaging of three-dimensional multicellular tumor spheroids with fluorescent reporter proteins using confocal microscopy, Molecular imaging, 7 (2008) 214-221.

[84] M. Wartenberg, H. Acker, Quantitative recording of vitality patterns in living multicellular spheroids by confocal microscopy, Micron (Oxford, England : 1993), 26 (1995) 395-404.

www.manaraa.com

[85] D. Donovan, N.J. Brown, E.T. Bishop, C.E. Lewis, Comparison of three in vitro human 'angiogenesis' assays with capillaries formed in vivo, Angiogenesis, 4 (2001) 113-121.

[86] S.R. Horman, J. To, A.P. Orth, N. Slawny, M.J. Cuddihy, D. Caracino, High-content analysis of three-dimensional tumor spheroids: investigating signaling pathways using small hairpin RNA, Nat Meth, 10 (2013).

[87] H. Thielecke, A. Mack, A. Robitzki, Biohybrid microarrays--impedimetric biosensors with 3D in vitro tissues for toxicological and biomedical screening, Fresenius' journal of analytical chemistry, 369 (2001) 23-29.

[88] Questions regarding the spheroid culture technique:, in, Spherogenex.de, pp. website.

[89] C.C. Hanot, Y.S. Choi, T.B. Anani, D. Soundarrajan, A.E. David, Effects of Iron-Oxide Nanoparticle Surface Chemistry on Uptake Kinetics and Cytotoxicity in CHO-K1 Cells, International journal of molecular sciences, 17 (2016).

[90] Prussian Blue Staining Protocol for Iron, in.

www.manaraa.com

Appendix

Experimental Data

Table A.1

Tilt diameter raw data

Degrees of Tilt	24 diameter	48 diameter	96 diameter
0.100	0.500	0.499	0.498
0.200	0.498	0.496	0.490
0.300	0.496	0.491	0.478
0.400	0.492	0.484	0.460
0.500	0.492	0.484	0.437
0.600	0.482	0.464	0.405
0.700	0.475	0.450	0.365
0.800	0.468	0.434	0.313
0.900	0.458	0.415	0.240
1.000	0.448	0.392	0.111
1.100	0.437	0.365	0.000
1.200	0.423	0.334	0.000
1.300	0.409	0.295	0.000
1.400	0.392	0.248	0.000
1.500	0.373	0.183	0.000
1.600	0.352	0.060	0.000
1.700	0.329	0.000	0.000
1.800	0.301	0.000	0.000
1.900	0.270	0.000	0.000
2.000	0.231	0.000	0.000
2.100	0.183	0.000	0.000
2.200	0.111	0.000	0.000
2.250	0.037	0.000	0.000

www.manaraa.com

Table A.2

Tilt area raw data

Degrees of Tilt	24 area	48 area	96 area
0.100	0.196	0.196	0.194
0.200	0.195	0.193	0.189
0.300	0.193	0.190	0.180
0.400	0.190	0.184	0.166
0.500	0.190	0.184	0.150
0.600	0.182	0.169	0.129
0.700	0.177	0.159	0.105
0.800	0.172	0.148	0.077
0.900	0.165	0.135	0.045
1.000	0.158	0.121	0.010
1.100	0.150	0.105	0.000
1.200	0.141	0.087	0.000
1.300	0.131	0.069	0.000
1.400	0.121	0.048	0.000
1.500	0.110	0.026	0.000
1.600	0.098	0.003	0.000
1.700	0.085	0.000	0.000
1.800	0.071	0.000	0.000
1.900	0.057	0.000	0.000
2.000	0.042	0.000	0.000
2.100	0.026	0.000	0.000
2.200	0.010	0.000	0.000
2.250	0.001	0.000	0.000

www.manaraa.com

Table A.3

Calculated percent differences of area

Percent Differences			
Degrees of Tilt	24 area	48 area	96 area
0.000	1.000	1.000	1.000
0.100	0.998	0.996	0.990
0.200	0.992	0.985	0.962
0.300	0.982	0.965	0.914
0.400	0.969	0.938	0.848
0.500	0.969	0.938	0.762
0.600	0.929	0.861	0.658
0.700	0.904	0.811	0.534
0.800	0.874	0.753	0.391
0.900	0.841	0.688	0.230
1.000	0.803	0.615	0.049
1.100	0.762	0.534	0.000
1.200	0.717	0.445	0.000
1.300	0.668	0.349	0.000
1.400	0.615	0.245	0.000
1.500	0.558	0.134	0.000
1.600	0.497	0.014	0.000
1.700	0.432	0.000	0.000
1.800	0.363	0.000	0.000
1.900	0.291	0.000	0.000
2.000	0.214	0.000	0.000
2.100	0.134	0.000	0.000
2.200	0.049	0.000	0.000
2.250	0.006	0.000	0.000

www.manaraa.com

Table A.4

Calculated percent error of area

Percent Error			
degrees of tilt	24 block	48 block	96 block
0.000	0.000	0.000	0.000
0.100	0.002	0.004	0.010
0.200	0.008	0.015	0.038
0.300	0.018	0.035	0.086
0.400	0.031	0.062	0.152
0.500	0.031	0.062	0.238
0.600	0.071	0.139	0.342
0.700	0.096	0.189	0.466
0.800	0.126	0.247	0.609
0.900	0.159	0.312	0.770
1.000	0.197	0.385	0.951
1.100	0.238	0.466	1.000
1.200	0.283	0.555	1.000
1.300	0.332	0.651	1.000
1.400	0.385	0.755	1.000
1.500	0.442	0.866	1.000
1.600	0.503	0.986	1.000
1.700	0.568	1.000	1.000
1.800	0.637	1.000	1.000
1.900	0.709	1.000	1.000
2.000	0.786	1.000	1.000
2.100	0.866	1.000	1.000
2.200	0.951	1.000	1.000
2.250	0.994	1.000	1.000

www.manaraa.com